UNIVERSITY of the
WESTERN CAPE

Natural Science Faculty
Earth Science Department

An assessment of water use by riparian and non-riparian invasive alien plants and the effects on water resources at the catchment scale

By

Yonela Princess Mkunyana

A thesis submitted in fulfilment of the requirements for the degree of Doctor of Philosophy

Supervisors:

Prof. D. Mazvimavi

Dr. S. Dzikiti

Dr. J. Glenday

February 2023

Abstract

An assessment of water use by riparian and non-riparian invasive alien plants and the effects on water resources at the catchment scale

Y.P. Mkunyana

Ph.D. Environmental and Water Science, Earth Science Department, University of the Western Cape

The diversity and increasing extent of invasive alien plants (IAPs) are currently a global ecological and economic problem, especially in semi-arid regions. The introduction of IAPs worsens the strain in South Africa's water resources by reducing the mean annual runoff by approximately 7%. Further work needs to be done to ensure that those IAPs that have the greatest impact receive priority. Effective management of IAPs promotes the conservation and sustainable use of the natural environment, the economies it supports, and the high quality of life in society. The monitoring of the distribution of IAPs is therefore an important consideration in catchment management. Remote sensing and cloud computing platform, Google Earth Engine (GEE) were used to map land use/landcover changes between the 1973 – 2021 period using Landsat imagery. The validation of this classification showed that Landsat 8 images had improved accuracy in classifying land covers. In the Nuwejaars Catchment, the extent of invasions decreased from 25 % in 1973 to 11 % in 2021. Most of these invasions were identified in the mountainous parts and lowland riparian zones. This decrease was attributed to the clearing activities that are actively taking place in the catchment.

Previous studies highlighted the detrimental impacts of IAPs on catchment water resources. Earlier research also emphasized that improved information about water use rates by IAPs is important in a semi-arid country where there are competing demands for limited water resources. *Acacia longifolia* was identified as the dominant invader in the Nuwejaars Catchment. This study compared water use rates by the *A. longifolia* species occurring in different locations, from headwaters to lowlands. Water use rates were quantified using the Heat Pulse Velocity (HPV) sap flow systems. Using a paired t-test, it

was observed that sap flux densities measured across the different stem sizes of instrumented trees and stand transpiration rates differed significantly ($p<0.05$). The results showed that the headwaters of the catchment received more rainfall than the other parts. Accordingly, *A. longifolia* stands in the headwaters used water similarly to those in the lowland and mid-slope riparian areas. Results obtained in this study support the hypothesis that riparian invasions use more water than invasions occurring in a non-riparian setting. Further, this study revealed that high tree densities are likely to occur in both riparian and non-riparian settings if moisture and/or rainfall that promotes plant growth is available. Furthermore, the analyses of soil water content and groundwater variations confirmed that the differences in water use rates by *A. longifolia* across the sites were a consequence of the differences in the groundwater water table from the headwaters to the lowlands. The assumption that IAPs act as groundwater pumps in areas they invade was also proven to be true.

Additionally, this study examined the hypothesis that IAPs use considerable amount of water than indigenous fynbos vegetation. This was done by comparing the water use rates by fynbos vegetation with that of the invasive *A. longifolia* stand occurring in a similar environment and/or setting. Actual evapotranspiration (AET) measurements from the fynbos stand were measured using an eddy covariance system, while AET from *A. longifolia* stand was modelled using in-situ weather, soil water content, and transpiration data. The paired t-test illustrated significantly ($p<0.05$) high rates of water use from *A. longifolia* stand (742 mm) compared to the indigenous fynbos stand (429 mm). These results validated the previous assumption of land rehabilitation and potential water savings that were assumed by clearing IAPs and replacing them with indigenous vegetation. At the catchment scale, IAPs in the Nuwejaars Catchment lost 61.94 Mm^3/year of water through AET. In the event that invaded areas (11 % of the catchment coverage) were replaced with indigenous vegetation, the volume of water lost through AET would be 35.81 Mm^3/year. Therefore, the restoration of invaded areas in the Nuwejaars Catchment would amount to 26.13 Mm^3/year of potential water savings.

February 2023

An assessment of water-use by riparian and non-riparian invasive alien plants and the effects on water resources at the catchment scale

Keywords

Actual evapotranspiration

Alien clearing

Eddy covariance

Fynbos

Groundwater-surface water systems

Heat pulse velocity

Hydrological benefit

Landcover/land-use

Penman-Monteith

Phreatophyte

Sap flow

Sapwood area index

Soil water content

Surface energy balance

Transpiration

Two-layer model

Declaration

By submitting this thesis/dissertation electronically, I declare that the entirety of the work contained therein is my original work, that I am the sole author of the thesis titled **'An assessment of water use by riparian and non-riparian invasive alien plants and the effects on water resources at the catchment scale'**, that it has not been submitted for any degree or examination in any other university. Reproduction and publication thereof by the University of the Western Cape will not infringe any third-party rights, and all the sources I have used or quoted have been indicated and acknowledged by complete references.

Co-authorship

The manuscript I co-authored included parts of Chapter 3. Contributions to the manuscript include collecting field data (for ground truth), supervising intellectual work, and reviewing. Mtengwana et al. (2020) evaluated the use of two multispectral remote sensing data sets (Landsat 8 and Sentinel-2) to map and monitor IAPs in the Heuningnes Catchment (with quaternary catchments G50B-F), which includes quaternary catchments G50B&C (Nuwejaars Catchment). The results from Mtengwana et al. (2020) justify the use of Landsat 8 in the mapping of IAPs in the Nuwejaars Catchment.

Yonela Princess Mkunyana

February 2023

Acknowledgements

"*Gratitude is the ability to experience life as a gift. It liberates us from the prison of self-preoccupation*." – John Ortberg.

The completion of this thesis is a testimony of Proverbs 31:25, "*She is clothed with strength and dignity, and she laughs without fear of the future*." I have been truly blessed and highly favoured by God. For that, I am forever grateful. When I look back at how many people contributed to the realization of this thesis, I am blown away by how lucky I have been and how very insignificant the words "thank you" seem when it comes to expressing the gratitude I feel. I could not complete this thesis without the support of many individuals and organisations. I would like to thank:

First, my parents, for raising me to value education, to have an enquiring mind, and not be afraid of a challenge. Thank you for instilling the ethical value of *Ubuntu* in me. This journey needed respect for others, helpfulness, sharing, caring, trust and unselfishness. Above all, you taught me that consistency, patience, and discipline are key determinants of success. To my mother (fondly known as Mam'Thembu): through you, I've seen how education polishes minds and reinforces our thoughts. I am glad to have witnessed you furthering your studies and made me realize what we are capable of. That gave me the courage to go the extra mile.

Enormous gratitude to my siblings: Zanekhaya, Abongile, and Zusiphe. Each one of us has had a fair share of challenges. We have shared some of those, but my greatest pleasure is seeing all of us persevering and making it against all odds. To all my family members (amaMpondo nabaThembu), thank you for the support, love, and motivation to pursue this dream, none of this would have been possible without you. In the words of Marianne Williamson "…*as we let our own light shine, we unconsciously give other people permission to do the same*. I hope my journey inspires you and generations to come, ndiyabulela!

To Siviwe, for all you have done, a thank you would not be enough. This was a lengthy journey. Thank you for being an ever- present source of motivation and support. You have truly been amazing, and I am grateful to have walked this journey with you.

My supervisor: Prof Mazvimavi, thank you for your patience, encouragement, and believing in me even when I doubted myself. Thank you for being both a supervisor and a father when needed. The honest discussions, and words of wisdom, truly kept me going. Without your constant drive and motivation that pushed me to realize my strengths, this thesis would not have been a success. Dr Dzikiti, I am forever indebted for transferring your technical skills for the monitoring equipment and analysis of data, thank you for your patience and contributions to this thesis. Special appreciation is also given to Dr Glenday, for her motivation and support. I sincerely acknowledge your assistance in the field, reviewing, and shaping this thesis to be what we all envisioned from the onset.

My sincere thanks to my fellow researchers and friends I met through research at UWC, the Dr(s) that made "*Women in Science"* fashionable: Nolusindiso Ndara, Faith Jumbi, Zanele Ntshidi, and Nompumelelo Mobe. Ladies, all your journeys were unique, and they inspired me in different ways; your support motivated and pushed me on. Dr Siyamthanda Gxokwe, it was the most beautiful thing to watch you grow. Eugene Maswanganye, your assistance throughout the research process was always appreciated, from driving me to the field to collecting data on my behalf. Thanks for being my go-to person when everything seemed impossible. Refiloe Maphiri, I may have never considered the role you played in this, but being around you, teasing and laughing in those cubicles was all therapeutic for me. *kea leboha,* I needed that. Munashe Mashabatu, and my other colleagues. You all made this journey bearable and unforgettable.

Thank you to the teaching staff of EWS- Earth Science department for building my theoretical background which was very helpful during this research. During this journey, I presented this work several times, thank you all for your contributions. I am also grateful to the technical staff for their support and involvement in fieldwork. Appreciation to Mrs. Mandy Naidoo, she made the administrative and logistical aspects of this research manageable.

This study would not have been complete without the community of Elim, I appreciate them for their hospitality, the braai nights we had after fieldwork are memorable. Thank you to the landowners in the Nuwejaars Catchment, for sharing their homes and allowing us in their properties whenever we needed access. I appreciate the engagements and sharing of experiences and knowledge about processes they have seen over years.

The Nuwejaars Wetlands Special Management Area (NWSMA) supported this work from the very beginning. Many thanks to Eugene and the team for availing themselves whenever we needed their assistance – your knowledge and time are most appreciated.

The research presented in this paper emanates from various Water Research Commission (WRC) projects. I am thankful to WRC for funding this study over the years and particularly grateful for insights and suggestions from Mr Wandile Nomquphu. I am thankful to the South African Environmental Observation Network SAEON-National Research Foundation (NRF) for funding and sharing their resources and facilities when needed. Last, but not least, thank you to the host institution- the University of the Western Cape, for providing us with the resources we needed especially during the COVID-19 wave. Thank you for the extra support, especially for the researchers.

Dedication

My father's passing left me scarred that I almost gave up, but I found strength through God, *He "...turned my mourning into joyful dancing. He took away my clothes of mourning and clothed me with joy,"* - Psalm 30:11

This thesis is dedicated to my late father, MzwaMampondo Wiseman Mkunyana. I am certain that even in the afterlife, you are still proudly bragging about me. Lala Ndamase!

Table of Contents

List of Figures

List of Tables

List of Abbreviations

AET	Actual Evapotranspiration
ANOVA	Analysis of Variance
CFR	Cape Floristic Region
DTW	Depth to The Water table
ET	Evapotranspiration
ET_g	Evapotranspiration from groundwater
ETo	Reference evapotranspiration
FAO-56	Food and Agriculture Organization, paper no 56.
GEE	Google Earth Engine.
HPV	Heat Pulse Velocity
IAPs	Invasive Alien Plants
LAI	Leaf Area Index
MLC	Maximum Likelihood Classifier
NBSAP	National Biodiversity Strategy and Action Plan
NIAPS	National Invasive Alien Plant Survey
NDVI	Normalised Difference Vegetation Index
NEMBA	National Environmental Management: Biodiversity Act
NSE	Nash-Sutcliffe Efficiency
ROI	Region Of Interest
SAPIA	Southern African Plant Invaders Atlas
SAI	Sapwood Area Index
SEBAL	Surface Energy Balance Algorithm over Land
SEBS	Surface Energy Balance System
SFRA	Stream Flow Reduction Activity
SWC	Soil Water Content
Sy	Specific yield
VPD	Vapor Pressure Deficit
WfW	Working for Water.

Symbols

Δ	Slope of the saturation vapour pressure against the temperature curve.
γ	Psychrometric constant.
λ	Latent heat of vaporisation of water.
G	Soil heat flux.
H	Sensible heat flux.
ρ	Density of air.
c_p	Specific heat of air at constant pressure.
k	Thermal diffusivity of the wood.
k_1	Maximum stomatal conductance of the plant.
ke	Extinction coefficient which was assumed as a constant with a value of 0.5.
r	Surface reflectance (albedo).
ET_g	Consumption of groundwater for transpiration.
ΔS	Change in storage.
R	Rate of the water table recovery.
θ	Measured volumetric soil water content.

Chapter 1
Introduction

1.1 Background

The term 'invasion' refers to the uncontrolled spread of an organism outside its native range, which has a detrimental effect on the environment, economy, or the health of humans, animals, and plants. For a non-native (alien) organism to be considered an invasive species, the negative effects that the organism causes outweigh any beneficial effects. Many alien introductions provide benefits to society and even among species that meet the definition of invasive, societal benefits may greatly exceed any negative effects. However, in some cases, positive effects are overshadowed by negative effects, and this is the concept of causing harm (The National Invasive Species Council, 2006). Meyerson et al. (2019) argued that species must cross distinct stages, or barriers before they can be described as "invasive". This agreed with Richardson et al. (2000) who broke down phases of invasion into five:

1. Introduction: organisms transported by humans across a geographical barrier and establish adult populations.
2. Colonization: the adult population is reproducing, spreads, and forms a colony.
3. Naturalization: the colony establishes new populations and continues to spread.
4. Invasive: the species rapidly reproduce and spread in a larger area.
5. Transformer: the species changes the condition, state, or nature of the natural ecosystem.

Invasive species are defined as species of animals, plants, or microorganisms translocated by humans into environments they do not naturally exist, in which they establish and spread, negatively affecting the dynamics of local ecosystems (The National Invasive Species Council, 2006). From the human health perspective, invasive species promote pathogen pollution in the invaded area leading to the emergence of diseases. For example, the introduction of the North American raccoon *Procyon lotor* to Central Europe *Baylisascaris procyonis*, a nematode causing *larva migrans* syndromes potentially inducing

severe central nervous system disease in humans (Chinchio et al., 2020). Invasion in fauna includes the case of the eastern-Asiatic brown marmorated stink bug (*Halyomorpha halys*) to Europe, a successful global invader that caused severe economic damage to crop and the North American crayfishes (*Procambarus clarkia*), infected with the fungus *Aphanomyces astaci* caused huge economic losses to fisheries, being the pathogen lethal to native crayfishes in Europe (Chinchio et al., 2020). In South Africa, recent introductions include the tomato leaf miner (*Tuta absoluta*), which was detected in 2016 and is now a major agricultural pest, and the polyphagous shot hole borer (*PSHB, Euwallacea fornicatus*), an ambrosia beetle from Southeast Asia which was first detected in 2017 in Pietermaritzburg and has now extended to other parts of the country (van Wilgen et al., 2020; Zengeya and Wilson, 2021).

In plants, examples include the south American coypu (*Myocastor coypus*), invasive in North America, Europe, and Asia, where it causes both environmental and economic impacts consuming aquatic vegetation and undermining riverbanks (Chinchio et al., 2020). The water hyacinth (*Eichhornia crassipes*) was identified as the world's worst aquatic weed due to its invasive potential, negative impact on aquatic ecosystems, and the cost it necessitates to control it. This weed, a native of the Amazon basin, has been popular in outdoor aquatic gardens but its escape to natural areas where its populations have expanded to completely cover lakes and rivers has devastated water bodies by reducing flow, which can result in flooding and damage to infrastructure and the life they support, especially in the south-eastern U.S (The National Invasive Species Council, 2006). The water hyacinth was first recorded in South Africa on the Cape flats in the early 1900s and since then, has spread throughout the country (Pérez *et al.*, 2011). Compared to many other countries, South Africa has invested in research on biological invasions (van Wilgen et al., 2020; Wilson et al., 2018). To date, the invasive alien species (IAPs) that are perceived to have had the largest impacts have been among those most studied including many tree species (van Wilgen et al., 2020).

Many invasive species are examples of "*the tragedy of the commons*," or how actions that benefit one individual's use of resources may negatively impact others and result in a significant overall increase in damage to the economy, the environment, or public health. The shrub *Parthenium hysterophorus* is suspected to have accidentally been introduced to Ethiopia through relief food donations in the mid-1980s but has since spread to Kenya,

Uganda, Tanzania, Somalia, and South Sudan (Makoni, 2020). The Australian acacias (wattles) have been introduced to many parts of the world for many purposes (Le Maitre et al., 2002) and they have played a major role in improving the livelihoods of communities (van Wilgen et al., 2012) and in economic growth (Le Maitre et al., 2011). *A. cyclops*, *A. longifolia* and *A. saligna* were introduced in the early 18th century by the Cape Colonial Secretary to stabilize dunes near Cape Town (Richardson et al., 2000). *A. decurrens*, *A. mearnsii*, and *A. melanoxylon*, were introduced for timber production (Dye and Jarmain, 2004; Le Maitre et al., 2011; Magona et al., 2018; Morris et al., 2011). Where these species were planted for forestry, the indigenous vegetation was removed to allow the acacias to establish without competition (Richardson et al., 2000). In the early 19th century, *A. baileyana*, *A. elata*, and *A. podalyriifolia* were introduced for ornamental purposes (Magona et al., 2018) and as a result of this long history, South Africa has the greatest recorded diversity of Australian acacia species introductions and the most widespread wattle invasions than anywhere in the world (Le Maitre et al., 2011; Magona et al., 2018; Richardson et al., 2000). Despite the benefits that led to the introduction of wattles, some wattle species have also become widespread invaders, threatening biodiversity by transforming ecosystems (Le Maitre et al. 2000, 2011). This resulted in an urgent need for objective protocols for dealing with conflicts of interest that arise when IAPs have both benefits and costs (van Wilgen et al., 2020, 2012; Wilson et al., 2018). Further work needs to be done to ensure that those IAPs that have the greatest impact receive priority attention when it comes to management. The effective management of IAPs promotes the conservation and sustainable use of the natural environment, the economies it supports, and the high quality of life in society (Makoni, 2020; van Wilgen et al., 2020).

1.2 Geographical coverage of IAPs and *Acacia longifolia* in South Africa

The diversity and increasing extent of IAPs encroaching on natural systems is currently a global ecological and economic problem, especially in semi-arid regions (Holmes et al., 2008; van Wilgen et al., 2012). The geographical patterns, modes of dispersal, reasons for introductions and key issues regarding the increased distributions of IAPs globally were discussed by Richardson et al. (2011). The study listed regions with the largest number of IAPs. Australia was the leading country with 183 woody IAPs, followed by Southern

Africa with 170, North America with 163, Pacific Islands with 147, and 107 in New Zealand. In the USA, *Tamarix* species (*T. chinensis*, *T. gallica*, and *T. ramosissim*) commonly known as saltcedar are problematic alien invaders in southern California and other areas of the southwestern United States (Hamada et al., 2007). Since the introduction of woody IAPs in the western United States during the 19th Century, saltcedar has dominated riparian zones, xeric, and halophytic plant associations; and the perennial river systems in the western U.S. and northwest Mexico (Nagler et al., 2005).

In South Africa, more than 200 IAPs have been reported as problematic in natural and semi-natural ecosystems (Chamier et al., 2012). These species cover approximately 10 million hectares of land, which is 8% of the country's surface area (Le Maitre, 2004; van Wilgen et al., 2004). Pines and acacias are among the common species found in many parts of the world and have become invasive particularly in South Africa. Due to the similar climates in South Africa and Australia, the Black wattle *(Acacia mearnsii)* is an example of a problematic Australian woody species that have become invasive in South Africa. *A.meansii* invades riparian areas in most cases (Dye and Jarmain, 2004) and as a result, the studies done on the hydrological impacts of IAPs have focused on this species. *Acacia longifolia* was introduced in South Africa as an ornamental and for dune stabilization but has spread along the coastal areas where it competes with and replaces the indigenous species (Henderson, 2007; Henderson and Wilson, 2017). *Acacia longifolia* is highly problematic in riparian areas of the wetter parts of the Western Cape, Eastern Cape, Kwa-Zulu Natal, and scattered parts of Mpumalanga Province (Henderson, 2007). However, *Acacia longifolia* has received less research attention than other IAPs such as the eucalypts, pines, and other wattle species like *A. mearnsii* because of its lower areal coverage nation-wide compared to other IAPs. Yet, there are settings where *A. longifolia* is the most dominant invader, such as in the Nuwejaars Catchment in the Western Cape.

Acacia longifolia is an evergreen shrub/tree that grows 2-8 meters high (Morais and Freitas, 2015, 2012), the bright yellow and cylindrical flowers are usually seen from August to October in South Africa. Like other IAPs, *A. longifolia* can adapt to harsh conditions, spread at rapid rates, and often develop deep roots, large canopy sizes, and/or dense stands (Calder and Dye, 2001), which allow them to outcompete the indigenous vegetation in accessing water, light, and nutrients. Most of the research on *A. longifolia*

impacts in invaded systems has been done in Portugal (Marchante et al., 2008; Morais and Freitas, 2012, 2015; Rascher et al., 2011b) where it was highlighted that the species *A. longifolia* is a water spending invader, so it is likely that its encroachment may have serious consequences for ecosystem function. However, water use patterns and impacts of *A. longifolia* on water resources are poorly understood in South Africa.

Various legislation in South Africa has been developed to emphasize the need of understanding the interrelationships between vegetation and water sources to promote the sustainable use of natural resources (South African Constitution, Act 108 of 1996). This includes the National Environmental Management: Biodiversity Act of 1998 which promotes the protection of species, ecosystems, and encourages sustainable use of indigenous biological resources. The declaration of plantation forestry as a stream flow reduction activity (SFRA) shows maintained interest in the issue of forest water use and its impact on catchment water yield (Calder and Dye, 2001). The increasing expansion of *A. longifolia* in the Nuwejaars Catchment, therefore, demands urgent intervention as the species is listed in category 1a in the National Environmental Management: Biodiversity Act (NEMBA, 2004). This category consists of invasive species that cannot legally be owned, grown, or imported into South Africa. These regulations place restrictions on the use of listed alien species and regulate how they are to be managed (van Wilgen et al., 2020). Consequently, in areas where they grow, property owners and government officials are required to control and/ or monitor their spread. This is done to reduce the risk of importing alien species that could become invasive and harmful, reduce the number of alien species becoming invasive, limit the extent of invasions, and reduce the impacts caused by these invasions while recognising that society should continue to benefit from alien species (van Wilgen et al., 2020).

1.3 The hydrological impacts of IAPs

The introduction of IAPs with high water use rates worsens the strain on South Africa's limited water resources and this has been recognised by policymakers. South Africa is dominated by arid and semi-arid regions with limited water availability. The country receives an annual average rainfall average of 490 mm/year compared to the global average of 840 mm/year, and less than 10% of the rainfall ends up as surface runoff with

the rest being lost through evapotranspiration (Enright, 2000). It is estimated that IAPs reduce the mean annual runoff in South Africa by approximately 7% (Calder and Dye, 2001).

The increasing expansion of IAPs demands urgent intervention as these species have mostly invaded the riparian zones (Holmes et al., 2008), leading to environmental problems such as a reduction in water availability. In riparian systems, the water table is generally closer to the surface and accessible for transpiration (Le Maitre et al., 2011; Loheide et al., 2005; Shakhane et al., 2017). The penetration of vegetation roots into the capillary fringe consequently results in declining water tables and that is one of the major impacts that IAPs have on these systems (Shakhane et al., 2017). In some cases, riparian IAPs change the hydraulic gradients of the groundwater and surface water systems which govern the interaction between surface and subsurface water (Shakhane et al., 2017). Consequently, a gaining stream can change into a losing stream or the other way around (Shakhane et al., 2017). At times, streams that usually flow throughout the year are converted to non-perennial systems. In some cases, IAPs have deep root systems that extract large quantities of water from depths of more than 10 m or sometimes more (Le Maitre et al., 2015). Therefore, they often behave as "groundwater pumps" and are sensitive to changes in depth to the water table (Banks et al., 2011; Loheide et al., 2005a). Thus, changes in the location and density of IAPs may serve as indicators of change in the local water table (Ahring and Steward, 2012). All these processes illustrate the great extent of connectivity between components of the hydrological cycle and align with observations by Sophocleous (2002) and Loheide et al. (2005) who emphasized that effective management of water resources requires an understanding of the basic principles of interactions between groundwater, surface water, and all components of the hydrological cycle. It is therefore imperative to understand the impacts of vegetation on groundwater and surface water systems, especially in arid-semi-arid catchments where woody vegetation is encroaching.

Contrary to the assumptions made about groundwater use by riparian IAPs, Snyder and Williams (2003) argued that not all woody IAPs in the forest used groundwater for transpiration as the term 'phreatophyte' implies. Riparian trees, especially IAPs growing under different conditions of water availability, can adapt their physiology to maximize their chances of survival (Schachtschneider and Reinecke, 2014). This implies that

different riparian species need to adapt to survive the different regimes (timing, frequency, magnitude, and duration) of water availability found in a catchment. This was also supported by findings from a study by Dzikiti et al. (2017) which illustrated that riparian invasions (*Eucalyptus* sp.) in semi-arid regions can rely on rainwater stored in shallow soil layers as an important source of water. This was also observed by Mkunyana et al. (2019) who also confirmed the scientific hypothesis that riparian (*Acacia longifolia*) trees use more water than the same species occurring on the non-riparian hillslope. The water use patterns by riparian *A. longifolia* declined with soil water content, which then raised uncertainties of whether riparian acacias may or may not be dependent on groundwater as earlier studies suggested. Results from Mkunyana et al. (2019) were insufficient to address these uncertainties because the water sources of *A. longifolia* were not investigated. Therefore, there is a gap in scientific knowledge about the characterization of the conditions that promote the use of alternative water sources in IAPs. This is necessary to accurately assess the differential impacts of IAPs on soil water, groundwater, and ultimately on catchment water balance.

1.4 The hydrological benefits of restoring invaded catchments.

Several studies in South Africa have investigated the impacts of woody alien plants on hydrological processes in invaded catchments by quantifying and comparing water use by IAPs above that used by indigenous species (Enright, 2000; Dye et al., 2001; Le Maitre et al., 2015, 2000; Morris et al., 2011; Cavaleri and Sack, 2010; Cavaleri et al., 2014, Dzikiti et al., 2017). The estimated annual reductions in surface water flows by Le Maitre et al. (2000) were 33 000 Mm^3. Chamier et al. (2012) illustrated that the reductions following alien invasions in the Western Cape and KwaZulu Natal provinces were quantified and showed reductions ranging from 55 % to 82 % respectively (Chamier et al., 2012). Dzikiti et al. (2016) showed that each hectare of land invaded by the invasive *Eucalyptus camaldulensis* along the Berg River used an additional ~ 2 million litres of water per year above that used by the indigenous vegetation growing along the same stretch of river. Accordingly, it was concluded that the restoration of hydrological flows in rivers and water benefits to humans can be achieved by clearing IAPs as this may result in significant reductions of annual ET (Prinsloo and Scott, 1999; Scott *et al.*, 2006; Dzikiti *et al.*, 2013).

Contrary to early studies, a study done by Dzikiti et al. (2017) in the Northern Cape

discovered that the invasive *Prosopis* trees transpired more than five times the water used by the indigenous *Vachellia karroo* at the stand scale. The water use differences were due to the higher plant density by the invasive *Prosopis* trees rather than higher transpiration rates by the individual tree. This was based on the lower sapwood to heartwood ratio in a *Prosopis* tree compared with that of a *V. karroo* (indigenous species) which suggested higher sap flux density in the indigenous species. These results were consistent with findings by Cavaleri and Sack (2010) who emphasized that in some cases indigenous vegetation is likely to use as much water as invasive species. Meaning that the hydrological benefits of clearing IAPs depend on the water use patterns of the replacing species (Cavaleri et al., 2014; Doody and Benyon, 2011; Dye and Jarmain, 2004). Therefore, one must consider the structural and physiological characteristics of both pre-clearing and post-clearing vegetation to predict the net benefits (Dye et al., 2001). Based on this, the reasons for increased water use patterns by IAPs require further investigations to understand whether this detrimental behavior should be expected from all invasions under all environmental conditions. There is a knowledge gap about the differences in water use rates IAPs occurring in different environmental conditions as well as how the environmental conditions affect the water use patterns by indigenous species. This information is important to make informed decisions as to where the restorations will produce higher benefits.

There is evidence that clearing of IAPs results in water salvages, but the quantified volumes of these benefits depend on the water use characteristics of the replacing species after clearing and the location in the landscape (Doody et al., 2011). These efforts are done worldwide to restore invaded systems (Fourie et al., 2013; Rebelo, 2006). In South Africa, the Working for Water Programme was established. However, further research is still needed to support informed decision-making for such programmes, especially in the Cape Floristic Regions (CFRs) where there is still a lack of understanding of the water use patterns and characteristics of these species.

1.5 Significance of the study

The Western Cape Province suffers from the increasing expansion of IAPs such that there is a need for urgent control measures because much of the encroachment is occurring in catchments that are the main sources of the region's water supply (Nel et al., 2013).

Therefore, there is a need for detailed studies to understand how specific IAPs influence a specific catchment's water resources, to make informed decisions on their management. In South Africa, detailed water use data on Australian acacias exists only for *Acacia mearnsii* (black wattle) (Dye and Jarmain, 2004). Little is known about the water use patterns of other acacia species. It is important to investigate and compare water use patterns of other species, such as *Acacia longifolia* to understand how these patterns are influenced by environmental factors and to quantify their impacts on water resources.

The results from this study are essential not only for understanding the hydrological impacts of IAPs but also contributes knowledge of water use patterns by indigenous species that are dominant in the Cape Floristic Region (CFR). The mountains, valleys and coast of the South-Western Cape are the natural habitats of the largest variety of plant species in the world - the Cape Floral Kingdom. This is one of the richest biodiversity biomes globally. However, the integrity of this biome is compromised by IAPs encroachment, associated with high rates of water use. South Africa is a semi-arid country with limited resources. It is therefore essential to manage or minimise the impacts of IAPs on our water resources by informing decision-makers on the sustainable use and management of the resource (Ramoelo et al., 2014).

1.5.1 Research Questions

1. To what extent do clearing activities affect the distribution of IAPs in the Nuwejaars Catchment?
2. How similar or different are transpiration patterns of *A. longifolia* occurring in different topographic positions/elevations?
3. How similar or different are water use rates by *A. longifolia* and indigenous fynbos stands?
4. To what extent do water use patterns of *A. longifolia* affect the variations in soil water and groundwater?
5. At the catchment scale, to what extent do IAPs affect water resources in the Nuwejaars Catchment?

1.5.2 Aim

This study aims to contribute knowledge about water use patterns and catchment-scale hydrological impacts of IAPs existing in semi-arid riparian and non-riparian environments. This study can assist decision-making in programmes that prioritize better management strategies for water resources.

1.5.3 Objectives

1. To determine the spatial distribution of IAPs in the Nuwejaars Catchment.
2. To compare water use rates of *A. longifolia* occurring at different positions/elevations.
3. To determine the impact of tree water use patterns from *A. longifolia* stands on soil water and groundwater variations at different locations.
4. To compare actual evapotranspiration rates of *A. longifolia* and the indigenous fynbos occurring in a similar setting.
5. To estimate the catchment scale impacts of clearing IAPs and/or quantify the potential water savings.

1.6 Thesis layout

This thesis comprises 8 chapters with Chapter 1 presenting the introduction, Chapter 2 is the study area description and research design. Chapters 3 to 7, each cover one of the research objectives. These chapters have been written in scientific journal format with the intention that each of these chapters be submitted for publication. Each chapter includes an introduction, methods, results, discussion, and conclusion. As a result, there are some slight repetitions in the descriptions of sites and methodologies in the results chapters (Chapters 3 to 7). Chapter 8 summarises conclusions made in Chapters 3 to 7, as well as the study recommendations.

Chapter 1 introduces the thesis, highlighting the background, scientific discussions and theories on the topic, as well as the significance of the study.

Chapter 2 describes the study area and research design.

Chapter 3 describes the spatial extent of IAPs in the Nuwejaars Catchment.

Chapter 4 quantifies and compares transpiration rates of *A. longifolia* occurring in different positions in the Nuwejaars Catchment.

Chapter 5 describes the relationships between transpiration patterns of *A. longifolia,* soil water and groundwater dynamics of the selected sites.

Chapter 6 compares actual evapotranspiration rates of *A. longifolia* and the indigenous fynbos stand occurring in a similar setting.

Chapter 7 quantifies the hydrological benefits of clearing *A. longifolia* and restoring the system by reintroducing fynbos.

Chapter 8 highlights the conclusions and recommendations from each chapter.

Chapter 2
Study area description and research designs

2.1 Introduction

The current study uses hydrological methods to investigate the impacts of IAPs on the water resources of the Nuwejaars Catchment. As part of the hydrological study, rates of transpiration from a dominant IAP species were measured at different locations within the Nuwejaars Catchment. To monitor the microclimate of the invaded sites, a network of automatic weather stations was established across the catchment. Furthermore, quantitative soil-water and groundwater monitoring were also conducted to better understand plant-soil-water processes. A comparison was made between the water use rates of fynbos stands and those of A. *longifolia*.

2.2 Study area

The Nuwejaars Catchment covers an area of 760 km^2 in the Cape Agulhas region, in the Western Cape Province of South Africa, and falls within the Breede-Gouritz Water Management Area. The area is commonly known as the southern-most part of Africa, located between the latitudes 34°27` and 34°50` S and longitudes of 19°35` and 20°1` E. The catchment consists of quaternary catchments G50B and C (Figure 2.1).

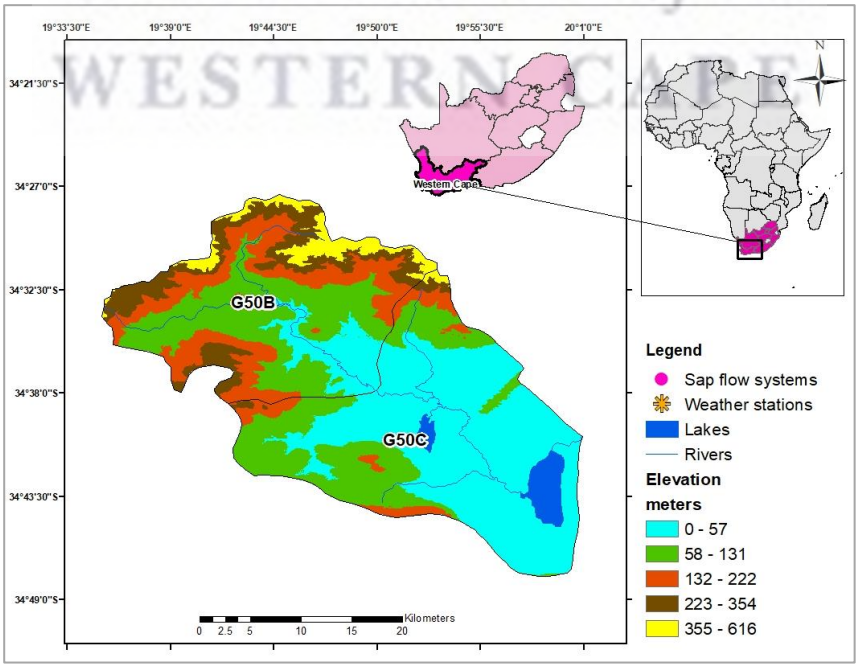

Figure 2.1: Location of the Nuwejaars Catchment.

2.2.1 Climate

The catchment lies within a Mediterranean climatic region, characterized by wet winters from mid-May to late August. The mean annual rainfall over most of the catchment is between 400-600 mm/year, with a mean annual precipitation of 650 mm/year on the mountains that form the northern watershed (Herdien et al., 2010; Kraaij et al., 2017). The dry summers occur from November to March, with maximum mean daily temperatures of 27 °C observed in January. The minimum temperatures occur in July and August (Cape, 2014; Hanekom et al., 2009; Herdien et al., 2010).

2.2.2 Geology and soil types

The geology of the area is very variable, dominated by geological formations of the Malmesbury, Table Mountain, Bokkeveld, Cape Granite Suite and Bredasdorp Groups. The upper catchment is dominated by formations of the Table Mountain Group (TMG) quarzitic sandstones. The Bokkeveld Group, including shale and sandy shales, covers the mid-sections of the catchment, overlaying the basement formations of the Malmesbury Group and Cape Granite, which transitions into calcified dune sands and sedimentary limestones of the Bredasdorp Group towards the lower parts of the catchment (G50C), in which most lakes and wetlands occur (Figure 2.2). The soil textures in the upper part of the catchment are loamy sand and/or sandy loam, and the lower part is mostly sandy.

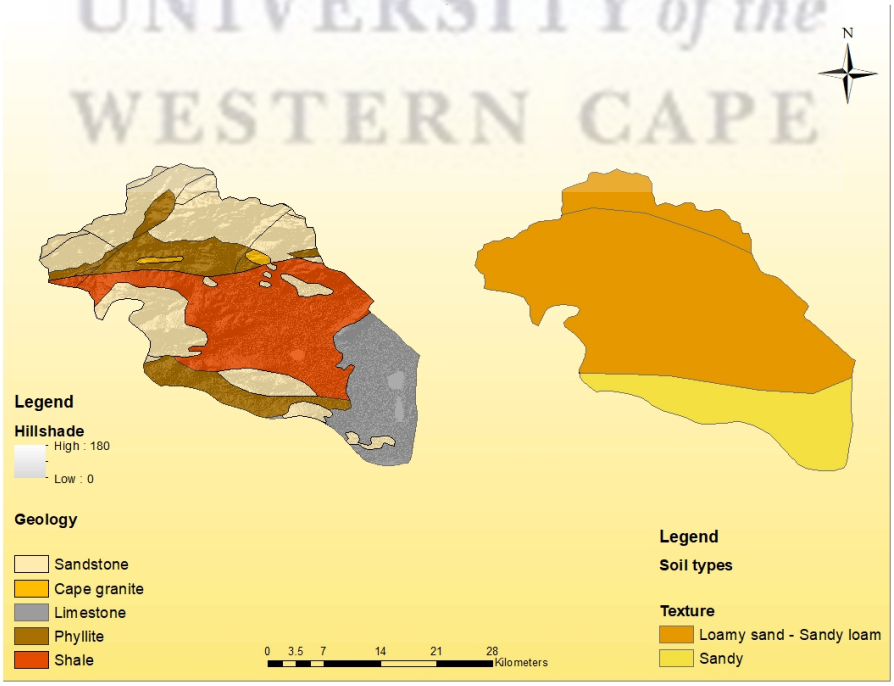

Figure 2.2: The geology (left) and soil types (right) in the Nuwejaars Catchment.

2.2.3 Topography and hydrology

The elevation in the Nuwejaars Catchment varies from 7 to 654 m above sea level. The mountainous areas cover the north-west, northern, and northern eastern parts of the catchment with altitudes ranging from 200 to 600 m above sea level. The elevation decreases sharply to less than 100 m after about 10 km along the main river, followed by lowlands that are 10–60m above sea level (Mkunyana et al., 2019). The flatter area of the catchment has numerous wetlands in the form of pans, lakes, and floodplains (Figure 2.3). Lowlands with altitudes less than 40 m occupy 35% of the catchment area, mid-slope (41 – 100 m) 27%, and uplands (>100 m) 38% (Mazvimavi et al., 2021).

The wetlands, pans, and lakes provide diverse habitats, resulting in this area having high biodiversity. The main river, Nuwejaars, is fed by Koue and Jan Swartskraal tributaries (Figure 2.3). A floodplain wetland which is about 22 km long and has a width of up to 1.5 km occurs along the Nuwejaars River between Elim and Soetendals vlei which is one of the major lakes in this catchment (3 km wide and 8 km long). The Nuwejaars River flows into the Soetendalsvlei which drains into the 18 km Heuningnes River, which then discharges into the Indian Ocean (Mazvimavi, 2018).

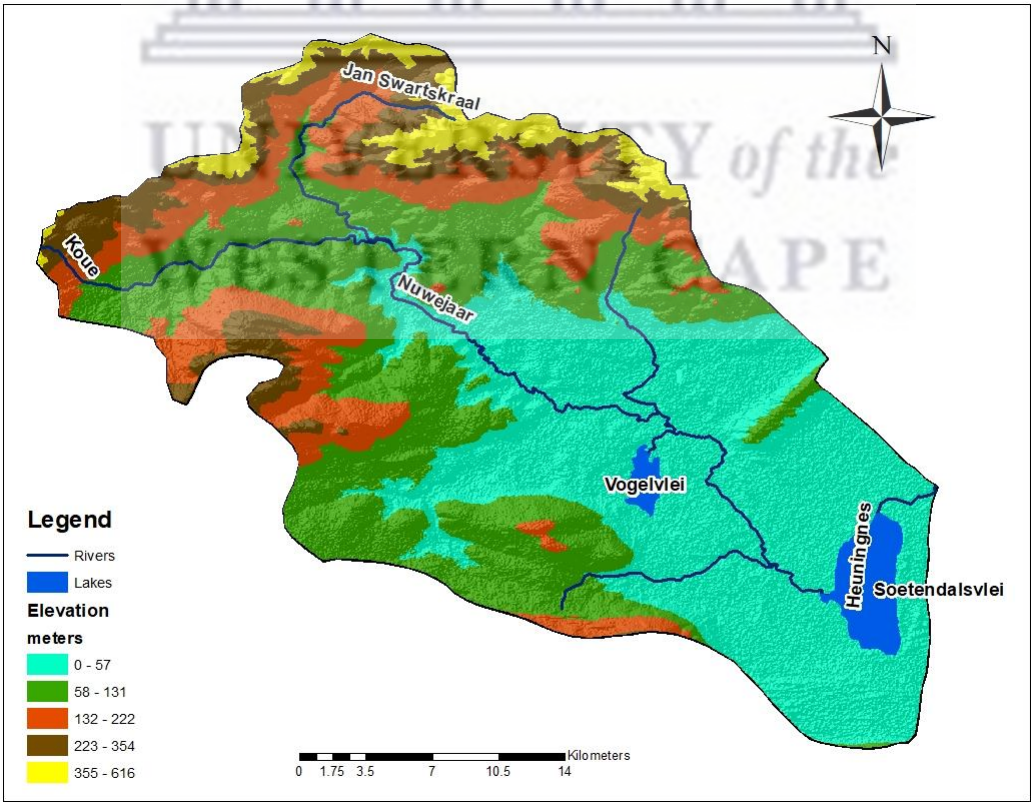

Figure 2.3:Elevations and water bodies in the Nuwejaars Catchment.

2.2.4 Vegetation

The Nuwejaars Catchment hosts more than 1 750 indigenous plant species (Nowell and Esler, 2011). The indigenous vegetation is mainly fynbos, which is a sclerophyllous shrub-dominated vegetation characterized by species of the *Proteaceae*, *Ericaceae* and *Restionaceae* families, typical of the Cape Floral Region or CFR (Scott, 1999; Mucina and Rutherford, 2006). Several sub-types of fynbos have been described: Mountain Fynbos, Proteoid Fynbos, Restioid Fynbos and Asteraceous Fynbos (ODM, 2004; Fourie *et al.,* 2013). The Mountain Fynbos occurs on shallow, sandy, acidic soils, most of which are derived from sandstones of the TMG and are highly infertile. The Mountain Fynbos is found extensively in moist areas on the steep south-facing slopes of the mountains and occurs in small patches on seaward-facing coastal slopes. Renosterveld is another shrub-dominated vegetation type of the CFR, which occurs in thin, but more fertile soils associated with shale. Renosterveld is mostly found in the lower central parts of the catchment, where agriculture also takes place. The low-lying areas are also dominated by Restiod Fynbos, these are tall reeds that are closely associated with vleis and may be flooded during the winter season. These are mostly found along the coast and east of Soetendalsvlei. The southernmost part of the catchment has the Overberg Dune Strandveld and the Cape seashore vegetation, are found along the coast. In the floodplains, sedges, reeds, and restios are common, with grasses being more dominant on drier land (Figure 2.4).

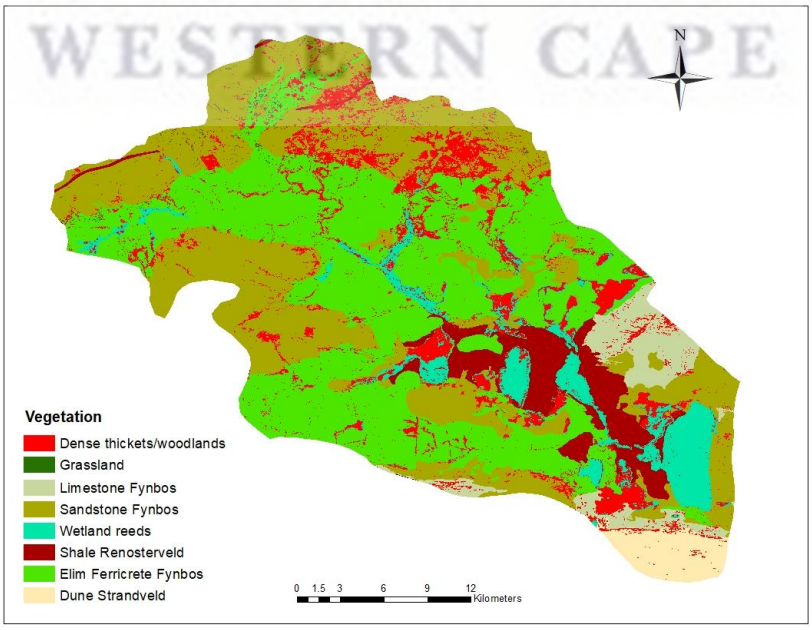

Figure 2.4: Types of vegetation in the Nuwejaars Catchment.

2.2.5 Land use and land cover.

Fynbos is the dominant landcover in the Nuwejaars Catchment, followed by cultivated lands (39 %) (Herdien et al., 2010; Mazvimavi et al., 2018). For the purpose of land use and land cover mapping, renosteveld has been lumped with fynbos. Agricultural activities taking place in the catchment include commercial dryland crop production (wheat, barley, etc.), sheep and cattle production, irrigated vineyards and orchards, and commercial forestry. These cultivated lands mostly occur on the mountainous and south-east coastal parts of the catchment (Figure 2.5). According to the National Invasive Alien Plant Survey done by Kotzé et al. (2010), IAPs covered 35% of the Nuwejaars Catchment. The dense bushes in the catchments are mostly formed by IAPs. Dense IAP thickets occur more on the mountainous part and stretch along rivers down to the lowlands. Bare surfaces in the map (Figure 2.5) represent exposed rock on mountain cliffs and peaks.

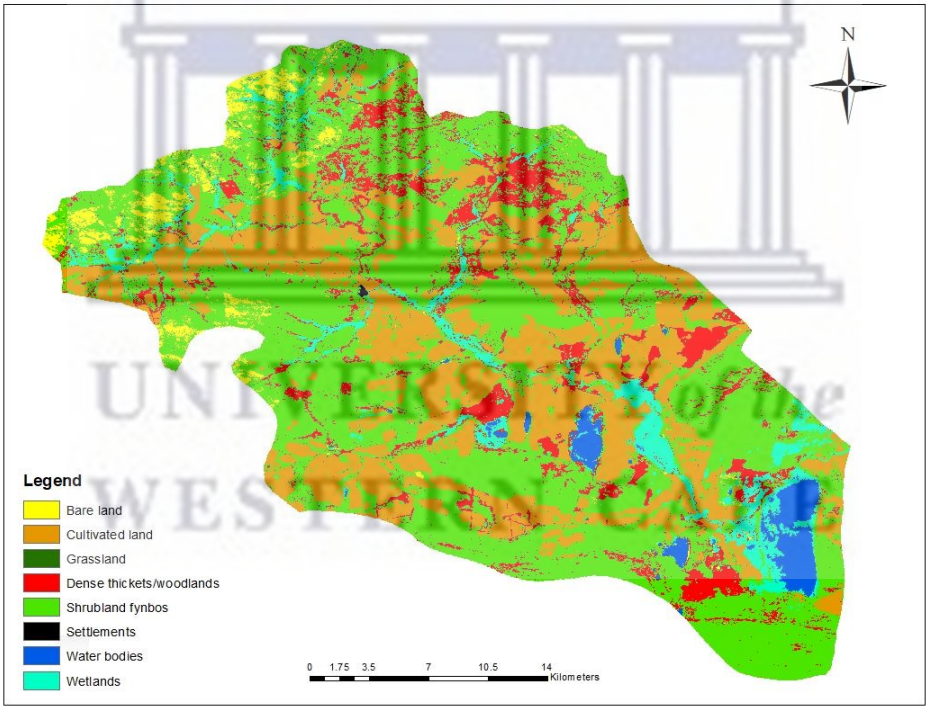

Figure 2.5: Land uses and land covers in the Nuwejaars Catchment.

2.3 Study sites

To investigate the impact of IAPs on the water resources of Nuwejaars Catchment, sap flow (transpiration) rates, soil water content (SWC), groundwater fluctuations, and evapotranspiration rates were monitored. The selection of sites and experimental setups

will be outlined in this chapter since they are relevant to all objectives; however, specific methods for each objective will be described in other chapters. Since most of the land in this catchment is privately owned, permission was sought from the respective landowner to install and regularly monitor the sites.

2.3.1 Selection of study sites

Several invaded sites were evaluated with the assistance of the coordinator of the IAP clearing programme run by the Nuwejaars Wetland Special Management Area forum. The objective of the site visit was to identify (i) the dominant invader in the catchment, and (ii) the highest elevation that these invasions occupied. Previously, Mkunyana et al. (2019), identified *Acacia longifolia* as a dominant invader on riparian and non-riparian sites. Two of the monitoring sites used in the current study were previously identified and used in a study by Mkunyana et al. (2019), namely Moddervlei and Spanjaardskloof. To quantify transpiration along a topographic gradient, two more sites were added i.e., Jan Swartskraal and Sandfontein. A total of four sites monitored transpiration by *A. longifolia*. The selection criteria for these sites were in areas that are:

(i) invaded by *Acacia longifolia* trees.
(ii) easily accessible for routine monitoring.
(iii) safe to keep equipment and avoid vandalism.

The hillslope sites are (a) an upland non-riparian site at Sandfontein, and (b) a mid-slope non-riparian site at Spanjaardkloof which is located on the southern hillslope of the Bredasdorp hills. The riparian sites included the lowland riparian Moddervlei (along the Nuwejaars River) and the mid-slope riparian at Jan Swartskaal which is one of the tributaries that discharges into the Nuwejaars River (Figure 2.6).

To quantify the implications of IAPs on water resources, water use rates by fynbos were also monitored using an eddy covariance system. The selection criteria used to select the site were:

(i) uniform/homogenous indigenous vegetation.
(ii) locally representative vegetation.
(iii) relatively flat terrain.

(iv) away from electrical poles to avoid the electric current.

(v) easy access for transport of heavy field equipment (close to a road)

A suitable site was identified at Tussenberge. The site was also advantageous as it was part of an ongoing hydrological monitoring project. This site had a weather station and boreholes for microclimate and groundwater monitoring, and therefore provided a good case study to investigate the water use patterns of fynbos (Figure 2.6).

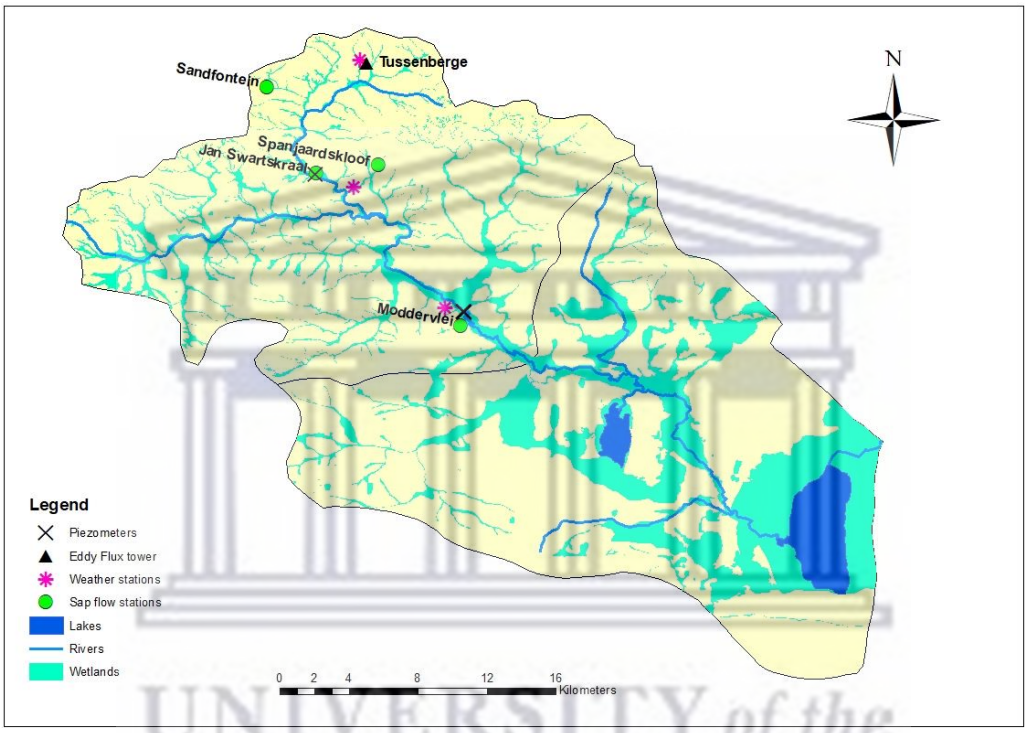

Figure 2.6: Selected study sites in the Nuwejaars Catchment.

2.3.2 Monitoring period.

Transpiration rates by *A. longifolia* were the main variable in this study. The monitoring period of transpiration was from October 2018 until November 2021. This period was selected to cover more than one wet and dry season to be able to estimate annual rates. This was decided based on previous experiences with sap flow systems that are sometimes faulty and thus cause gaps in the data, resulting in the misrepresentation of seasonality. The eddy flux tower was installed in August 2019. Seasonal variations of actual evapotranspiration (AET) by fynbos were also important for comparison with water use rates by *A. longifolia*. Therefore, it was important that the transpiration monitoring overlaps with the monitoring of AET by fynbos.

2.4 Instrumentation and data collection

To quantify transpiration rates from *A. longifolia* at different locations, sap flow data was collected hourly from three to four selected trees at each of the four sites listed above.

Close to the sap flow monitoring stations, the variation of soil water content (SWC) was monitored using soil water probes, data was also collected hourly to overlap with sap flow monitoring. Field visit and routine downloading of data from these stations were done every two weeks from October 2018 to November 2021, to check and change batteries. Weather data were collected to monitor the microclimate of the sites using the automatic weather stations established across the sites. Groundwater levels were monitored hourly from a network of boreholes and piezometers across the study area. Hourly AET rates from fynbos at the Tussenberge site were measured using the eddy covariance system. High-frequency data from the flux tower was downloaded monthly from the microSD card to avoid data being overwritten. The experimental set-up for each site is explained in detail below:

2.4.1 Moddervlei

This is a lowland riparian site located on a wetland floodplain. The site is approximately 20 m from the Nuwejaars River, with an elevation of 25 m above sea level. At Moddervlei, four *Acacia longifolia* trees were selected for sap flow measurement. Soil water sensors were installed at 25 cm intervals from 10 to 100 cm depth below the surface. Three piezometers with a depth of 3 meters were installed along a transect at distances of 3, 15, and 20 m from the river channel. The site has a nest of 5 monitoring boreholes with depths ranging from 8, 20 and 50 m located at about 50 m from instrumented trees. An automatic weather station was established ~100 m outside the *Acacia longifolia* stand (Figure 2.7).

Figure 2.7: Moddervlei's monitoring set-up. Soil water sensors were in proximity to the sap flow (Source: Google Earth Image of 6th February 2021).

2.4.2 Jan Swartskraal

This is a mid-slope riparian site located at ~10 m from the Jan Swartskraal River. The elevation of the site is approximately 67 m above sea level. Three *Acacia longifolia* trees were selected to measure sap flow. Soil water sensors were also installed at 20 cm intervals from 10 to 90 cm depth below the surface. Water table fluctuations were monitored by a piezometer ~ 2 m from the river channel. Two monitoring boreholes were located ~30 m from the instrumented trees (Figure 2.8). An automatic weather station located about 2 km away (at Spanjaardskloof) was used to monitor relevant weather parameters.

Figure 2.8: Jan Swartskraal's monitoring set-up. Soil water sensors were in proximity to the sap flow system (Source: Google Earth Image of 6th February 2021).

2.4.3 Spanjaardskloof

This is a non-riparian hillslope site located on the southern slopes of the Bredasdorp Hills (Figure 2.9). The elevation of the site is 145 m above sea level. Sap flows were monitored for three selected *A. longifolia* trees. SWC variations were also monitored at 20 cm intervals from 10 – 90 cm below the surface. There are two monitoring boreholes with depths of 20 and 60 m at ~ 30 m from the instrumented trees. Weather conditions were monitored from an automatic weather station located at an elevation of 85 m.a.s.l. was 1.6 km from the sap flow monitoring site.

Figure 2.9: Spanjaardskloof's monitoring set-up. Soil water sensors were in proximity to the sap flow system (Source: Google Earth Image of 15th January 2021).

2.4.4 Sandfontein

This is a non-riparian, upland hillslope site located at an elevation of 228 m.a.s.l. and is 58 m from a small headwater stream (Figure 2.10). The selected tree stand is outside the riparian zone on sloping ground with a gradient of 0.10. Based on the assessment done during site selection, this site represents the highest elevation at which *A. longifolia* trees occur within the Nuwejaars Catchment. Sap flows were monitored on four selected trees. Variations in SWC were monitored from 10 – 40 cm below the surface. An unconsolidated material was observed below 40 to 100 cm depth, where solid bedrock was observed. A soil water sensor was installed vertically into a hole in the bedrock at a depth of 100 cm. Two monitoring boreholes, 11 and 50 m deep were drilled ~15 m from the instrumented trees. The Tussenberge automatic weather station which is 4.8 km away and at an elevation of 230 m was used to determine the weather conditions at this site.

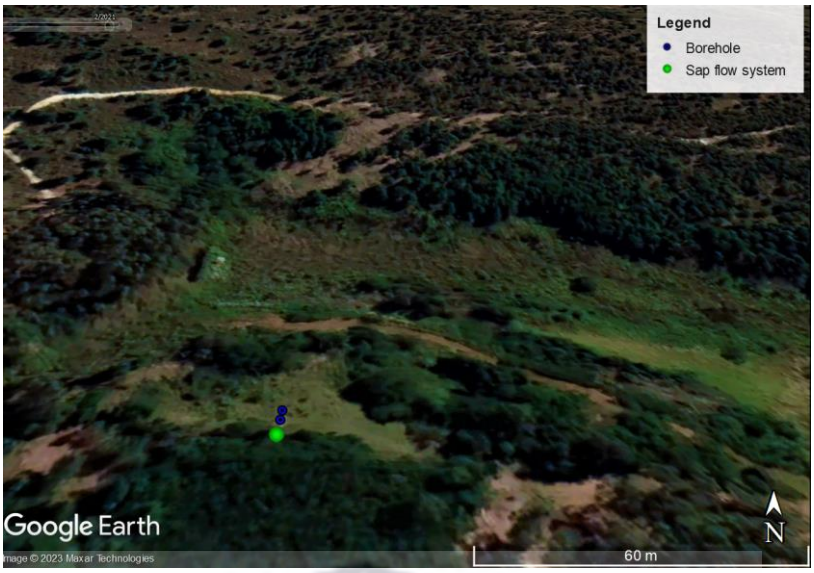

Figure 2.10: Sandfontein's monitoring set-up. Soil water sensors were in proximity to the sap flow system (Source: Google Earth Image of 6th February 2021).

2.4.5 Tussenberge

This site is mostly dominated by indigenous fynbos shrubs (dominated by proteas, erica, and restios). The elevation of the site is 230 m above sea level, and the gradient is about 0.10. An eddy covariance system was installed to monitor actual evapotranspiration (AET) rates. An automatic weather station was also installed 300 m away from the flux tower to monitor weather conditions. Three monitoring boreholes at a distance of ~ 250 m southeast of the flux tower were drilled and have depths of 12, 30 and 50 m (Figure 2.11).

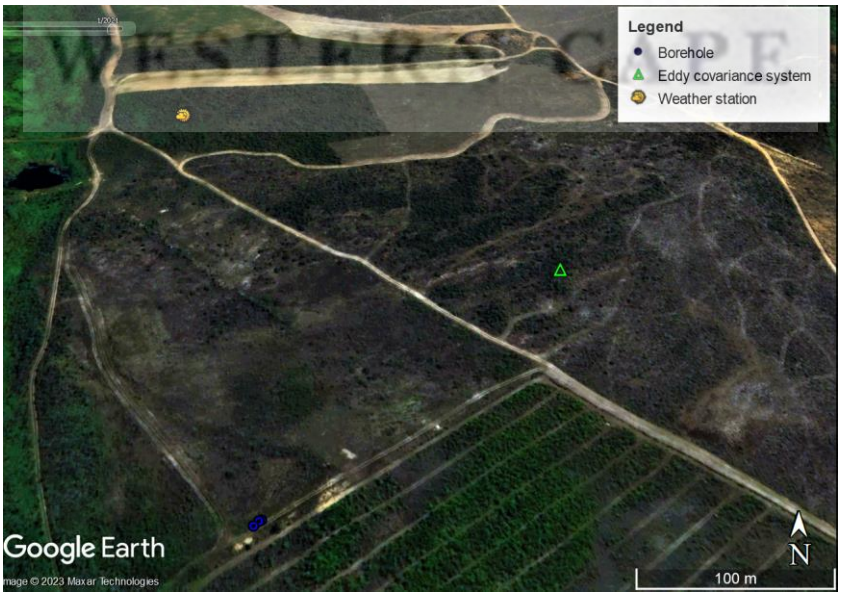

Figure 2.11: Tussenberge's experimental set-up (Source: Google Earth Image of 15th January 2021).

Chapter 3
The spatial extent of IAPs in the Nuwejaars Catchment

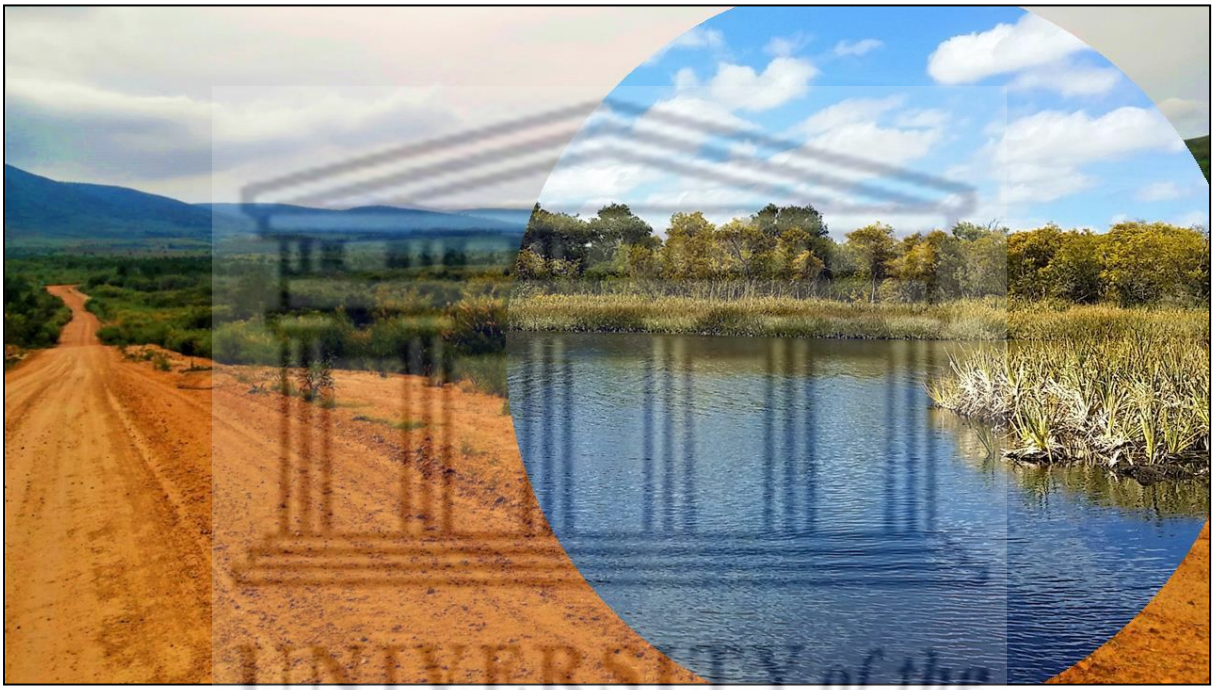

IAPs along hillslopes and on riparian areas in the Nuwejaars Catchment.

Parts of this chapter were published as:

Mtengwana B., Dube T., **Mkunyana Y.P**., and Mazvimavi D. (2020) 'Use of multispectral satellite datasets to improve ecological understanding of the distribution of Invasive Alien Plants in a water-limited catchment, South Africa', *African Journal of Ecology*, 58(4), pp. 709–718. Available at: https://doi.org/10.1111/aje.12751.

3.1 Introduction

Land cover changes over time occur mainly due to urbanization, agricultural practices, and invasion by alien plants (Rouget et al., 2003). IAPs are plants that survive and rapidly expand outside their native distributional range (van Wilgen et al., 2012, 2004). These plants are introduced into the ecosystem either deliberately as commercial or ornamental garden plants, or accidentally (Enright, 2000). Accidental introductions occur when species are dispersed by seed pollution, human transport, wind, or birds into new geographical regions (Enright, 2000; van Wilgen et al., 2012). Due to inadequate control, these species have spread into natural ecosystems, thus being considered invasive (Enright, 2000). Their impacts include habitat loss, ecosystem changes, and disruption of hydrological processes.

The diversity, abundance, and impacts of alien plants on natural systems cause global ecological and economic problems, especially in semi-arid countries (Blanchard and Holmes, 2008; Wilson et al., 2014). Globally, IAPs have been reported to threaten biological diversity by eroding gene pools and thus resulting in the extinction of endemic species, especially in freshwater ecosystems (Rai and Singh, 2020). In hydrology, their impacts include increased evapotranspiration rates compared to indigenous species, reductions of stream flows (Prinsloo and Scott, 1999), and lowering of groundwater levels (Dzikiti et al., 2013; Fourie et al., n.d., 2013; Scott and Le Maitre, 1998). They can alter soil properties and expand into grazing lands (Ndhlovu et al., 2011), which may consequently change soil productivity. In semi-arid countries such as South Africa, the monitoring of the distribution of IAPs is an important consideration for the management of catchments for water security (Preston et al., 2018).

This chapter aims to map the extent and distribution of IAPs and landcover changes in the Nuwejaars Catchment. The Nuwejaars Catchment is among the heavily invaded catchments in the Western Cape Province. This catchment was also identified as a biodiversity hotspot, hosting various indigenous species and thus falls under the Cape Floristic Region (CFR). The CFR is the most invaded terrestrial area in South Africa (Wilson et al., 2014) because of the natural fire regime that creates opportunities for the establishment and proliferation of woody plants. The effectiveness of clearing programmes in these regions requires knowledge about the spatial distribution of IAPs.

Pines, eucalypts, and acacias are among the common species that have become invasive in many parts of the world where they are not indigenous, and this is particularly the case in South Africa (Chamier et al., 2012; Sebinasi Dzikiti et al., 2013; Meijninger and Jarmain, 2014). The invasive acacia species are native to Australia and have been widely distributed for over a century in many parts of the world (Le Maitre et al., 2011). Alien species from Australia reproduce quite rapidly in South Africa, due to similar climatic conditions. The invaded areas in the Nuwejaars Catchment are dominated by Australian *Acacia longifolia*.

To prevent the spread of IAPs, the South African Department of Water and Sanitation established a clearing strategy through organizations, such as the Working for Water (WfW) programme, local municipalities and property owners in areas where benefits, such as increased surface runoff and groundwater recharge will be maximised (Meijninger and Jarmain, 2014). The objective of clearing is to enhance and prioritise the removal of alien species occurring in water-sensitive areas to save water and create employment in the process (van Wilgen et al., 2004). The Nuwejaars Wetland Special Management Area forum started clearing IAPs in 2009. Clearing and managing IAPs should ideally operate at a landscape scale and therefore require up-to-date information on the land cover to make informed and appropriate resource management decisions. This is particularly true given that IAPs spatial distribution and cover can change rapidly, within time scales as short as one year, impacting management decisions (Nowell and Esler, 2011).

Mapping of these IAP distributions can also be applied to spatial conservation plans (Rouget et al., 2013). This emphasizes the need to map the spatial extent and distribution of IAPs routinely over time. Unfortunately, invasion maps are typically not updated at appropriate time intervals and spatial scales to inform management. National surveys of the spatial distribution have been undertaken, for example, the Southern African Plant Invaders Atlas, SAPIA (Henderson and Wilson, 2017), and the National Invasive Alien Plant Survey, NIAPS (Kotzé and Beukes, 2010). These are the most comprehensive IAP maps available in South Africa, however, they were mapped at a very coarse scale (27.78 km^2), designed for use at a tertiary catchment level (Kotzé and Beukes, 2010), while local management and planning would need information about locations and coverage at a sub-quaternary level (van Wilgen et al., 2004). Furthermore, these surveys were

undertaken after 10 years, with NIAPS data reflecting 2007 and 2008 conditions, and do not provide information necessary for implementing effective clearing on an annual basis (Kotzé et al., 2010). Thus, what is lacking is a sub-quaternary catchment scale time series mapping that can provide reliable data on the abundance and distribution of IAPs in a catchment (Preston et al., 2018). This information is important not only for identifying areas to prioritize for clearing, but, if this is done for an area where clearing efforts have already commenced, time series mapping can assist in identifying the successes of failures of the clearing initiative taking place in a catchment. This is the case for the Nuwejaars Catchment.

The availability of remote sensing data bridges the time interval gaps of mapping IAPs on a larger scale. Remote sensing imagery in combination with Global Positioning System (GPS) and Geographic Information System (GIS) technologies can provide a platform on which to base sound decisions and IAP management strategies (Rogan and Miller, 2006). A recent study by Holden et al. (2021) provided an accurate and up-to-date understanding of the occurrence and density of invasive alien trees in an important water tower for the southwestern Cape of South Africa at a 20 m resolution. Holden et al. (2021) stated that there is an urgent need to integrate technology and research advances into invasive alien plant management and decision-making. The results from this study showed the importance of using a transdisciplinary approach including the freely available satellite imagery (Sentinel-1 and -2) and Google Earth Engine (GEE) processing power for mapping IAPs in the water towers of South Africa. Holden et al. (2021) highlighted that due to high spatial resolutions, drone technology improved the mapping process and outputs by managers and decision-makers.

A study by Mtengwana et al. (2020) evaluated the feasibility of determining the spatial distribution of IAPs in the Nuwejaars Catchment using images from Landsat 8 and Sentinel 2. The improved spatial resolution and the presence of the red-edge bands in Sentinel-2 (S2), demonstrated more potential in the discrimination of vegetation species. Pixels in the imagery from both sources were classified into land cover types using a supervised classification maximum likelihood approach based on the same set of ground-truthed training sites. The classification method applied to Landsat 8 (LT8) data was not able to detect small patches of IAPs within the catchment but also resulted in somewhat greater coverage estimates than when using S2 data. However, Mtengwana et al. (2020)

showed that both the LT8 and S2 classifications resulted in similar distribution patterns for the invaded areas, demonstrating the capability of both satellites for use in detecting the IAPs and other cover classes of interest within the catchment, despite the slight differences in the classification accuracies. Both satellite data sets provide the time scale and spatial complementarity required for ecological monitoring (Mtengwana et al., 2020).

The availability of large volumes of free Landsat imagery since 1972 motivated the use of Landsat images in the current study compared to Sentinel 2 which was launched in June 2015. The benefit of using Landsat time series imagery enables the provision of baseline conditions important for determining changes in the distribution of IAPs in the Nuwejaars Catchment before and after the clearing activities.

3.2 Methods and materials

3.2.1 Study area

The study was conducted in the Nuwejaars Catchment. The catchment's description and location are explained in chapter 2.

3.2.2 Ground truthing data

Ground truthing points were collected using a handheld Geographical Positioning System (GPS) with less than 5% error during August 2018, which coincided with the flowering period for most IAPs. Three hundred and sixty-five ground truth points representing different land cover types were identified and recorded. The observed classes were water bodies, IAPs (mostly dominated by *Acacia longifolia*), cultivated lands, and fynbos shrublands. These points were used during classification and overall accuracy assessment. Additional training data points based on local knowledge were collected using Google Earth to improve the classification of each image. The historical images from Google Earth matched the years that Landsat had available images.

3.2.3 Remote sensing data and analysis

Using the recently introduced cloud computing platform, Google Earth Engine (GEE). Landsat images were obtained from the online USGS earth observation database: http://earthexplorer.usgs.gov using the image collection function in GEE.

Landsat scenes (Path 174/Row 84) that covered the study area were obtained for the periods 1973 – 2021. All the images were filtered by catchment area (region of interest, ROI), dates, and selecting imagery with minimal cloud cover (Table 3.1). Cloud cover was high in 1996 and 2006 images, but the percentage of clouds over land pixels in a scene was less than 2%, which minimized misclassification risks.

Table 3.1: The characteristics of the Landsat images used in this study.

Description	Date	Number of bands	Resolution	Scene cloud cover (%)	Land cloud cover (%)
Landsat 01	1973/09/09	4	80 m	1	1
Landsat 05	1996/11/10	7	30 m	11	0
Landsat 05	2006/11/14	7	30 m	23	1
Landsat 08	2015/12/17	11	30 m	0.1	0
Landsat 08	2020/11/12	11	30 m	0.4	0.4
Landsat 08	2021/07/10	11	30 m	0.9	0.3

i. Classification

The collected ground truthing points were imported on GEE for training sites. Moreover, a drawing tool on GEE was used to supplement the training data in all the images by selecting regions of interest (ROIs). In supervised classification, the training dataset with known labels is used to guide a mathematical classifier in labelling the spectral space in the image composite (Figure 3.1). The study area was then classified into four categories: water bodies, IAPs, cultivated lands, and fynbos using maximum likelihood classifier (MLC) to derive a landcover thematic map from each Landsat image of the study area. The classified images were exported as raster and used in ArcMap for further analysis.

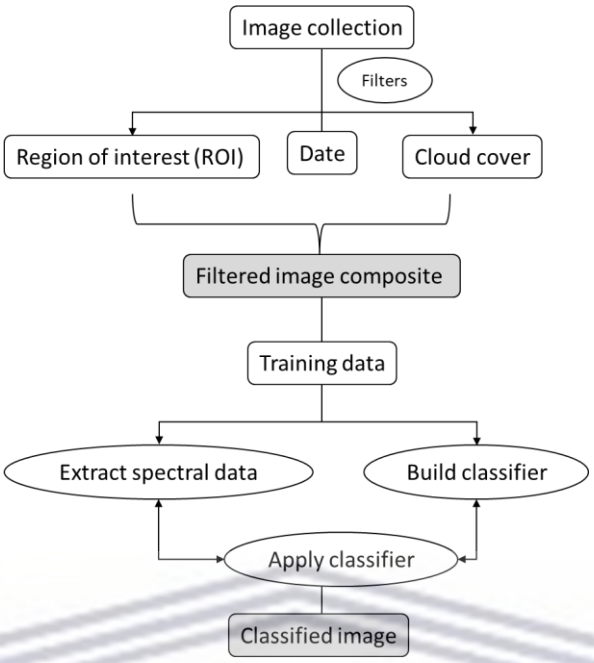

Figure 3.1: Steps undertaken on Google Earth Engine (GEE) to produce land-use/landcover maps. The functions used in GEE are shown by oval shapes and the shaded squares show images produced.

ii. Validation

Validation was done using an error/confusion matrix which contains information about actual (ground truth) and predicted classes done by a classification process. This means that the pixels that had been categorized from the satellite image were compared to the same site in the field. Change detection analysis was also performed to determine the spatial extent of different land cover types between the years.

The vegetation density in the catchment was analysed using the Normalised Difference Vegetation Index (NDVI). NDVI is the most common measure of vegetation cover in remote sensing (Nowell, 2011). It uses red (R) and near-infrared (NIR) spectral bands.

$$NDVI = \frac{NIR-R}{NIR+R} \qquad (3.1)$$

NDVI values range between -1 and +1. Positive values indicate greener vegetated areas, and a value closer to +1 indicates vegetation with higher water content and a higher rate of photosynthesis. Negative NDVI values are characteristic of non-vegetated areas such as water or bare land.

3.3 Results

3.3.1 Classification accuracy assessment

Compared to the earlier remote sensing images, the 2015 - 2021 images had better user and producer accuracy across all land use/landcover classes (Figure 3.2). It shows that Landsat8 images have improved in landcover/land use accuracy. Overall accuracy increased from 60% in 1973 to 82 % in 2021, with the highest overall accuracy of 97 % in 2020. Using Landsat 8 images, the user's accuracy for IAP and fynbos land covers was over 90% (Figure 3.3). Therefore, the catchment scale land-use / landcover distributions are reliable and can be used for further analysis.

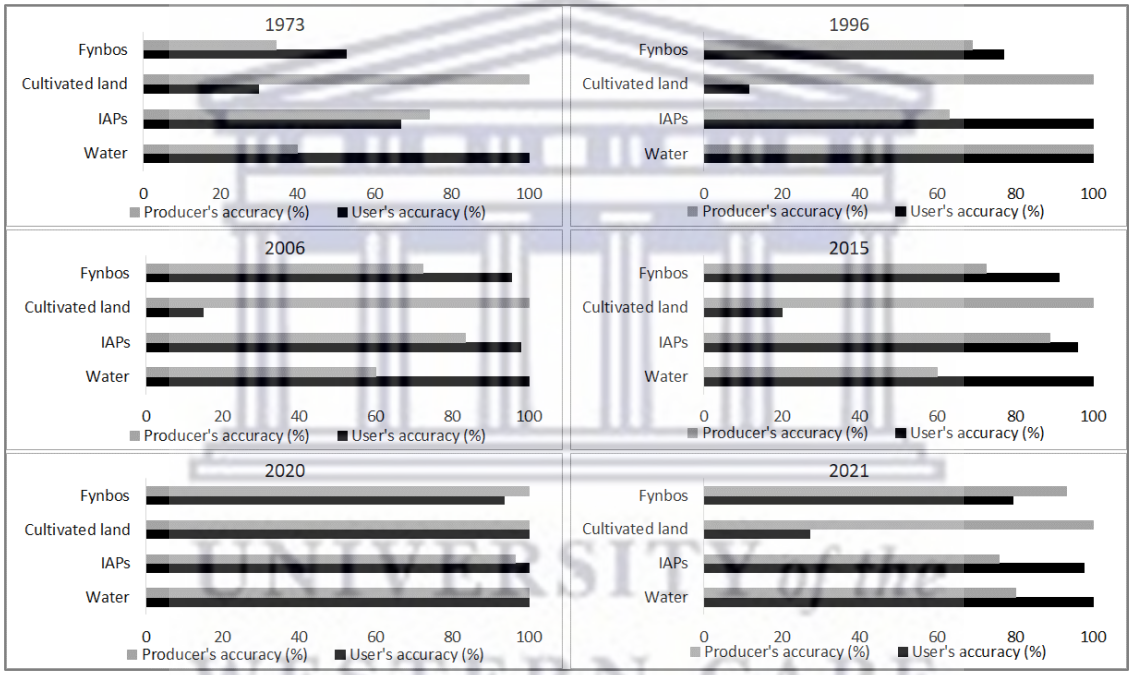

Figure 3.2: Producer and User's accuracies of the classified images.

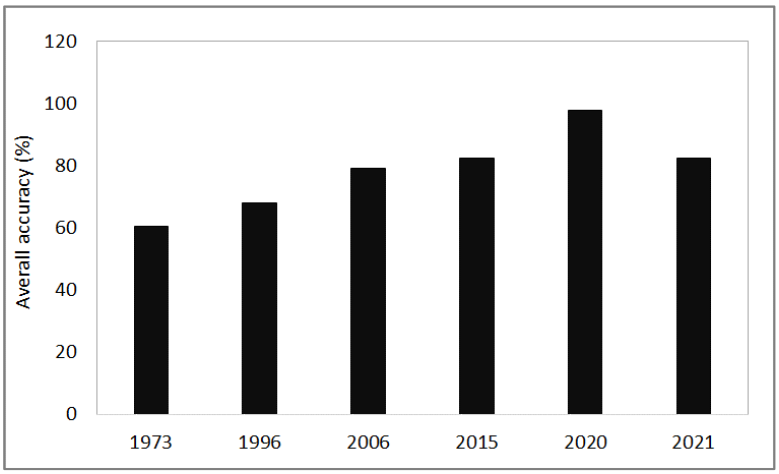

Figure 3.3: Overall accuracies of the classified images.

3.3.2 The spatial extent of land-use/landcover types in the Nuwejaars Catchment

Between 1973 and 2020, cultivation has become the most dominant land use activity in the catchment (Figure 3.4), Since 1973, the area covered by fynbos shrubs has decreased by 5%. Most of the northern headwaters and riparian zones are occupied by IAPS. A decrease in the spatial extent of IAPs has been observed between 1973 and 2021, from 25 % to 11 % of the catchment area (Figure 3.5).

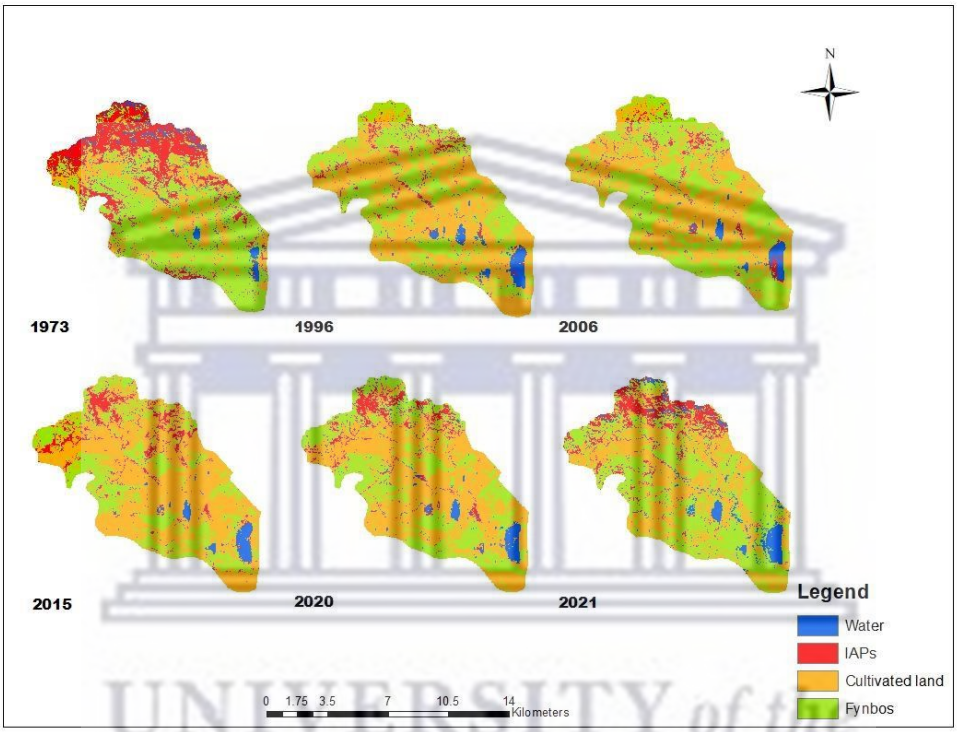

Figure 3.4: Land use/landcover from 1973 – 2020 in the Nuwejaars Catchment.

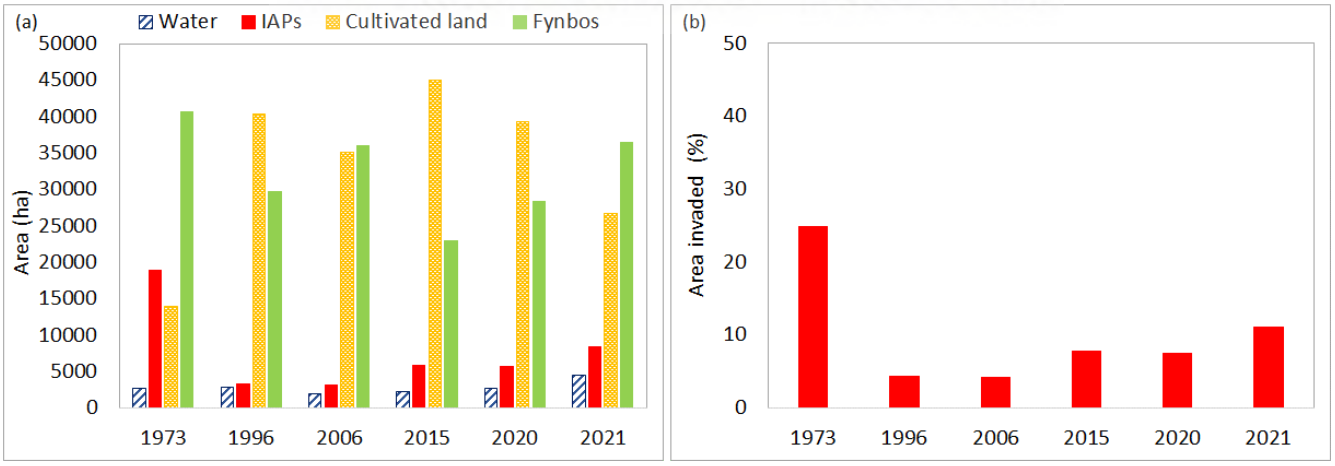

Figure 3.5: (a) Area covered by each land-use/landcover from 1973-2020, (b) total area invaded by IAPs in the Nuwejaars Catchment.

IAPs are confined to mountainous parts and the riparian zones of the Nuwejaars Catchment. These were seen to be areas with relatively high NDVI during the dry season, in December 2018 and November 2020 (Figure 3.6). The IAPs found in the Nuwejaars Catchment such as the dominant *Acacia longifolia* are evergreen, hence the high NDVI in locations they occur. High NDVI indicates the plants are actively growing and consuming water. This has the potential to affect both groundwater and surface water in both riparian and non-riparian zones. Images taken in July 2019/2021 illustrate the recovery of the Nuwejaars Catchment from the drought experienced in the Western Cape during 2017/2018 (Figure 3.6), as the water indices were more prominent during July 2021 showing refilling of wetlands and water bodies.

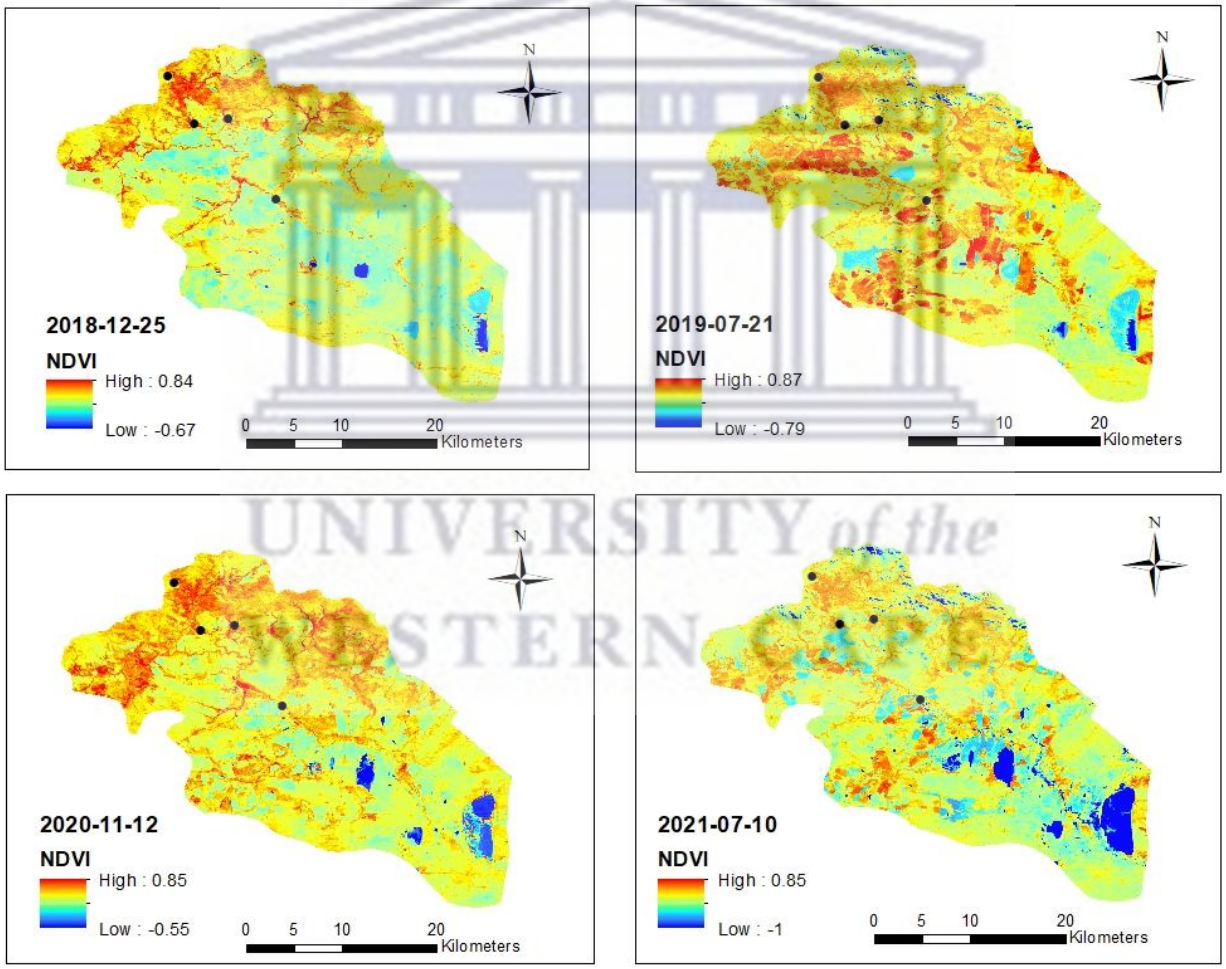

Figure 3.6: Normalised Difference Index (NDVI) in the Nuwejaars Catchment (source: Landsat 8).

3.4 Discussion and conclusion

Cultivation and fynbos shrubs are the dominant land covers in the Nuwejaars Catchment.

However, significant areas in the headwaters and along the riparian zones have been dominated by IAPs. Generally, the headwaters receive slightly higher rainfall than other parts of the catchment. The deep sandy soils and shallow water tables have also encouraged the invasion of riparian areas.

As a way of controlling and reducing the negative impacts of IAPs in invaded ecosystems country wide (Le Maitre et al., 2011), the national "Working for Water" programme was established in 1995. Local farmers and landowners also made efforts by establishing the Wetland Special Management Area forum in the Nuwejaars Catchment which began clearing IAPs in 2009, likely contributing to the observed decline in IAP cover from an estimated 25 % of the catchment in 1973 down to coverage of 11 % or less, maintained between 1996 and 2021.

The improved accuracy of Landsat 8 images in this study confirms that the use of Landsat is the better option to improve the knowledge of IAP coverage, compared to the NIAPS taken every 10 years at a very coarse scale (Kotzé and Beukes, 2010; van Wilgen et al., 2004). Although the distribution of IAPs showed a decline between 1973 and 1996, the geographic spread and proliferation of IAPs in the Nuwejaars Catchment have increased between 2006 and 2021 and have been predicted to increase further due to climate change effects. Future climate predictions for this area are characterized by reduced rainfall and increased temperatures (Mtengwana et al., 2021). IAPs have broad environmental tolerance, and increased temperatures facilitate and increase invasions by accelerating physiological processes and plant growth (Chen et al., 2017). Mtengwana et al. (2021) showed that riparian zones, low-lying areas, and indigenous shrublands are the most vulnerable areas for invasions and should be prioritized in management efforts to reduce the impacts on biodiversity and water losses through increased evapotranspiration. The NDVI results show that areas that invaded areas generally had the highest NDVI in the landscape during the dry season, which indicates the plants are actively growing and consuming water at this time. These patterns were in line with findings from previous studies that IAPs tend to use more water than indigenous vegetation (Calder and Dye, 2001; Dye et al., 2001; Everson, 2016; Gush, 2018; Scott-Shaw et al., 2017). The result from this study suggests that IAPs were able to access water despite the dry conditions during 2018.

Chapter 4

Comparing transpiration patterns of selected A. longifolia stands occurring on different topographic positions.

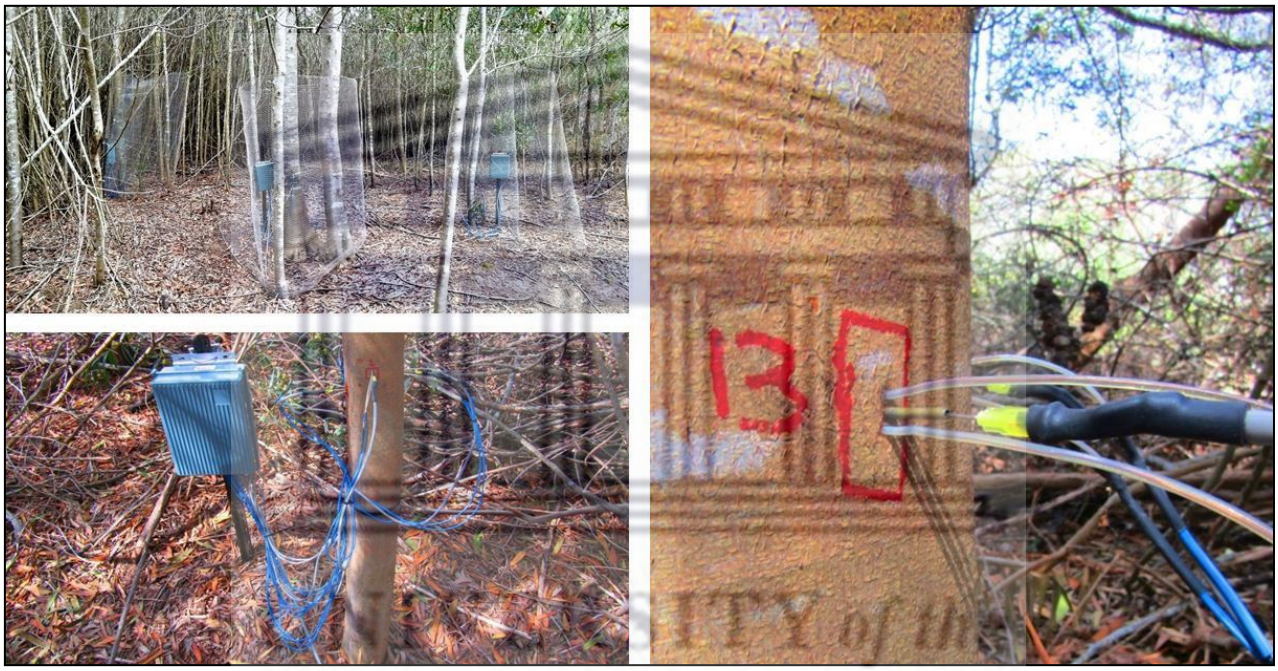

The Heat Pulse Velocity (HPV) sap flow system.

4.1 Introduction

Evapotranspiration (*ET*) is often not well quantified, despite being an important variable in understanding eco-hydrological systems. Globally average *ET* is estimated to be about 67% of the precipitation (*P*) (Zhang et al., 2016), while in dry regions is as high as 95% (Pilgrim et al., 1988). The relative importance of the different components of *ET* varies in different regions depending on the biophysical and anthropogenic characteristics (Zhang et al., 2016). At a global scale, it is estimated that transpiration (*Tr*) makes up 65 % of ET, 25 % is from soil water evaporation (*Es*), and 10 % is the evaporation of water intercepted by plant canopies (*I*) (Schlesinger and Jasechko, 2014). Thus, transpiration is the largest water flux of terrestrial ET, especially in forests (Le Maitre et al., 2015; Tfwala et al., 2019).

Natural forests in southern Africa are limited in their extent; they cover less than 0.25% of the landscape (Le Maitre et al., 2002). The lack of a natural source of fast-growing timber trees led to the establishment of plantations with alien species, beginning in the late 18th century (Richardson et al., 2000; Le Maitre et al., 2002). Plantations of alien trees, primarily pines and eucalypts, now cover 1.52 million ha in South Africa (Allen, 1998). Some of these plantations have spread and invaded areas where they have not been purposefully planted, and the surveys by Kotze et al. (2010) and van den Berg (2010) showed that the extent of invasion by alien species increased from 1 736 million ha in 1996 to approximately 1 813 million ha in 2008. The volume of water consumed by alien plants was estimated to be equivalent to 6.7 % of the Mean Annual Runoff (MAR) at the national level and 15.8 % in the Western Cape Province (Enright, 2000; Shackleton et al., 2015; van Wilgen et al., 2012). Such water use is an environmental problem in a country like South Africa where the average precipitation is approximately 500 mm per year, well below the world average of 860 mm per year (Fourie et al., 2013). This resulted in the enactment of legislation in South Africa that prohibits establishing commercial forest plantations in riparian areas where impacts on streamflow are greatest (Dye et al., 2017).

Despite these efforts, extensive self-established stands of gums (*Eucalyptus* spp.), black wattle (*Acacia mearnsii*) and poplars (*Populus* spp.) occupy long stretches of river systems and they are expanding their range in South Africa (Le Maitre et al., 2002). Several studies have observed that invasive alien plants (IAPs) have water use rates higher than

indigenous vegetation (Calder and Dye, 2001; Dye and Jarmain, 2004; Dye et al., 2008; Le Maitre et al., 2015; Mapeto et al., 2018; Scott-Shaw et al., 2017). Studies by Dye and Poultera (1995), Prinsloo and Scott (1999), and Dye and Jarmain (2004) found that there can be notable increases in catchment water yield after the removal of IAPs. Improvement of information about water use rates by IAPs is important in a semi-arid country where there are competing demands for limited water resources. Land managers and policymakers require a better understanding of the ecological and socioeconomic status of invaded systems so that water resource management can be improved in invaded catchments (Huddle et al., 2011).

Acacia longifolia is the dominant invader in the Nuwejaars Catchment and it is one of the least studied invasive acacia species in South Africa. *Acacia mearnsii* (black wattle) is ranked as the highest water user among the well-studied invasive species (Dye and Jarmain, 2004). The black wattle emerged as the alien plant species of highest priority in the fynbos biome (van Wilgen et al., 2008), because of its significant impacts on water, biodiversity, fire hazard, and its ability to occupy both riparian and non-riparian areas. *A. longifolia* has not received in-depth research attention in South Africa and worldwide. A review of current knowledge on the consequences of the invasion by *Acacia* genus in Mediterranean ecosystems by Souza-Alonso et al. (2017) established that *A. longifolia* possesses eco-physiological traits and mechanisms that assist them to outcompete the native species, this includes high tolerance to wide range of salt concentrations compared to native species (Morais and Freitas, 2015, 2012). Increased salinity concentrations in the lowland parts of the Nuwejaars Catchment were reported by Mazvimavi et al. (2021). This is where dense thickets of *A. longifolia* were mostly observed.

In South Africa, besides the use of groundwater, *A. mearnsii* was liable for the estimated reduction of the mean annual runoff produced by all invasive plants (Le Maitre et al., 2000) and possess traits that enable them to withstand drier conditions than some native species. This is a major environmental problem in regions with limited water resources. Increasing coverage of *A longifolia* in riparian areas of the wetter parts of the Western Cape, Eastern Cape, Kwa-Zulu Natal, and scattered parts of Mpumalanga Province was reported by Henderson (2007). If *A longifolia* has similar characteristics to *A. mearnsii* then it is likely to have a detrimental impact on the water resources of the invaded catchments.

A. longifolia was the third *Acacia* species on the priority list of IAPs encroaching the fynbos biome, and the fifth overall out of the 23 species ranked invading the fynbos biome (Figure 4.1). There are no adequate and quantitative estimates of the water use rates of *A. longifolia* stands in the environment setting where they are dominant in South Africa.

Figure 4.1: The relative importance and the final ranking of invasive alien species in the fynbos biome (adopted from van Wilgen et al. (2008)). The numeric numbers show the order of priority -from high to low.

The impacts of *A. longifolia* have mostly been studied in Portugal (Marchante et al., 2008; Morais and Freitas, 2015, 2012; Rascher et al., 2011). Findings from these studies show that *A. longifolia* thrives in areas with moderate to low water stress and that water stress condition induces morphological changes in these trees (Morais and Freitas, 2012). It was also demonstrated that *A. longifolia* trees alter soil nutrients (Marchante et al., 2008) and properties (Rascher et al., 2011a) to outcompete the indigenous vegetation. These findings highlight the ability of *A. longifolia* to thrive under a variety of conditions. However, no study has been done to investigate how transpiration rates or patterns by *A. longifolia* vary in different landscape positions within the same climatological region. The spatial and temporal variations in magnitudes of tree water use patterns among species in a given landscape can be explained by variations in topography, micro-climate, and species-specific physiological and structural properties, including rooting depth, hydraulic architecture, leaf area and tree size (Hassler et al., 2017; Rossatto et al., 2012; White et al., 2002). Within stands, variation in sap velocities between species can occur

because of competition for light and water resources (Hassler et al., 2017). At the landscape scale, site-specific characteristics such as geology, soil type, soil depth or depth to groundwater, elevation, slope position and aspect could potentially affect spatial variation in transpiration patterns because they influence water and energy availability (Hassler et al., 2017).

Although there is a growing number of vegetation water use studies undertaken in arid and semi-arid regions, few have compared rates of water use by riparian and non-riparian plants and communities (Dzikiti et al., 2013; Mkunyana et al., 2019; Nagler et al., 2005; Scott, 1999) and these patterns have rarely been compared on different topographic locations such as lowland floodplains, mid-slope, and upland positions in the same catchment. The current study was birthed from previous findings by Mkunyana et al. (2019) who established that riparian *A.longifolia* used two times more water than *A. longifolia* occurring in a non-riparian setting in the Nuwejaars Catchment during June 2016 to June 2017 observation period. The groundwater fluctuation and other driving factors for the transpiration of *A. longifolia* were not analysed in the previous study. The current study seeks to contribute to this knowledge gap by comparing water use rates from *A. longifolia* trees occurring under different environmental conditions and locations, from the headwaters to lowlands in the same catchment. Understanding and quantifying transpiration and its landscape-scale variability are essential for improving the parameterisation of hydrological and soil-vegetation-atmosphere transfer models, as well as formulating appropriate management decisions.

4.2 Methods and materials

The location and selection of the study sites are explained in chapter 2 of this thesis.

4.2.1 Site requirements

To address the research objectives, suitable study sites with dense invasions of *Acacia longifolia* located in different elevations, gradients, and positions in the Nuwejaars Catchment were identified.

4.2.2 Monitoring the micro-climate of the study sites.

Weather data were collected from three automatic weather stations within the catchment.

Tussenberge weather station which monitors meteorological variables at the headwaters (230 metres above sea level, m.a.s.l.) was established in April 2019, while the Spanjaardskloof weather station at a mid-slope location (85 m.a.s.l.) was established in December 2015, and the Moddervlei weather station in the lowland (25 m.a.s.l.) was established in June 2016. The locations of these stations were representative of the landscape units used for the comparison of transpiration rates at different topographic locations.

All the weather stations stored hourly data for air temperature, relative humidity, atmospheric pressure, solar radiation, wind speed and direction, and rainfall (Figure 4.2). These data were used to estimate the daily reference evapotranspiration (ETo, mm) during the study period according to the following formula FAO Penman-Monteith method (Allen, 1998):

$$ETo = \frac{0.408\Delta(R_n - G) + \gamma\left(\frac{900}{Ta+273}\right) * u_2(e_s - e_a)}{\Delta + \gamma(1 + 0.34 * u_2)} \qquad (4.1)$$

where Δ is the slope of the saturation vapour pressure at air temperature Ta (kPa/°C); R_n is the net radiation (MJ/m²); G is the soil heat flux (MJ/m²), which is assumed to be negligible on a daily scale; γ is the psychrometric constant (kPa/°C); e_s is the saturation vapour pressure (kPa); e_a is the actual vapour pressure (kPa); u_2 is the mean wind speed (m/s) at a 2 m height, and Ta is the air temperature (°C) at a 2 m height.

Figure 4.2: Automatic weather stations established at the sites.

4.2.3 Monitoring sap flow velocities

Four study sites representative of the different conditions in which *A. longifolia* occurs within the Nuwejaars Catchment were selected for investigation (Figure 4.3):

i. a lowland riparian floodplain (altitude 25 m.a.s.l.) *Acacia longifolia* stand within a 50 m wide zone adjacent to the Nuwejaars River at Moddervlei.
ii. a mid-slope riparian (altitude 67 m.a.s.l.) *Acacia longifolia* stand within a 30 m wide zone adjacent to the Jan Swaartskraal River.
iii. a non-riparian mid-slope (altitude 145 m.a.s.l.) *Acacia longifolia* stand with no nearby stream at Spanjaardskloof.
iv. a non-riparian upland (altitude 228 m.a.s.l.) *Acacia longifolia* stand located 60 m from a headwater stream at Sandfontein.

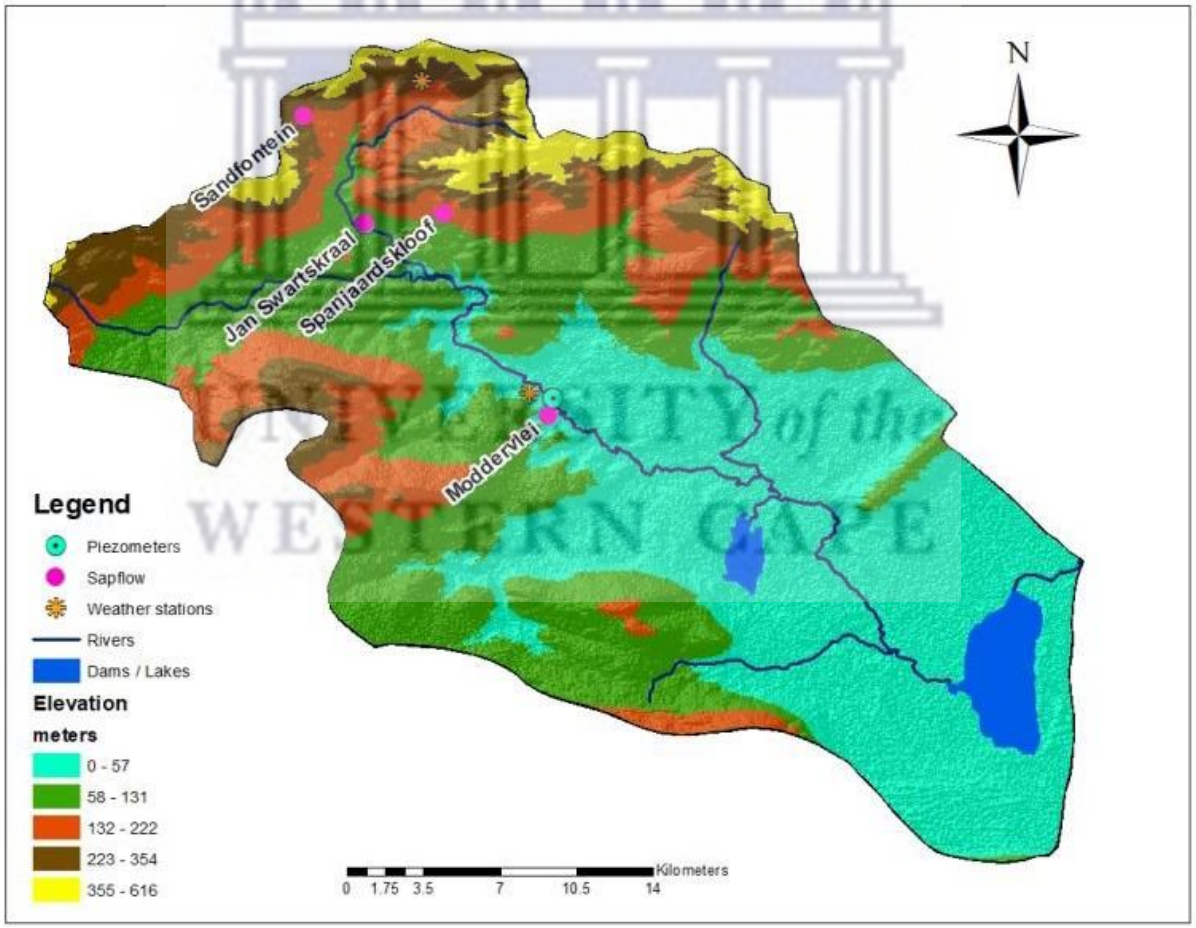

Figure 4.3: The layout of the study sites in the Nuwejaars Catchment.

4.2.4 Selection of trees

When suitable sites were located, the selection of trees for instrumentation required a stem survey at all the sites to identify representative trees. The selection criteria for trees to be monitored were the following:

v. actively growing and healthy trees, without visible evidence of fungal infestation.
vi. trees with relatively straight trunks and no knots which distort sap flow movement.
vii. trees that are representative of the different stem sizes present in the stand.

The HPV method can only be used on stems with diameters larger than 3 cm (Smith and Allen, 1996), and therefore trees selected at the riparian sites (Moddervlei and Jan Swartskraal) had diameters between 9.64 and 22.60 cm, while tree diameters at non-riparian sites (Spanjaardskloof and Sandfontein) were between 7.16 and 19.26 cm (Table 4.1).

Table 4.1:Stem diameters of the selected trees at each site

Site names	Elevation (m.a.s.l.)	Diameter (cm) and (size class)
Moddervlei	25	9.64 (S) 14.01 (M) 17.19 (M) 21.65 (L)
Jan Swartskraal	67	10.35 (S) 18.14 (M) 22.60 (M)
Spanjaardskloof	145	7.16 (S) 9.07 (S) 14.80 (M)
Sandfontein	228	7.48 (S) 12.41 (M) 14.96 (M) 19.26 (L)

*Size classes assumed for tree diameters where S is small, M is medium, and L is a large size class.

There are seven established theoretical methods, and several empirical or dual methods, to measure sap flow (Forster, 2017). Four of the seven theoretical HPV methods have been extensively tested and include the compensation heat pulse method (CHPM), heat

ratio method (HRM), T-max heat pulse, and sapflow+ method (Burgess et al., 2001; Forster, 2017). A review by Forster (2017) stated that a major difference between these methods is their limited measurement range; the CHPM and T-max methods cannot measure slow or reverse flows, while the HRM cannot measure high flows. The sapflow+ method can measure a wide range of flows. Forster (2017) found the precision of the HPV methods when compared to an independent method of measuring plant water use, in this case weighing lysimeters, gave an average R^2 of 0.82. The sapflow+ method had the greatest precision with an R^2 of 0.98 (Table 4.2). This method was selected for use in this study. The sap flow measurements were done using the Heat Pulse Velocity (HPV) sap flow technique which was adopted by Burgess et al. (2001). This method was chosen because the HPV method is appropriate and cost-effective for the transpiration measurement of various tree species (Dzikiti et al.,2017; Dzikiti et al., 2013; Everson, 2014; Forster, 2017; Ntshidi et al., 2018; Scott-Shaw et al., 2017).

Table 4.2: A summary of descriptive statistics derived from a study by Forster (2017) on the accuracy of HPV methods against an independent measurement of plant water use.

Method	n	R^2	Slope	Deviation from the slope (%)	Minimum range (cm/h)	Maximum range (cm/h)
All methods	104	0.82	0.86	34.70		
T-max	10	0.85	0.67	36.56	5 to 10	>200
CHPM	59	0.72	0.86	30.61	2 to 5	>200
HRM	11	0.91	0.83	16.94	-10	45
Sapflow+	7	0.98	0.62	38.00	-10	>200
Dual pulse	17	0.89	1.07	59.70	-10	>200

** Values for R2, slope and deviation from slope are means from the studies compiled in supplementary materials (Forster, 2017).*

4.2.5 Instrumentation of selected trees

After suitable sites were identified. The morphology of the trees had to be established, particularly the depth range or thickness of the sapwood (conductive xylem). This was done to determine the depths to which the HPV probes must be inserted in the selected trees to ensure that they were inserted within the sapwood. To do this, trees adjacent and

representative of the selected trees at each site were cut and these samples were used to measure the thicknesses of the bark, sapwood, and non-conductive heartwood.

A drilling template consisting of three holes was tied around the stem of the selected trees at breast height. The central hole (~1.8 mm) was used for the heater while the other two 2 mm holes located 5 mm below and above the central hole were used to insert the thermocouples (Figure 4.4). Four (4) sets of probes were installed on each tree. The depths of these probes varied across the sapwood area to account for radial variations in sap velocity. The T-type thermocouples were marked to indicate the depths to which they would be inserted. Each heater probe released a heat pulse for about 0.5 seconds at hourly intervals throughout the study period. The sapwood temperature was measured before injecting a heat pulse and then one and a half minutes after the initiation of the heat pulse. The thermocouple cables were connected to a multiplexer (AM16/32) that allowed multiple measurements of sap flow velocities to take place (Figure 4.4). The multiplexer was connected to a CR 1000 data logger which stored all the data collected.

The HPV systems were powered by 12V batteries charged and changed approximately every two weeks. A safe box was used to store all the equipment as shown in Figure 4.4 since the sites are in remote locations. When equipment installations were completed, fencing was done to keep away primates, cattle, pigs, and other animals that could damage the wiring on and around the systems. Data were collected at hourly intervals from October 2018 to November 2021. Due to the misalignments of probes, the sap flow velocities at Sandfontein had unrealistic peaks between October to November 2018, which resulted in the readjustment of probes in the instrumented trees. Therefore, data collection at this station began in December 2018. There were faults with the data logger at Jan Swartskraal in March 2020, due to the depletion of the lithium battery, thus data could not be retrieved (from March 2020). Additional gaps in transpiration data occurred due to faulty probes and battery discharging below 12V.

Figure 4.4: HPV system comprising heat and temperature probes connected to a safety box that enclosed a multiplexer, datalogger, and a 12V battery. The soil water data logger was also enclosed in the box to protect soil water sensors installed at various depths close to the selected trees.

4.2.6 Quality control of sap flow data

HPV data were downloaded bi-weekly when the batteries of the systems were changed. After every download, the HPV data were regularly checked for proper functioning. Data of poor quality were flagged with NAN (not-a-number), and unrealistically high or low values in the data were checked if they occurred in other probes, if not, the values were removed. In cases with one (hourly) data missing, the averaging method was applied using data collected before and after the missing data. In cases where there were successive missing data, the patching process using data measured by the other functional probe sets from the same tree or the tree closest to the one with a faulty probe was used. Where there was more than one non-functional probe in a tree, the probe with the highest correlation with the faulty probe was used.

Diurnal sap signals are expected to be low in the early morning, peak in the afternoon, and then decline after sunset. Thus, the velocities in the morning and at night are often assumed to be zero, as most trees close their stomata. Although night-time transpiration occurs in some woody species, these rates were found to be accountable for 5 – 15 % and

sometimes 30 % of the total daily transpiration (Frickle,2019). However, Dawson et al. (2007) also established that night-time transpiration is only beneficial in low-nutrient settings when soil water availability and night-time VPD are high. These conditions only occur during the wet season in the Mediterranean ecosystems, and thus were considered negligible in this study. Due to other causes, such as the misalignment of probes, the night-time values do not always stabilise around zero. Therefore, it is important to determine the true zero of each probe. This was done by felling the instrumented trees and monitoring for a further 24 hours at the end of the monitoring period (Figure 4.5). The offset value for each probe was applied to the HPV signals by subtracting or adding the value from the entire dataset to subsequently adjust the signals to match the zero flow conditions.

Figure 4.5: Felled A. longifolia tree used to determine the probe readings for zero-flux sap flow velocities.

4.2.7 Analysis of the sap flow data

i. Correcting sap velocities

Sap flow velocities were measured and calculated using Equation (4.2) described by Marshall (1958):

$$V_h = \frac{k}{x} In(v_1/v_2)3600 \qquad (4.2)$$

where V_h is the heat pulse velocity (cm/hr), k is the thermal diffusivity of the wood, x is the distance (cm) between the heater and the temperature probe, and v_1 and v_2 are increases in temperature (from initial temperatures) at equidistant points downstream and upstream, respectively.

The velocities were corrected by accounting for sensor misalignment and tree wounding due to the drilling using the following Burgess et al. (2001) method based on the modification of the Swanson and Whitfield (1981) empirical model:

$$V_c = bV_h + cV_h + dV_h \quad (4.3)$$

where V_c is the corrected heat pulse velocity, V_h is the heat pulse velocity estimated from Equation (4.2). Coefficients b, c and d are used to adjust for wound width (w, cm):

$$b = 6.62 * (w^2) + (3.33 * w) + 0.92 \quad (4.4)$$

$$c = -0.15 * (w^2) + (0.04 * w) - 0.004 \quad (4.5)$$

$$d = 0.03 * (w^2) - (0.009 * w) - 0.0008 \quad (4.6)$$

Sap velocities (cm/hr) from the four probes in a tree were converted to an estimate of the tree's total sap flow in L/hr. This was done by dividing the cross-sectional area of sapwood into four concentric bands, or rings, based on the insertion depths of the four probes. The cross-sectional area of each band was assumed to have the sap velocity measured by the relevant probe to calculate an L/hr flux in that ring. These were summed to estimate the total sap flow of the tree per day.

4.2.8 Upscaling sap flow to stand-level transpiration rates.

i. Characterising stand properties

The results obtained from the HPV sap flow system were used to determine the water use (transpiration) rates of the selected trees from the headwaters to lowlands in litres per day. The stem size distribution, tree density, sapwood area index (SAI, m^2 of sapwood per m^2 of ground area), wounding widths, wood moisture fraction, and the wood densities of the

instrumented trees were needed to derive the transpiration rates of individual trees and scale up tree water use to stand level.

ii. Tree densities

Tree density (defined as the number of trees per unit area) was determined where possible by demarcating 10 x 10 m^2 quadrants. However, there were *A. longifolia* stands at some study sites with very high densities of young, small-diameter trees, such as at Jan Swartskraal and at Sandfontein where it was not possible to lay out 10x10 m^2 quadrants. Consequently, 2 x 10 m plots were used in these cases (Table 4.4). One of the four quadrants surveyed at Jan Swartskraal was a 2 x 10 m plot, divided into 2 x 2 m subplots to facilitate stem measurements. At Sandfontein, all four plots were 2 x 10 m due to the high density of small trees. The area of *A.longifolia* dominated stand was small at Spanjaardskloof, due to the presence of other species resulting in highly mixed stands, hence only two 10 x 10 m plots could be demarcated at this site (Table 4.4).

iii. Stem size distribution

The stem size distribution was determined to scale up water use from single trees to stand level at each site. This was done by measuring the circumferences at breast heights of all trees within the demarcated quadrants and converting measurements to tree diameter (*dbh*). Thereafter, three *dbh* size classes were defined based on the tree size distribution across the sites and the sizes of the instrumented trees.

iv. Sapwood area index

The Sapwood Area Index (*SAI*) was calculated using the stem size survey data and the relationship between tree stem size and sapwood area was determined through field measurement. Various trees with different stem sizes were felled at each site. The stem circumferences, bark, sapwood, and heartwood thicknesses were measured from the cut trees. These were used to derive a sapwood area vs stem cross-sectional area relationship (allometric equation). The sapwood areas of the trees that were measured during stem surveys were then estimated using the established equation. The *SAI* of trees in a particular stem size class was calculated as the ratio of the total sapwood area for the trees of the correct size in a sample plot to the ground area. Plot SAI values were averaged to get a value for each site.

v. Determining the size of the wounding widths

The size of the wounding width indicates the extent of damage that resulted from drilling and sensor implantation into the trees. The wounding widths were determined at the end of the experiment when all thermocouples and heaters were disconnected. Wood samples were collected from the stems which were drilled and cut out to identify and measure the widths of the area that showed signs of disturbance that could have resulted from drilling. Discoloration on and around the drilled holes indicated the extent of the wound (Figure 4.6).

Figure 4.6: Shows the wounding width (yellow line) measured on A. longifolia tree.

vi. Moisture fraction and wood density

The moisture fraction of the trees was determined by cutting a section of the stem (a disk of ~ 6 cm thickness) from the instrumented trees at the end of the sap flow measuring period (Figure 4.7). The samples were placed in zip-lock bags to minimize the loss of moisture which may affect the mass of the fresh sample. The samples were then taken to the laboratory and weighed. The mass of the fresh wood (in grams) was denoted as *Mw*. The samples were oven-dried at 70^0 C and were weighed at 24-hour intervals until the weight was constant. The weight of the dry sample was denoted as *Md*. The moisture fraction of each sample (ΔM) was then given using Equation (4.7):

$$\Delta M = \frac{Mw - Md}{Md} \qquad (4.7)$$

The wood density of the samples was determined as the ratio of the dry mass to the volume of the wood. The volume of the wood was determined by placing the oven-dry sample into a measuring cylinder with water of a known volume. The volume of the wood was calculated as the change in the volume filled in the beaker when the sample was submerged in the beaker.

Figure 4.7: Samples collected from the instrumented trees to the lab to determine the moisture faction and wood density across the study sites.

The sap flux density (U_i, mm/day) per unit area of sapwood for each instrumented tree was determined by Equation (4.8):

$$U_i = \frac{V_c}{A} \qquad (4.8)$$

Where U_i, is the sap flux density of sapwood (mm/day) for a tree belonging to size class i, V_c is the corrected sap flow (m^3/day,) and A (m^2) is the measured sapwood area of the tree.

Transpiration rates for all the trees in each class size in a stand were estimated as the product of the class's sapwood area index (SAI) and the sap flux density (U_i, in mm/day) from the instrumented trees in each class size. Total stand-level transpiration (Tr in

mm/day) was then determined as the sum of transpiration by trees in each stem size category:

$$Tr = \sum_{i=1}^{n} SAI_i * U_i \quad (4.9)$$

where SAI_i is the sapwood area index (sapwood area/ground area), and U_i is the sap flux density(mm/day) in each class size $_i$.

4.3 Data analysis

The significance of differences in weather variables across the study sites was tested using ANOVA.

Data from October 2018 - November 2021 were analysed using paired t-tests to compare sap flux densities (transpiration per sapwood area) of the instrumented trees at each site to assess variation in sap flux density with tree size, within and across sites. Analyses were limited to the days for which all four sites had data. Due to equipment failure, Jan Swartskraal's dataset ended in March 2020, limiting the analysis period. However, for the other three sites with longer datasets, another set of paired t-tests was performed using days when all three had data.

Paired t-tests were also done to compare stand-level transpiration rates across all the study sites. Again, this was done only using the days when all four sites had data, as well as for the longer period for which three of the sites had data.

Box plots were used to graphically demonstrate the variation of sap flux densities and transpiration rates from individual trees at each site and across the different sites for the periods with data at all sites.

To estimate the annual rates of transpiration for each site, daily transpiration for each calendar month using the longer period for which three of the sites had data was estimated. The values were multiplied by the number of days in a month and then summed to get the annual value.

4.4 Results

The results presented in this chapter will be from the onset of the sap flow monitoring period in October 2018 until November 2021 when the experiments ceased.

4.4.1 Microclimate across the study sites

The weather conditions differed across the sites (Table 4.3). During the period of the study, in the lowland of the catchment, at Moddervlei, daily solar irradiance ranged between 8.85 to 26.41 MJ/m^2, with daily average temperatures from 11.8° to 21.7 º C. In the mid-slopes, represented by the Spanjaardskloof station, daily solar irradiance was between 9.38 – 26.04 MJ/m^2 with average temperatures of 12.1° – 22.1 º C. On the headwaters, solar irradiance ranged from 7.91 to 24.51 MJ/m^2 with average temperatures of 12.1° – 20.8 º C (Figure 4.8).

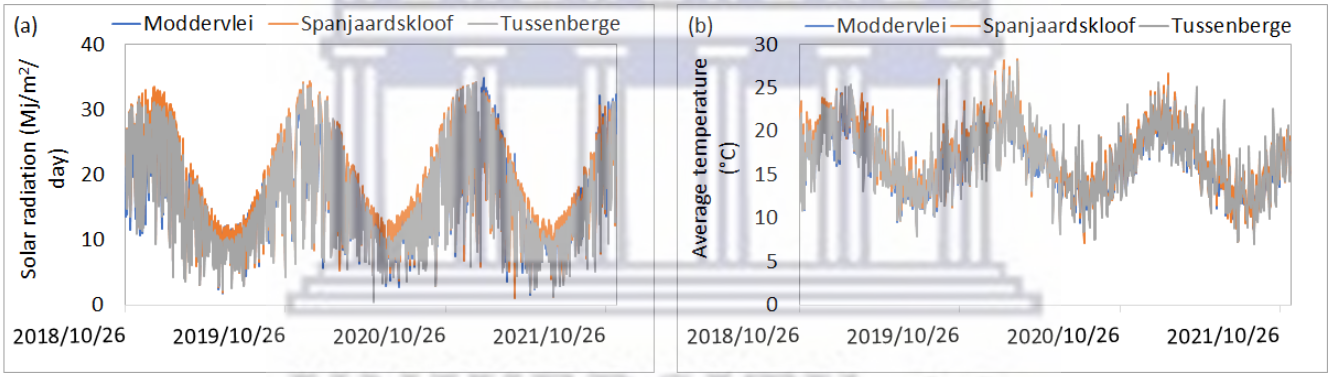

Figure 4.8: Daily solar radiation (a) and temperature (b) variations from October 2018 until November 2021 period.

On monthly averages, solar irradiance, and temperature at the lower sites, Moddervlei and Spanjaardskloof, were slightly higher than the solar irradiance and temperatures in the headwaters at Tussenberge. Although solar irradiances across the sites showed similar seasonal patterns, they were significantly different from one another ($p<0.05$) (Table 4.3). The differences in solar irradiance also resulted in significant differences in average temperatures across the sites (Figure 4.9).

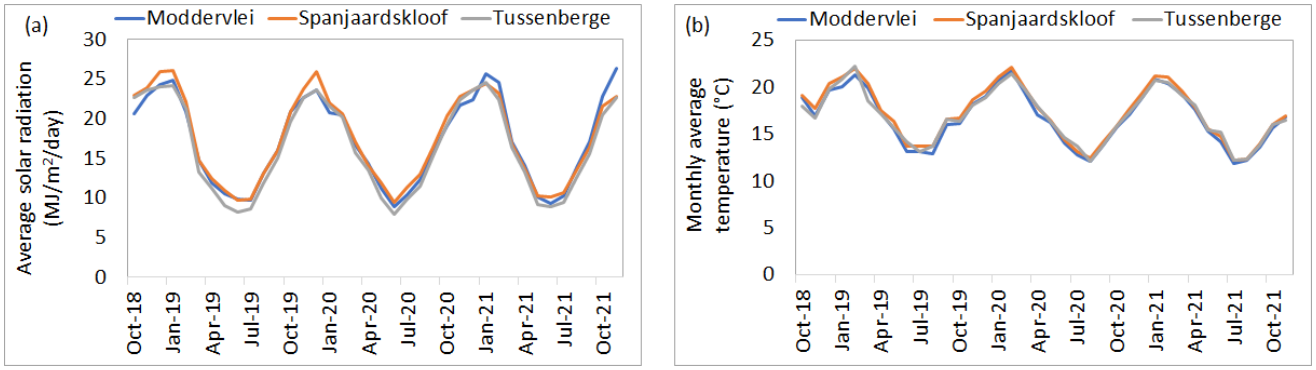

Figure 4.9: Average monthly solar radiation (a) and temperature variations (b) from October 2018 until November 2021 period.

The lower solar irradiance in the headwaters resulted in significant differences in reference evapotranspiration (ETo), where daily reference evapotranspiration at Moddervlei reached 8.4 mm, 8.7 mm at Spanjaardskloof, and 7.8 mm at Sandfontein (Figure 4.10a). The lower ETo rates in the headwaters were also evident when the average monthly reference ET at Moddervlei and Spanjaardskloof reached 165.3 and 164.4 mm, respectively. While, at Tussenberge, the average monthly reference ET only reached 159.5 mm (Figure 4.10b).

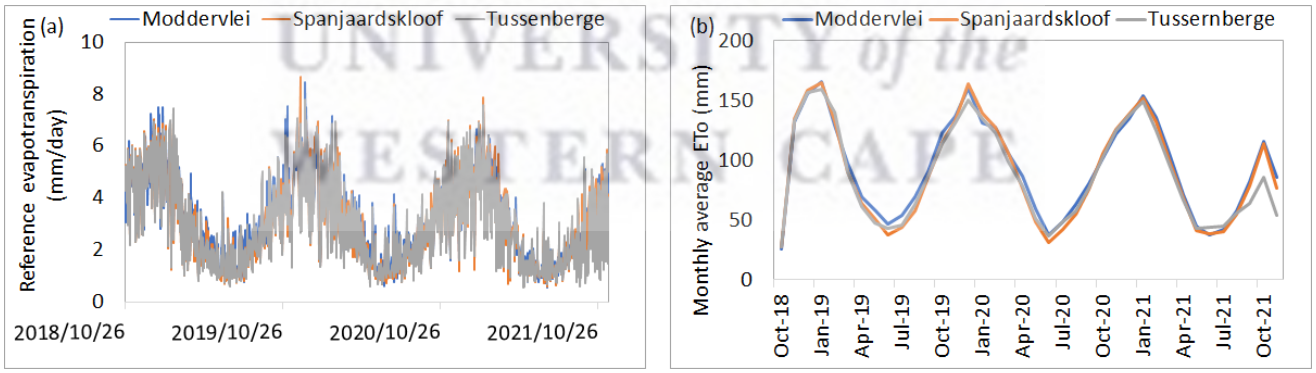

Figure 4.10: (a) Daily and (b) monthly reference ET variations from October 2018 until November 2021 period.

While the solar radiation and temperatures were lower at Tussenberge, the daily wind speeds were higher (0.17 – 6.65 m/s) than at Spanjaardskloof (0.32 – 5.82 m/s). Moddervlei had significantly high wind speeds with minimum and maximum daily wind speeds of 0.16 – 8.79 m/s (Figure 4.11a).

Tussenberge was slightly humid compared to other sites, with daily relative humidity between 33 and 98 %, while at Spanjaardskloof, the relative humidity ranged between 54 to 9 2%, which was slightly close to 53 - 97 % observed at Moddervlei (Figure 4.11b).

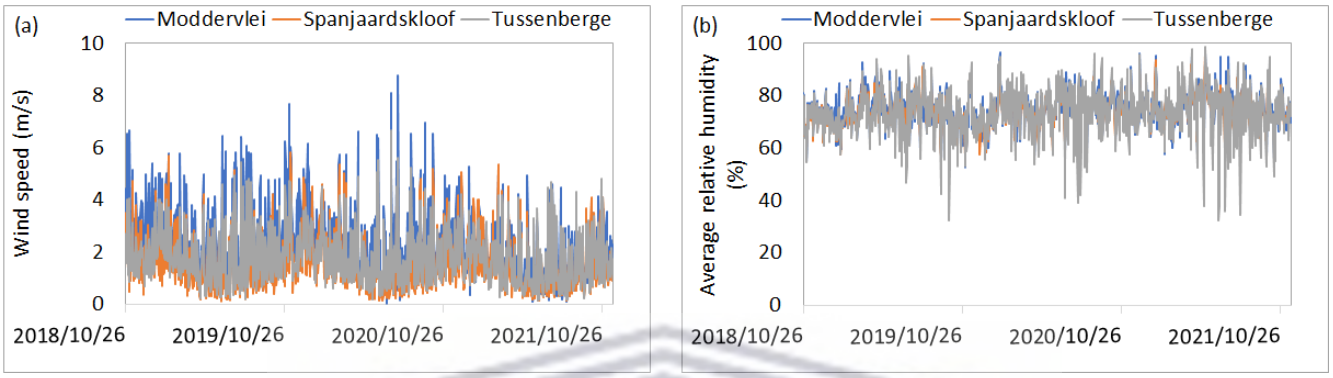

Figure 4.11: Variations in daily wind speeds (a) and relative humidity (b) from October 2018 until November 2021 period.

The slightly humid conditions at Tussenberge also explained the low ETo rates compared to other sites and high mean monthly rainfall of up to 273 mm, followed by 239 mm at Moddervlei, and 195 mm at Spanjaardskloof during May 2021. Generally, Figure 4.12b illustrates that Tussenberge had higher mean monthly rainfall, followed by Modderrvlei, while Spanjaardskloof received the least rainfall throughout the study period.

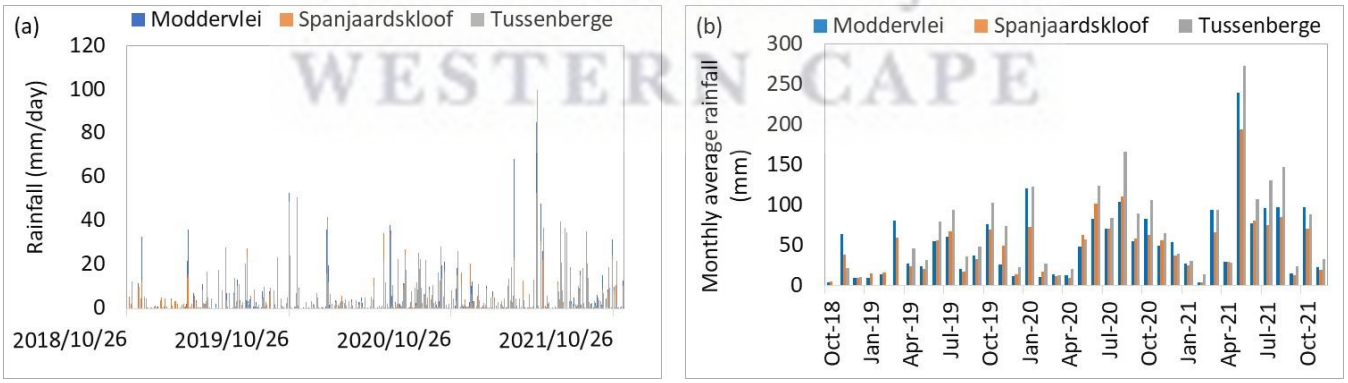

Figure 4.12: Daily (a) and average monthly (b) rainfall from October 2018 until November 2021 period.

Table 4.3: Comparing means of the weather variables monitored from the three weather stations in the catchment.

Variables	ANOVA P-values
Solar radiation (MJ/m^2)	0.01
Wind speed (m/s)	0.00
Average temperature (°C)	0.03
Relative humidity (%)	0.00
ETo (mm)	0.02
Rainfall (mm)	0.02

4.4.2 Characterizing the instrumented stands.

(i) *Tree densities*

The estimated total number of trees per hectare at each site illustrates that Jan Swartskraal had the highest density of 55 625 trees/ha, followed by 48 833 trees/ha at Sandfontein, Moddervlei with 13 875 trees/ha, and Spanjaardskloof had the lowest density of 8 650 trees/ha (Table 4.4).

Table 4.4: Estimations of tree densities per hectare (ha) at the study sites.

Moddervlei

Quadrants	size of the quadrant (m^2)	No. of trees	Trees/m^2	**Trees/ha**
1	100	62	0.62	6200
2	100	44	0.44	4400
3	100	167	1.67	16700
4	100	282	2.82	28200
	average number of trees per hectare			**13 875**

Jan Swartskraal

Quadrants	size of the quadrant (m^2)	No. of trees	Trees/m^2	**Trees/ha**
1	100	74	0.74	7400
2	100	119	1.19	11900
3	20	343	17.15	172000
4	100	312	3.12	31200
	average number of trees per hectare			**55 625**

Spanjaardskloof

Quadrants	size of the quadrant (m^2)	No. of trees	Trees/m^2	**Trees/ha**
1	100	64	0.64	6400
2	100	109	1.09	10900
	average number of trees per hectare			**8 650**

Sandfontein

Quadrants	size of the quadrant (m^2)	No. of trees	Trees/m^2	**Trees/ha**
1	20	48	2.40	24000
2	20	136	6.80	68000
3	20	109	5.45	54500
	average number of trees per hectare			**48 833**

(ii) *Stem size distribution*

The trees surveyed and measured in the demarcated quadrants were categorized into three classes of diameter at breast height (*dbh*). These were small (< 11 cm), medium (12–19 cm) and large trees (> 19 cm). The small-diameter trees (<11 cm) dominated, making up over 88 % of trees in all the study sites (Figure 4.13). It was also apparent that the riparian sites, Moddervlei and Jan Swartskraal had more medium and large trees compared to those occurring at Spanjaardskloof and Sandfontein sites.

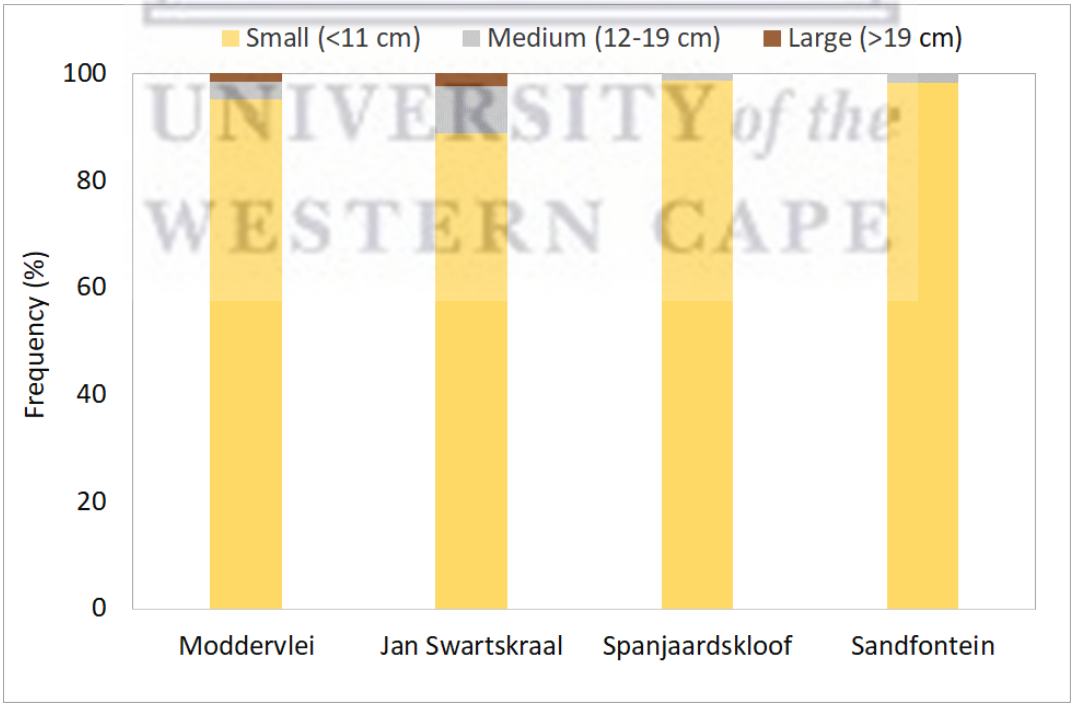

Figure 4.13: The distribution of stem diameters estimated from the circumferences of trees occurring in the quadrants.

(iii) *Sapwood area index*

A strong linear relationship was observed between sapwood and stem cross-sectional area (Figure 4.14).

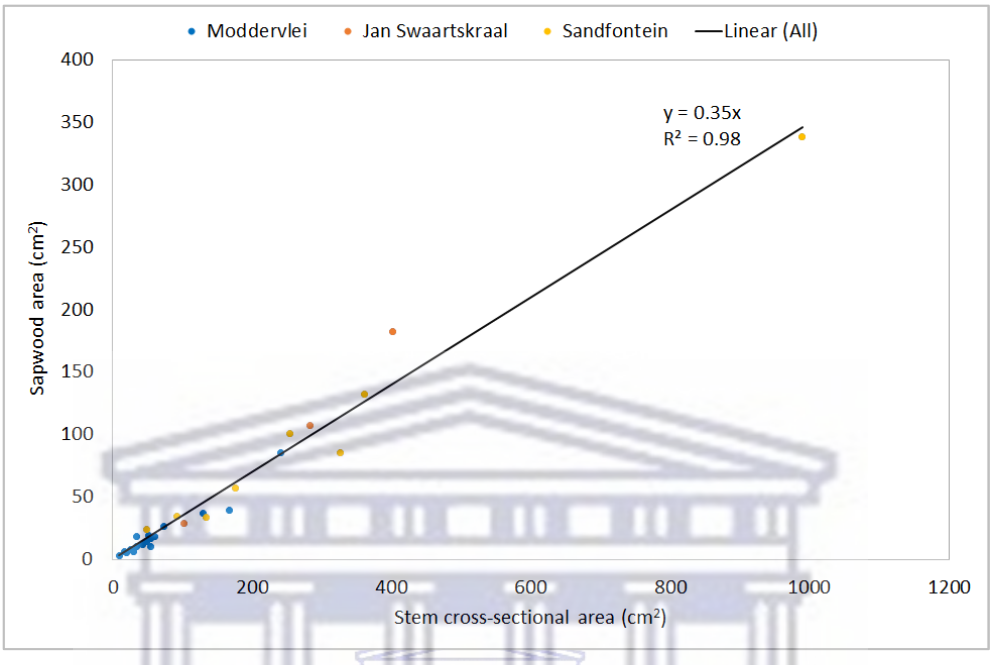

Figure 4.14: Allometric relations of sapwood and cross-sectional areas of A. longifolia trees at Moddervlei, Jan Swartskraal, and Sandfontein.

The estimated average sapwood per ground area across the sites using the allometric equation shows that the small trees at Sandfontein had more sapwood than the small trees from other sites, Sandfotein was followed by trees at Jan Swaartskraal and Moddervlei. The small trees at Spanjaardskloof had smaller sapwood per unit of ground. The medium-sized trees at Jan Swartskraal had more sapwood compared to the medium trees at other sites. These were followed by medium trees at Sandfontein and Moddervlei while the medium trees at Spanjaarsdkloof had the least sapwood areas. Both riparian sites had large trees with trees at Jan Swartskraal having more sapwood areas than the large trees at Moddervlei (Figure 4.15). These results suggest that trees at Sandfontein had sapwood areas similar to trees occurring in the lowland and mid-slope riparian, while the trees at Spanjaardskloof had the least sapwood areas.

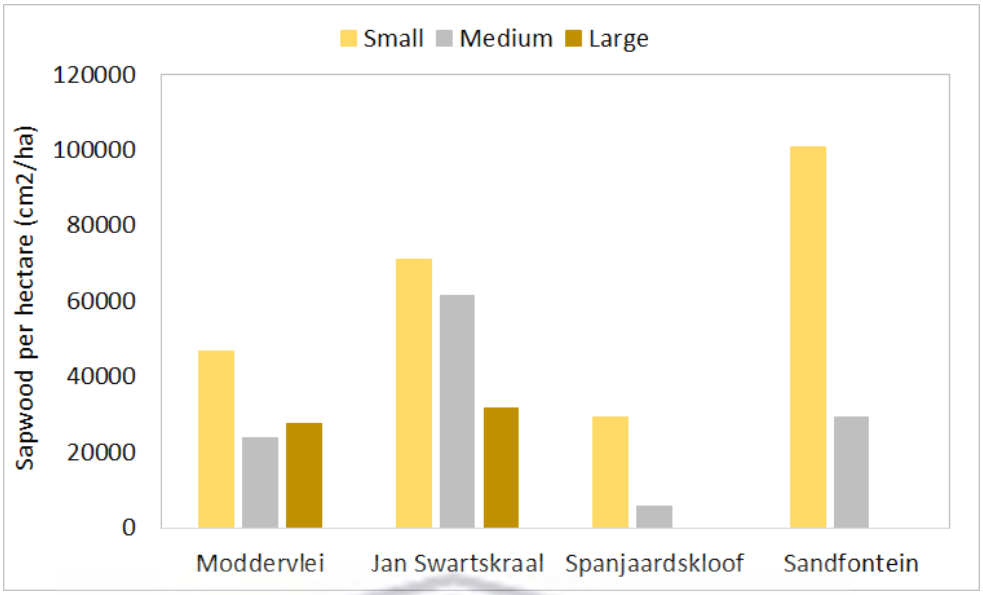

Figure 4.15: Average sapwood per ground area (1 hectare) of the surveyed trees belonging to class size.

4.4.3 Individual tree water use rates across the sites

Sap flux densities differed across the various stem diameters (Table 4.5).

Table 4.5: Paired t-tests of sap flux densities from instrumented trees at Moddervlei (MDV), Jan Swartskraal (JSK), Spanjaardskloof (SPK), and Sandfontein (SDF) with similar diameters.

Pairs	P(T<=t) two-tail
SPK_7.16 cm and SDF_7.48 cm	0.00
SPK_9.07 cm and MDV_9.64 cm	0.00
MDV_14.01 cm and SPK_14.80 cm	0.00
SPK_14.80 cm and SDF_14.96 cm	0.00
MDV_14.01 cm and SDF_14.96 cm	0.00
MDV_21.65 cm and JSK_22.60 cm	0.00

*The values are the measured stem diameters in cm

During the analysis period, the average daily sap flux density from the small-diameter trees ranged from 0.08 to 0.30 L/day/cm^2. The small tree at Jan Swartskraal (10.35 diameter) had the highest sap flux, while the small tree at Spanjaardskloof (7.16 cm diameter) measured the lowest transpiration rate per unit sapwood (Figure 4.16). According to a comparison of transpiration per unit sapwood from the small class size,

which is a dominant class across all sites, the small trees at the riparian sites (Moddervlei and Jan Swartskraal) had higher sap flux densities than those at the non-riparian sites. Additionally, the comparison of small trees with similar diameters from non-riparian Spanjaardskloof and Sandfontein also suggests that trees in non-riparian areas transpire differently. This was evident from the high average sap flux density measured from the 7.48 cm diameter at Sandfontein compared to the tree with a 7.16 cm diameter at Spanjaardskloof

Across all sites, medium-class trees transpired at higher rates per unit sapwood than large stem-sized trees. In addition, the medium trees at Moddervlei and Spanjaardskloof measured higher sap flux densities than those at Jan Swartskraal and Sandfontein. A medium tree at Moddervlei with a diameter of 14.01 cm measured an average sap flux density of 0.76 L/day/cm^2, followed by a medium tree at Spanjaardskloof with a diameter of 14.80 cm measuring 0.56 L/day/cm^2. However, medium-sized trees only made-up 2% of trees in the studied area and were more common along the riparian zones (Moddervlei and Jan Swartskraal) (Figure 4.13). A large tree at Sandfontein had an average sap flux density of 0.44 L/day/cm^2, which was two times higher than the average transpiration per unit sapwood at Moddervlei (21.65 cm).

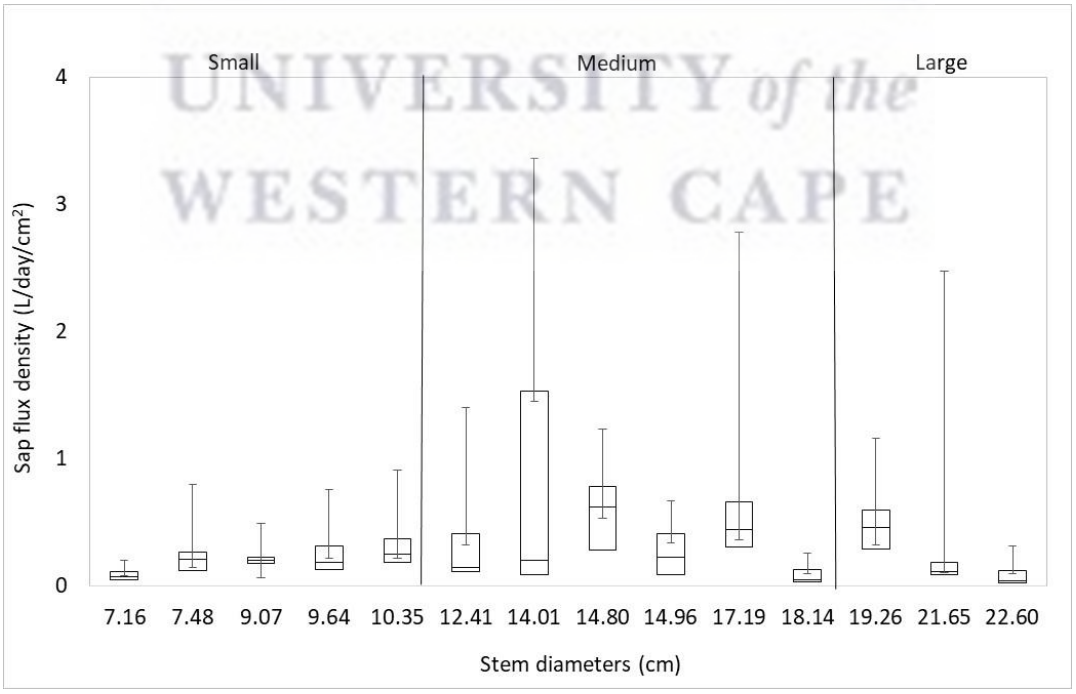

Figure 4.16: Sap flux densities of the instrumented trees across the sites. The diameters of trees are listed in ascending order.

4.4.4 Transpiration rates by A. longifolia stand on different topographical positions.

Across the sites, transpiration at the stand level differed significantly ($p<0.05$). On average, the lowland and mid-slope riparian stand at Moddervlei and Jan Swartsraal had rates of transpiration at 3.2 and 2.9 mm/day, respectively. On the non-riparian mid-slope Spanjaardskloof and upland at Sandfontein, the average transpiration rates of 0.7 and 2.9 mm/day were observed (Figure 4.17). According to these results, the non-riparian mid-slope section of the catchment, at Spanjaardskloof, transpired the least, while the *A. longifolia* stand on the uplands transpired at higher rates similar to those in riparian areas.

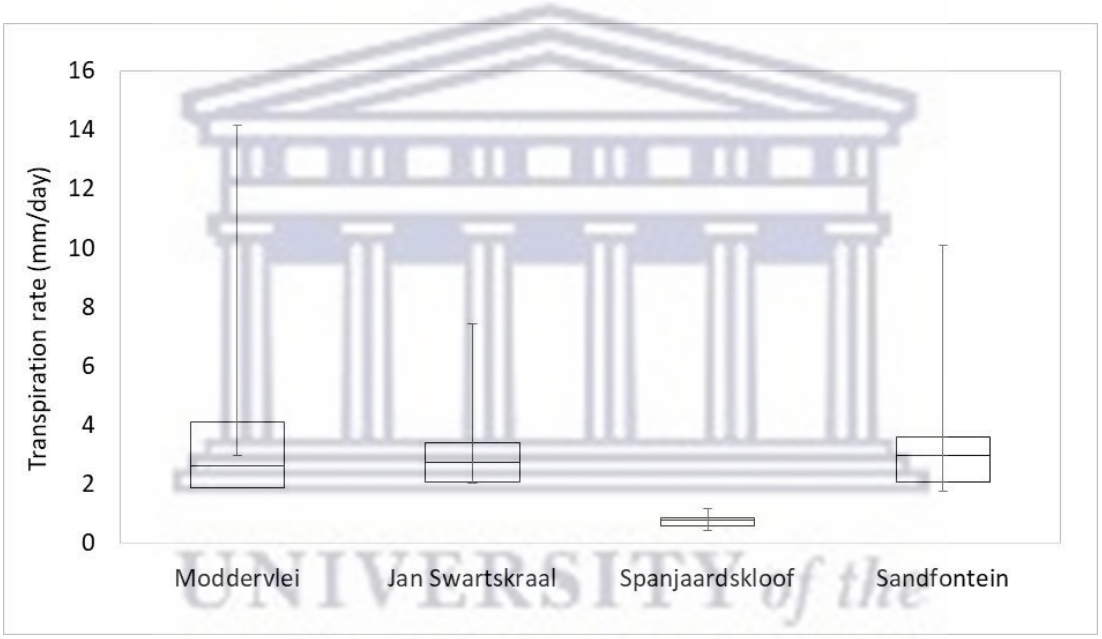

Figure 4.17: Box and Whisker plots for daily transpiration rates across the sites. These are days from October 2018 until March 2020, when the sap flow systems were working across the sites.

As illustrated in Figure 4.18, the COVID-19 lockdown restriction had a detrimental effect on monitoring, resulting in data gaps after March 2020. Due to the depletion of the lithium battery on the data logger at Jan Swaartskraal, data logging ended in March 2020. As a result, the comparison of annual estimates was only done for the other three sites (Moddervlei, Spanjaardskloof, and Sandfontein). For the period with data across the three sites between October 2018 and November 2021, the annual stand-level transpiration was estimated to be 825 mm at Moddervlei, 193 mm at Spanjaardskloof, and 664 mm at Sandfontein. In translation, *Acacia longifolia* stands on the lowland riparian areas and

upland of the catchment transpired at higher rates than those on the non-riparian mid-slopes.

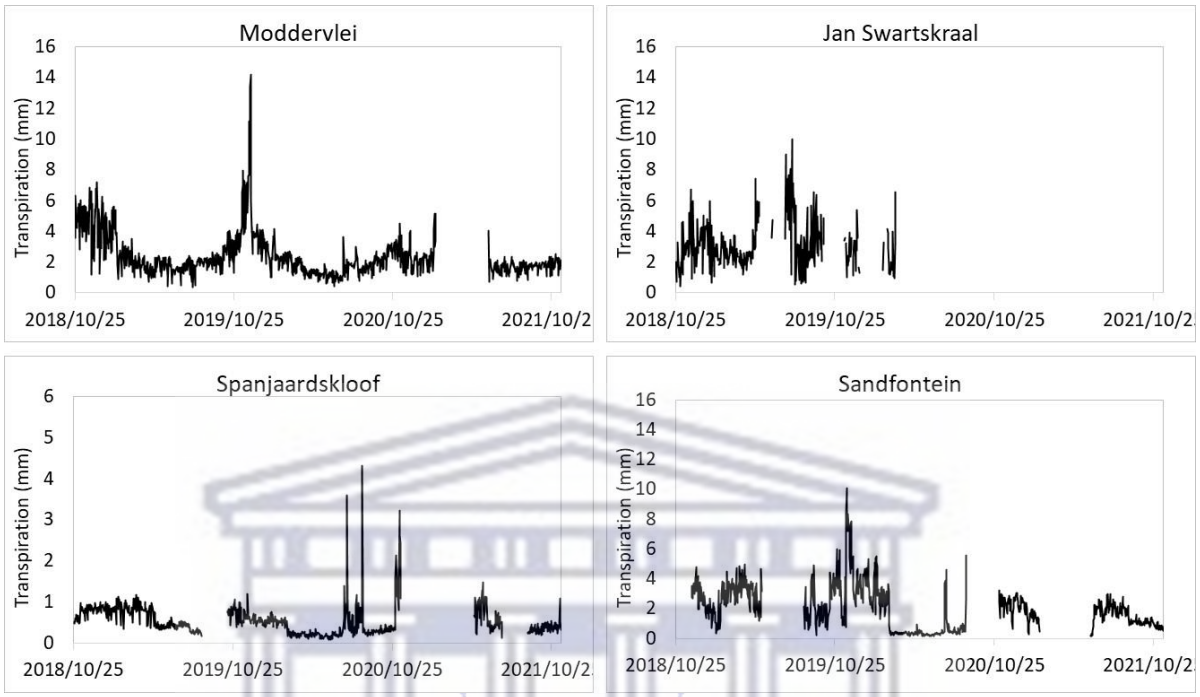

Figure 4.18: Daily transpiration rates across the study sites from October 2018 to November 2021 period (gaps showing the periods with faulty probes and/or when battery discharged below 12V).

4.5 Discussion

This chapter compared transpiration patterns of *A. longifolia* stands occurring in different topographical settings. Our understanding of the spatio-temporal dynamics and drivers of transpiration patterns in complex terrain is still limited by lacking knowledge of how systematic interactions of energy and moisture patterns shape the ecosystem and water fluxes as well as the adaptation of the vegetation to these patterns (Metzen et al., 2019). Thus, understanding the interaction of topography, soil moisture, and vegetation dynamic is important to identify vulnerable species and the resulting impacts on ecosystem services in complex terrain as species along these hydrologic gradients also have contrasting water-use patterns, which may further interact with climate (Hawthorne and Miniat, 2018). However, in this study, the impacts of soil moisture on tree water use will be analysed in a subsequent chapter. This chapter only focused on the contrasting water use patterns by *A. longifolia* occurring on different topographic positions. Previous

research showed spatio-temporal variations in factors that may drive transpiration patterns (Hawthorne and Miniat, 2018; Tromp-van Meerveld and McDonnell, 2006). This is the first study to compare the water use rates by the same species (*A. longifolia* stands) occurring at different slope positions in the same catchment.

4.5.1 Microclimate

The weather variables differed significantly across all the sites in the Nuwejaars Catchment. The differences in microclimate were highlighted by differences in total rainfall over the 3 years, whereby the headwaters (uplands) received more rainfall than other parts of the catchment. It was also noted that over the same period, the humid conditions on the headwater compared to mid-slope and lowlands also influenced ETo rates across the sites. ETo increased from the headwaters to the lowlands. Temperature and humidity were identified to be drivers of water use in other studies (Chen et al., 2014; Ping et al., 2006; Xu and Yu, 2020). In semi-arid and arid areas, it is generally known that transpiration is determined by the evaporative demand (which is often represented by ETo), available soil water, and the ability of trees to extract water from the water table to the atmosphere (Ping et al., 2006; Xu and Yu, 2020a). Based on the differences in microclimates of the study sites, contrasting transpiration patterns at different topographical positions were therefore expected.

4.5.2 Characterization of stands and individual tree water use patterns.

The characterization of the studied stands shows that the dense *A. longifolia* stands across the sites were dominated by small-diameter trees. The stem diameters and sapwood areas were related by a linear function. This suggests that trees with smaller stem diameters have smaller sapwood areas which indicates less water use rates. A similar relationship was derived by representing allometric equations by *Acacia arioloba* and *Acacia flecki* (Lubczynski et al., 2017). Sap flux measurements which are widely accepted as indicators of the magnitude and patterns of transpiration (Poyatos et al., 2016) illustrated the highest sap flux rates from the medium-sized trees than the larger trees. This is because the fraction of heartwood as a proportion of the total area for the large trees was greater than the proportion of the sapwood from all the instrumented trees. Meaning, as the tree size increased, the sapwood and heartwood of trees also increased. However, the sapwood width is regulated by the formation of heartwood (Morais and

Pereira, 2007) and consequently, tree water use from the large sized trees can be less than smaller sized trees as a result of sapwood regulation.

The comparison of small-sized trees which were dominant across the sites revealed that trees at Spanjaardskloof had the least average sap flux compared to small trees occurring at other sites. This may be a possible explanation for the low stand-level rates of water use observed at Spanjaardskloof compared to the other sites. Besides the differences in sap flux densities of the instrumented trees, stand densities showed the lowest number of trees per hectare at Spanjaardskloof. Thus, the cumulative total water use by *A. longifolia* at Spanjaardskloof was less compared to the other sites. These findings agree with earlier research findings of identifying priority areas for clearing programs which established that ecosystems dominated by IAPs are more likely to have high rates of water use in areas with denser stands than sparsely stocked stands (Cavaleri and Sack, 2010; Dzikiti et al., 2017).

4.5.3 Comparing stand-level transpiration rates of A. longifolia across the sites.

The stand-level rates of transpiration by *A. longifolia* differed significantly from the headwater to the lowland riparian site along the Nuwejaars Catchment. *A. longifolia* on the lowland riparian site transpired two times more (77 %) than *A. longifolia* on the non-riparian mid-slope site, at Spanjaardskloof. Those occurring in the uplands (Sandfontein) transpired 71% more than the *A. longifolia* at Spanjaardskloof.

Although the HPV system at Jan Swartkraal stopped functioning in March 2020, the sap flux densities measured from the instrumented trees show that the magnitude of transpiration per unit sap flux from trees at Jan Swartskraal was similar to those measured from the lowland riparian at Moddervlei. As a result, across the studied sites, *A. longifolia* in the mid-slope non-riparian at Spanjaardskloof had the lowest rates of transpiration, while high rates were observed at the lowland riparian sites, Moddervlei and Jan Swartskraal, as well as on the upland hillslope of the catchment, at Sandfontein. These results confirm earlier work by Mkunyana et al. (2019) who established that *A. longifolia* stands occurring in the lowland riparian use twice more water compared to those occurring in the non-riparian setting. Dzikiti et al. (2013) made similar findings for riparian pines using 36 % more water than the self-sown pines occurring in a non-riparian setting.

These differences were attributed to the shallow water tables that are found in riparian zones that become accessible for riparian vegetation to use resulting in substantially more water transpired by riparian vegetation than vegetation occurring in other topographical settings. Both studies, however, only focused on riparian and non-riparian settings, whereas the current study also considered the topographical influence on transpiration patterns. Other studies have established that in arid or semiarid areas, topography significantly influences the microclimate, soil properties, and hydrological processes, resulting in distinct vegetation types occupying different slope positions with different water use patterns (Yang et al., 2020).

Unexpectedly, the stand at Sandfontein had high rates of water use close to those observed in the lowland and mid-slope riparian Moddervlei and Jan Swartskraal stand. This was rather interesting and contrary to earlier findings that non-riparian species used less water. It was also established in this study that the non-riparian stands in the mid-slope and upland parts of the catchment had significant differences in transpiration patterns. This was evident from the comparison of sap flux rates from similar tree diameters as well as the stand transpiration. The headwaters of the catchment received higher rainfall than other parts, and therefore, the high rates of water use by *A. longifolia* at Sandfontein can potentially be attributed to the differences between moisture availability between the two non-riparian mid-slope (Spanjaardskloof) and upland (Sandfontein) sites in the catchment. Also, Sandfontein had the largest tree density, while Spanjaardskloof had the smallest. These tree densities and stand level transpiration were related since the results on *A. longifolia* stand in Portugal showed that this species tends to be more invasive as a result of a faster growth rate in areas that are wetter and moist (Morais and Freitas, 2012). It was also established by Souza-Alonso et al. (2017) that high rates of water use at the stand-level by *A. longifolia* are a community-level strategy promoting collective invasiveness rather than individual plants. Meaning the differences in stand-level transpiration across the sites may be a result of the dense thickets and do not indicate the individual or single tree impact.

4.6 Conclusions and recommendations

The variation of transpiration patterns by *A. longifolia* stands occurring on different topographical positions was driven by the differences in the microclimate across the study sites. The lowlands and headwaters received significantly higher rainfall than the mid-slope section of the catchment. The increased moisture in these parts of the catchment explained the higher tree densities at the riparian Moddervlei and Jan Swartskraal, as well as the headwaters, Sandfontein. This resulted in higher stand-level transpiration at these sites. Based on these observations, it is therefore confirmed that the widely reported adverse impacts of riparian invasions on water resources are a result of the ability of riparian species to form very high tree densities The hypothesis that riparian invasions use more water than invasions occurring in a non-riparian setting is supported by the results obtained during this study. Moreover, this study revealed that high tree densities are likely to occur in both riparian and non-riparian settings depending on moisture availability and/or rainfall that promotes plant growth. Therefore, the adverse impacts of IAP on water resources can be found in both riparian and non-riparian settings. Dense invasions should be flagged as high-priority areas for alien plant clearing regardless of whether the area is in a riparian or non-riparian setting. It is recommended that further work be done on monitoring tree water use on different IAP species occurring in the Nuwejaars Catchment.

Chapter 5

Relationships between soil water, groundwater, and transpiration patterns of Acacia longifolia occurring on different topographic positions.

Equipment for soil water and groundwater monitoring.

5.1 Introduction

Transpiration by terrestrial vegetation is a dominant flux in the global water cycle, accounting for 60–80% of total evapotranspiration on land (Schlesinger and Jasechko, 2014). In forested ecosystems, transpiration by trees constitutes a significant part of the water balance compared to other vegetation types. Trees can sustain higher transpiration rates during drought periods due to their deep root systems (Chen et al., 2014). The relatively high-water demand for trees makes forested ecosystems vulnerable to climate change. Therefore, it is critical to understand the mechanisms of transpiration and quantify its variation in response to changing environmental factors and water availability, to guide integrated water management. This is needed to predict the effects of climate change in South Africa.

The accurate quantification of transpiration rates is often complicated by the limited knowledge of how stomatal regulation responds to changes in the available energy (Chen et al., 2012). Environmental variables which affect transpiration include solar radiation (R_s), air temperature (T), vapour pressure deficit (VPD), wind speed (u), soil moisture, groundwater, and precipitation (P) (Xu and Yu, 2020). The responses of transpiration to environmental variables have been investigated to characterize the spatial heterogeneity of water fluxes within stands (Chen et al., 2014; Xu and Yu, 2020). These studies aimed to understand the primary driving factors for transpiration in water-limited ecosystems, as well as to determine the extent to which transpiration is controlled by environmental variables. This was done to improve our understanding of the water, energy and carbon exchange between vegetation and the atmosphere, and assess ecosystem adaptation to climate change in arid and semi-arid regions (Xu and Yu, 2020). These studies found that the spatial and temporal variations of solar radiation, temperature, windspeed, *VPD*, and rainfall influence the variations of transpiration (Xu and Yu, 2020).

Another important factor that affects tree water use is water availability, in the form of soil water and groundwater (Hou et al., 2018). In the field of ecohydrology, further work is needed to understand plant-soil-water interactions across a wide range of environmental conditions. The impacts of topography, vegetation and soil properties on subsurface rainfall redistribution have been focal issues for studies on water use in semi-arid areas (Li et al., 2015; Zhang et al., 2010). As a result, the dynamics of soil water have been found to influence plant water use relations (Bell et al., 2010). Soil water content

(SWC), relative extractable soil water (REW) and soil water potential (Chen et al., 2014; Li et al., 2017; Song et al., 2020) are used for determining the effects of soil water supply on plant transpiration. Thus, there is a need to understand how the spatio-temporal variation of SWC affects tree water use at different locations.

In arid and semi-arid regions where water is limited, there are complex feedback mechanisms between transpiration rates and groundwater dynamics (Zhang et al., 2020). The spatio-temporal variations of plant water use patterns can be largely determined by variations in groundwater availability. Consequently, the work by Loheide et al. (2005), Dzikiti et al. (2017), and Yang (2018) illustrated that trees sometimes extend their roots and behave like groundwater pumps and therefore affect and change the local hydraulic gradient leading causing changes in groundwater-surface water processes. However, there is a limited understanding of the role that tree water use affects variations in groundwater. To test this hypothesis, the early work by White (1932) attributed diurnal fluctuations of shallow water tables to groundwater consumption by phreatophytes. Since then, diurnal fluctuations in groundwater levels have been used to estimate evapotranspiration (ET). Due to the highly complex nature of this relationship, there is uncertainty about whether trees are dependent on groundwater, soil water, or stream water for growth (Pettit and Froend, 2018). Research has shown that the upward flux of groundwater into the root zone depends on several factors including the depth of the water table, soil hydraulic properties, vegetation types, evapotranspiration demand, and root development (Xu et al., 2016). Transpiration rates will differ depending on the depths of the water table and soil conditions. However, the effects of water table fluctuations on vegetation transpiration can be site and species-specific and remain poorly understood (Xu et al., 2016). This study seeks to understand these impacts at sites where *Acacia longifolia* stands occur.

The relationship between transpiration and water availability can be explained in two ways. Understanding the effect of stand transpiration on soil water, and groundwater variability in different locations is crucial for (i) improving the knowledge of how tree water use patterns are affected by spatial variation of water availability, or (ii) conversely, how transpiration affects the variation of soil water and groundwater in different topographical positions. Even though the influences of soil water and groundwater on transpiration are largely well understood. There are uncertainties in the relations between

transpiration rates and the spatial variation in available soil water and groundwater in different topographic positions i.e., lowlands, mid-slopes, and upland (headwater) regions. Moreover, little is known about whether *A. longifolia* stands are (a) water limited in some locations, (b) utilizing shallow groundwater, or (c) different in water use patterns between species occurring in wetter and drier areas of the landscape. This study will analyse the relations between transpiration patterns by *A. longifolia* stands and water availability and estimate evapotranspiration from groundwater (ET_g) in areas dominated by *A. longifolia* stands.

5.2 Methods and materials

This study required meteorological data, soil water and groundwater variations from the different topographic positions invaded by *A. longifolia* within the Nuwejaars Catchment. Four study sites in different topographic positions were selected. In the context of this study, topographic positions relate to the differences in elevation. Whereby, the selected sites were in the lowland, mid-slope, and uplands of the catchment. The installation of soil water sensors followed the installation of sap flow systems. The sap flow systems were installed in October 2018, while soil water monitoring started in February 2019. Thereafter, the piezometers were installed and started collecting data in June 2019. Since the monitoring of different components started at different times, a period that had transpiration, soil water, and groundwater data was selected for this analysis.

5.2.1 Study site

This study was conducted in the Nuwejaars Catchment in the Cape Agulhas region of the Western Cape Province which falls within the Breede-Gouritz Water Management Area. The study area, site descriptions, experimental setups, and the criteria used for selecting sites are explained in detail in chapter 2.

5.2.2 Sap flow measurements

Stand transpiration rates of each site were measured using the heat pulse velocity of the heat ratio method (as explained in chapter 4).

5.2.3 Monitoring microclimate

Weather data were collected from three automatic weather stations within the catchment.

The location and criteria used for selecting these stations are explained in chapter 4.

5.2.4 Soil water and groundwater measurements

i. Soil water content monitoring

Adjacent to the sap flow monitoring systems, SWC was monitored at various depths, up to a depth of 1 meter, where most of the *A. longifolia* roots were observed. Based on site observations, A. *longifolia* trees do not have tap roots and are primarily dominated by lateral roots. The depths where sensors were installed at each site are shown in Table 5.1.

Table 5.1: Soil water sensors installation depths with minimum and maximum average soil water content at the study sites.

Site names	Depths of soil sensor installation (cm)	Minimum and maximum average SWC (m^3/m^3)
Moddervlei	10,25,50,75, and 100	0.05 and 0.35
Jan Swartskraal	10,30,50,70, and 90	0.05 and 0.35
Spanjaardskloof	10,30,50,70, and 90	0.02 and 0.12
Sandfontein	10,20,30,40, and 100*	0.05 and 0.29

*The rocky surface below 40 cm depth at Sandfontein resulted in the sensor at 100 cm being installed vertically.

SWC was monitored to determine the effects of soil water variation on transpiration rates by *A. longifolia* during the period from February 2019 to November 2021. As the COVID-19 lockdown came into effect in March 2020, there were often difficulties in organising field visits. As a result, there are gaps in data at Spanjaardskloof from October 2020 until April 2021 that was caused by discharged batteries from the data logger during that period. The missing data from March 2021 at Sandfontein resulted from a faulty data logger and data could not be retrieved (Figure 5.1).

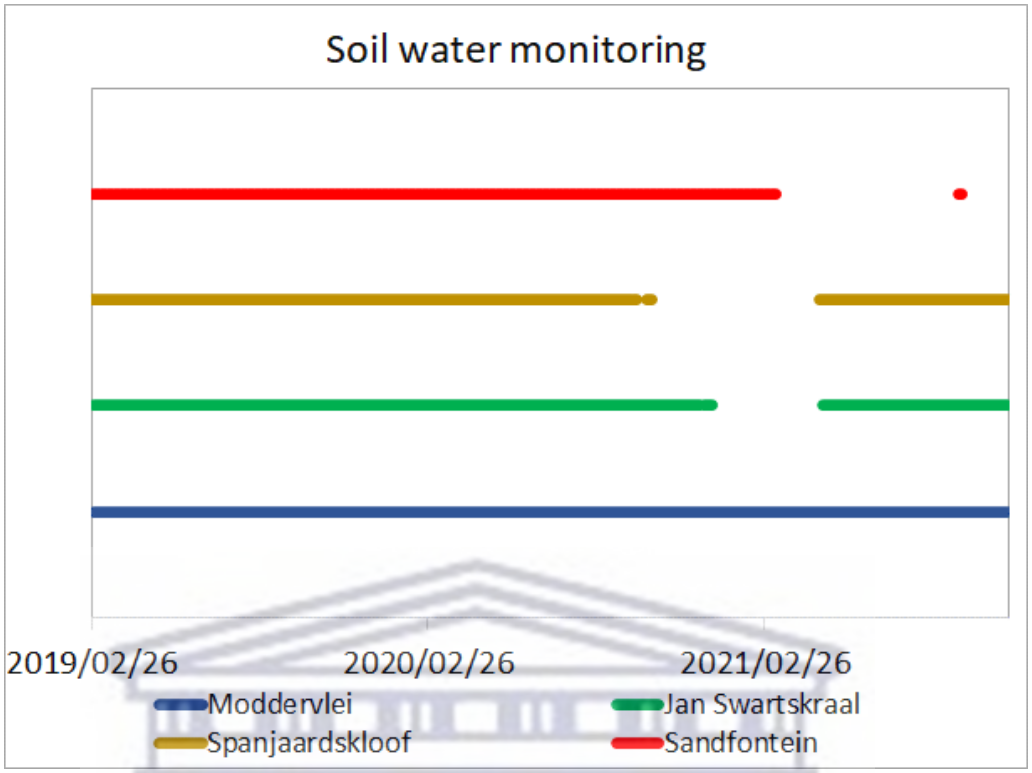

Figure 5.1: Soil water monitoring period at the study sites.

SWC was monitored using 5TE decagon sensors (Decagon Devices, Inc., NE, USA) connected to a data logger (Em50) and programmed to collect data at 60-minute intervals from February 2019 to November 2021 (Figure 5.2). The 5TE decagon sensors measured hourly temperature (°C), EC (mS/cm), and volumetric water content (m^3/m^3). The sensors measure the dielectric permittivity of the soil medium which is related to the volumetric water content. The 5TE decagon sensors use a 70 MHz frequency, which minimises salinity and textural effects, and thus improves its accuracy in most soils (Kanso et al., 2020).

After the installation of sensors into the undisturbed soil of the excavated soil pit wall, sensors were scanned to check if they worked properly. Thereafter, the pit was backfilled taking into consideration the sensitivity of the sensors and cables. Backfilling was done with the disturbed soil material that was stacked next to the pit during excavation in piles ordered by depth. The procedure was done to ensure the backfilling of the pit resembled the natural state and the layering of the surrounding undisturbed soil, to minimize preferential flow.

Figure 5.2: Decagon soil water sensors installed at various depths (left) and the Em50 data logger (right).

The water-holding capacity of soils is affected by soil texture and bulk density. Therefore, at each site, disturbed and undisturbed soil samples were collected at the depths where soil water was monitored. Wet conditions during sample collection led to pit collapse at Moddervlei such that samples could only be taken to 70 cm depth. At Spanjaardskloof, unconsolidated dry sand also restricted the collection of soil samples below 70 cm depth due to collapse. At Sandfontein, the surface was rocky below 40 cm depth and thus was difficult to get samples below 40 cm.

ii. Soil water analysis

Volumetric soil water content (m^3/m^3) was converted into mm of water stored in each soil layer. This conversion method was also used by Klaus (2013) using:

$$S_w = [\theta * S_t] * 1000 \qquad (5.1)$$

Where S_w is the soil water stored (mm), θ is the measured volumetric soil water (m^3/m^3), and S_t is the layer thickness (m). This method takes into consideration the SWC measurements taken at various depths. The total soil water storage for the shallow ($S_{shallow}$), 0-50 cm and deep (S_{deep}) 50-100 cm soils, were calculated as the sum of soil water stored (mm) in the probe sublayers within these larger layers, where:

$$S_{shallow} = \sum_{i=1}^{n} S_{w_{10}} + S_{w_{25}} + (0.5 * S_{w_{50}}) \quad (5.2)$$

$$S_{deep} = \sum_{i=1}^{n} (0.5 * S_{w_{50}}) + S_{w_{75}} + S_{w_{100}} \quad (5.3)$$

Since soil water monitoring began in February 2019, rainfall measured from the 1st of March to the 28th of February the following year was used to determine the annual total rainfall received during the soil water monitoring period. The year 2021 will only include rainfall data from the 1st of March 2021 until the 17th of November 2021, when both sap flow and soil water monitoring ceased.

iii. Groundwater monitoring

To monitor water table fluctuations, a network of monitoring boreholes in the upland (headwaters), mid-slopes and lowlands were drilled, piezometers were hand-augured in the riparian sites (Table 5.2). To monitor groundwater levels at hourly intervals, the solinst water level data loggers (Model 3001, Georgetown, ON, Canada) were installed in the boreholes and piezometers. The average depth to water table was very shallow (<1.0 m) on the headwaters (Sandfontein) and lowlands (Moddervlei) compared to the mid-slope site, Spanjaardskloof (~ 4.2 m) (Table 5.2).

Table 5.2: Piezometers and boreholes for groundwater monitoring from June 2019 until October 2021 period.

Site names	Piezometer or borehole ID	Piezometer or borehole depth (m)	Distances from the sap flow system (m)	Average depth to the water table (m)
Moddervlei	Pz1	3	12	1.42
	Pz2	3	9	1.17
	Pz3	3	6	1.21
	BH8	8	25	1.74
Jan Swartskraal	Pz4	2.5	4	0.77
	BH24	50	27	3.95
	BH25	7	23	4.46
Spanjaardskloof	BH9	60	20	4.22
	BH10	20	22	4.29
Sandfontein	BH28	50	10	0.53
	BH29	11	12	0.91

*Pz and BH represent the piezometer and borehole

In the lowland (Moddervlei) and mid-slope (Jan Swartskraal) riparian sites, piezometers were installed to monitor shallow (up to 3 m) groundwater tables (Figure 5.3). A borehole in this study refers to a deep hole drilled for monitoring the water table, whereas a piezometer is a shallow hole augured by hand.

Figure 5.3: Typical hand-augured piezometer (left) and drilled boreholes (right) at sites to monitor water table fluctuations.

A study by Mazvimavi et al (2021) showed the following drilling profiles at the study sites:
i) Moddervlei site has silt occurring in the top 1 m, followed by 3 – 10 m clay, and then underlain by shale formation. Piezometers 1 to 3 at Moddervlei were augured to 3 m depth as it was difficult to hand-auger through the clay layer.
ii) The mid-slope riparian site at Jan Swaartkraal has coarse-grained sandstone for the first 2 m, followed by shale from 2 to 29 m, and medium-grained sandstone up to 50 m. The piezometer at Jan Swartskraal (Pz4) was 2.5 m deep as it was difficult to hand auger below the fine-grained shale mixed with water as the water table level was at 1.5 m depth during the installation period.
iii) At Spanjaardskloof, BH9-60m and BH10-20m are in weathered and fractured sandstone.
iv) At Sandfontein, the lithology of the site is as follows (Mazvimavi et al, 2021);

- Sandy soil 0 – 1 m.
- Weathered sandstone 2 – 3 m.
- Fractured sandstone 4 – 10 m.
- Sandstone 12 – 40 m.
- Shale 41 – 47 m.
- Hard sandstone 48 – 50 m.

Sandfontein's piezometer installation failed due to weathered rocks below 40 cm depth, which made auguring difficult. There was also a confining layer below 1 m depth at Sandfontein.

The hourly depth to water table data was used to relate the diurnal variations in transpiration rates by *A. longifolia* trees located close to the monitored boreholes. Therefore, diurnal water table fluctuations can be considered a diagnostic indicator of groundwater consumption by phreatophytes (Butler et al., 2007) in cases where transpiration withdrawal exceeds the rates of groundwater inflow at the site. The impacts of stand transpiration on the water table were estimated using a method that analyses diurnal trends in hydrographs constructed from boreholes and piezometers neighboring the sap flow monitoring systems (White, 1932). In the absence of rainfall events, and/or stream-stage changes, the diurnal pattern of water use by plants produces a readily observable pattern of fluctuations in the depth of the water table (Loheide et al., 2005b).

The installation of piezometers was done in June 2020. Therefore, groundwater monitoring was between June 2020 after the installation until November 2021 when the sap flow experiment ceased (Figure 5.4)

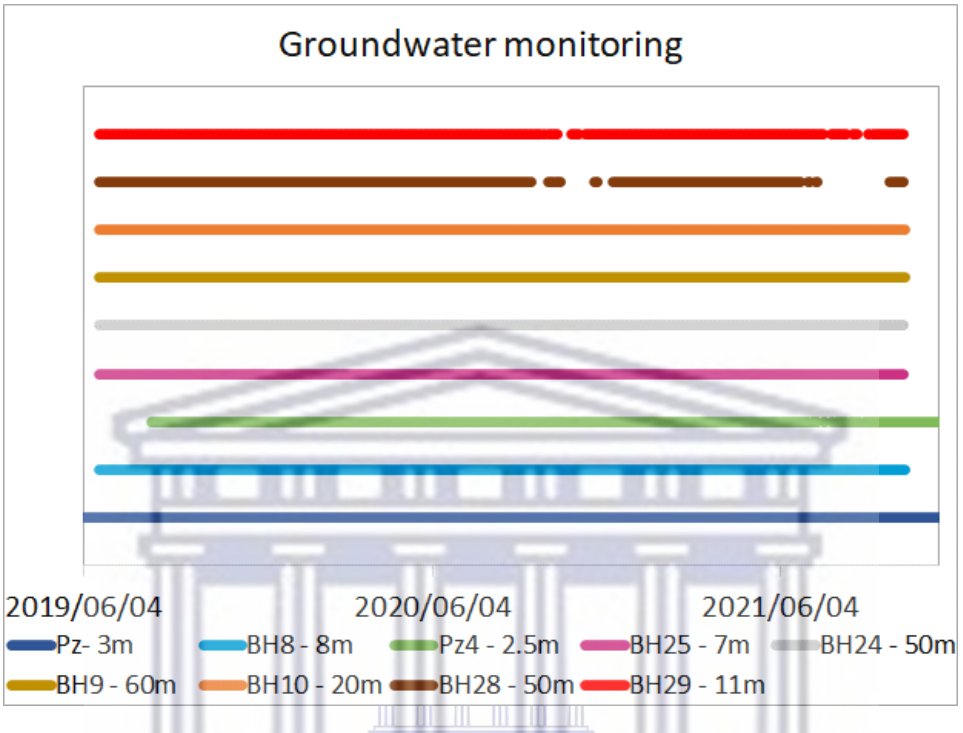

Figure 5.4: Groundwater monitoring period from a network of boreholes and piezometers in the catchment.

iv. Groundwater analysis

To assess the effects of transpiration on groundwater, an extended period without rainfall was selected to examine any diurnal patterns in the water table that can be considered due to transpiration. The assumption was that groundwater inflow would be relatively slower than plant water extraction, so the effect on the water table would be noticeable. For this analysis, hourly transpiration, and water table fluctuations during the 20 – 30th November 2019 period were selected to investigate the impacts of tree water use on the water table fluctuations using the White (1932) method:

$$ET_g(t) = S_y * (R\ (t) \pm \Delta S(t)) * 1000 \qquad (5.4)$$

where ET_g *(t)* is the consumption of groundwater for transpiration over 24 hours (mm/day). *ΔS (t)* is the daily change in storage (m/day), *ΔS (t)* is positive when the water table rises and becomes negative when it drops, and *R (t)* is the rate of the water table recovery (m/night) during times when evapotranspiration becomes negligible. *Sy* is the depth-dependent specific yield (dimensionless) of the subsurface material (Loheide et al., 2005; Lv et al., 2021). *Sy* for water table close to the surface (< 1m) was estimated using:

$$Sy = (\theta_s - \theta_r) * DTW(t) \quad (5.5)$$

This means, the closer the water table is to the surface, the smaller (close to zero) is *Sy* because the capillary fringe has no storage (Lv et al., 2021). When the water table was deep (>1m), the capillary fringe was ignored (Fan et al., 2014) and *Sy* was:

$$Sy = (\theta_s - \theta_r) \quad (5.6)$$

Where θ_s is the maximum water content that the material can hold, θ_r is the residual water content estimated using the material texture and bulk density from the collected soil samples. This information was used on the retention curve (RETC) model (van Genuchten et al., 1991), and *DTW (t)* is the measured depth to the water table. The water content between two equilibrium moisture profiles changes with the depth of the water table (Lv et al., 2021). The closer the water table is to the ground surface, the smaller the specific yield will be. Specifically, because the capillary fringe zone has little or no storage capacity, the specific yield is almost equal to zero once the water table is close enough to the ground surface (Lv et al., 2021). The assumptions of the White method are (i) diurnal water table fluctuations result from plant water use, (ii) groundwater consumption by plants is negligible between midnight and 4 A.M, and (iii) a constant rate of flow into the near-borehole region occurs over the entire day; that is, impacts of recharge events, cyclic pumping, etc. are assumed negligible (Loheide et al., 2005, Butler et al., 2007).

5.3 Results

5.3.1 Soil texture and bulk density at various depths across the study sites

The soil texture of the unsaturated zone at the study sites was mainly sandy (sand content greater than 90%). The general threshold for bulk density that is ideal for root growth in sandy soils is 1.6 g/cm^3 (USDA,1987). The bulk density at Moddervlei increased with increasing depth, with the highest bulk density of 1.56 g/cm^3 at 50 cm depth (Figure 5.5a). The overall soil type at Jan Swartskraal was sand. The top 10 cm depth was a mixture of sand and clay (6%) and silt was observed from 30 to 90 cm depth, with 10% content observed at 50 cm depth. The bulk density also increased with depth. Similarly, to what was observed at Moddervlei, the highest bulk density of 1.54 g/cm^3 was observed at 50 cm depth (Figure 5.5b). At Spanjaardskloof, the bulk density decreased with increasing depth with 1.38 g/cm^3 observed at 30 cm depth and declined to 1.19 g/cm^3 at 70 cm depth (Figure 5.5c). At Sandfontein, the bulk density decreased between 10 and 20 cm depths (from 1.41 to 1.27 g/cm^3, respectively) and thereafter increased to 1.65 g/cm^3 at 40 cm depth (Figure 5.5d). The riparian sites had a mixture of sand and silt content, especially between 50 to 90 cm depths. The non-riparian sites had a mixture of sand and clay.

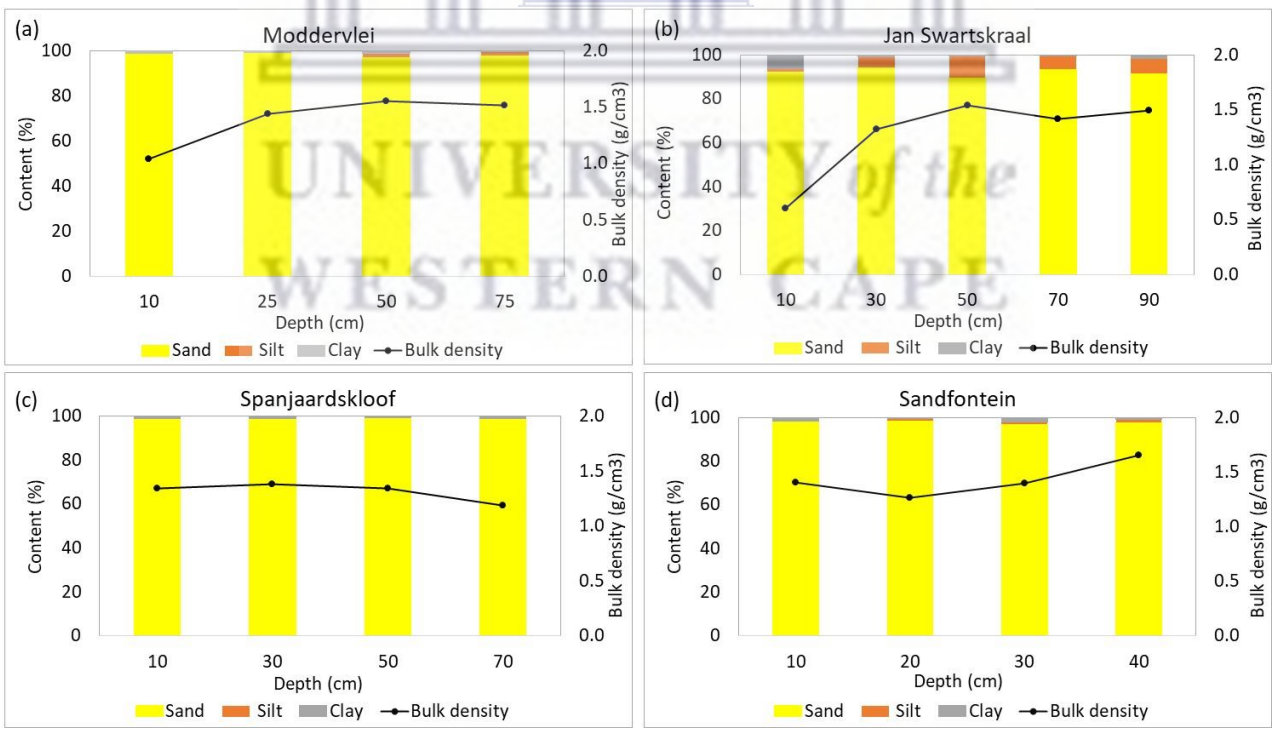

Figure 5.5: Classification of soil textures and bulk densities at various depths across the study sites.

5.3.2 The response of soil water to rainfall

As explained in the methodology, the monitoring of soil water content began in February 2019 and continued until November 2021. Generally, the annual rainfall increased from 2019 to 2021 (Figure 5.6). In total, over the 2 year-8months period, the headwaters received 21% and 28% more rainfall than what was received in the lowland (Moddervlei) and mid-slope (Spanjaardskloof) of the catchment, respectively. During this period, across all stations, May 2021 had the highest rainfall across the sites, where Moddervlei received 239 mm/month, 196 mm/month at Spanjaardskloof, and 273 mm/month measured at Sandfontein (Figure 5.6).

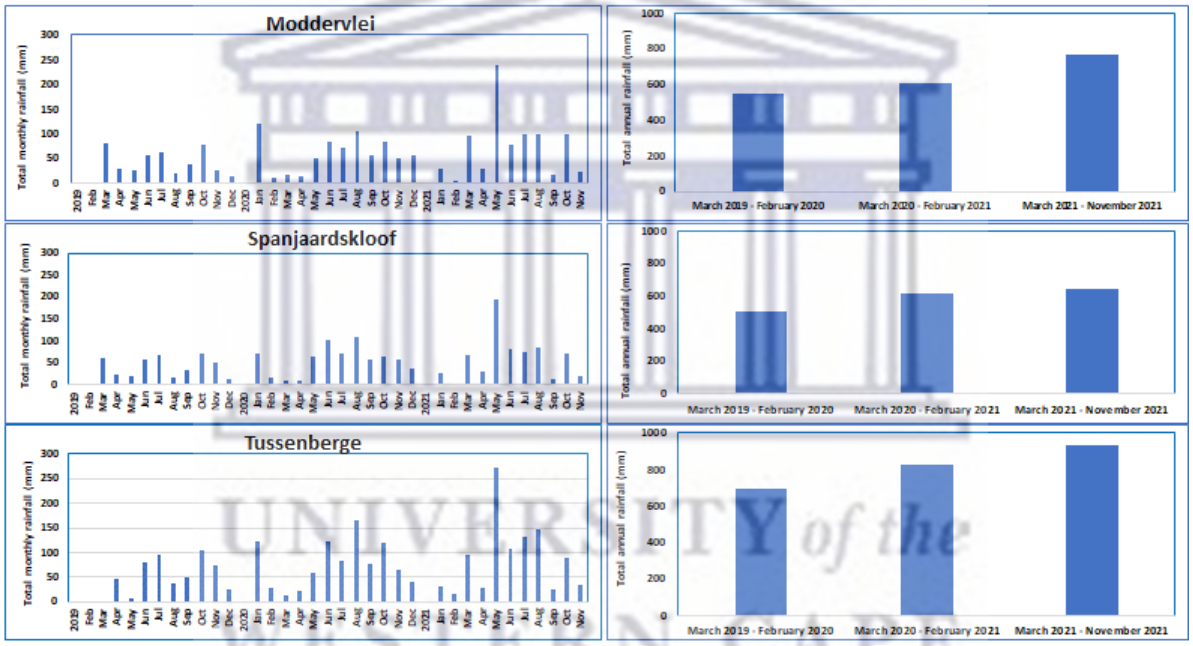

Figure 5.6: Monthly and annual rainfall from February 2019 to November 2021 period at the sites.

The shallow and deep soil layers responded differently to the rainfall events across the sites. At Moddervlei, large increases in SWC measured in the deep soil layers were observed in June 2019, June 2020, and May 2021 (Figure 5.7). SWC in the shallow layers had minor changes in June 2019 but showed notable responses in May-June 2020 and May 2021. These results illustrate that the deep soil layers at Moddervlei had higher SWC than the shallow soil layers.

In the mid-slope riparian site, at Jan Swartskraal, increases in SWC in the deep soil layers were observed from 96 mm in July 2019 to 176 mm in November 2019. Thereafter, the deep soil layers maintained higher SWC than the shallow soil layers throughout the monitoring period (Figure 5.7).

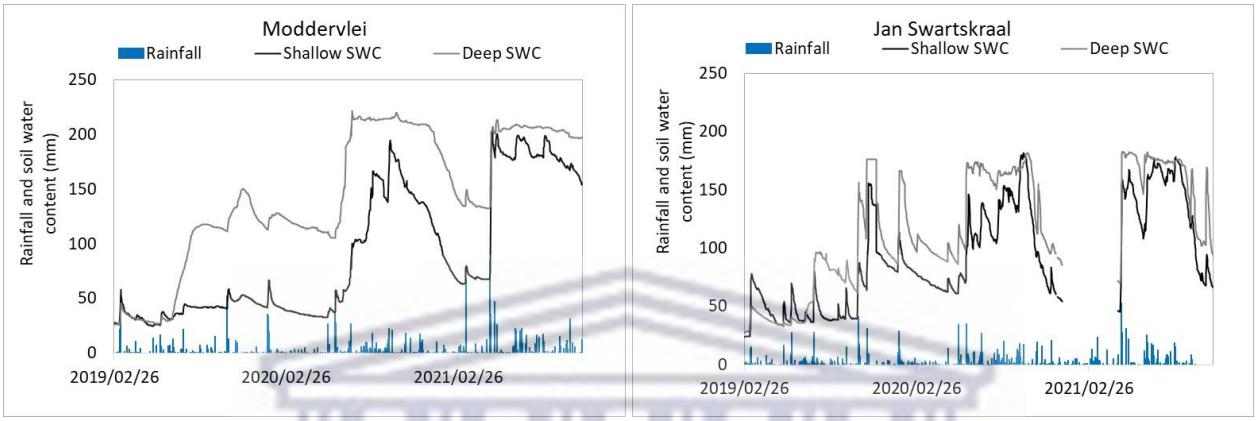

Figure 5.7: Moddervlei and Jan Swartskraal's daily soil water content response to rainfall in the shallow (0 – 50 cm, black) and deep (50 – 100 cm, grey) soil layers during February 2019 to November 2021 period.

Spanjaardskloof, a mid-slope hillslope site, received the least rainfall during the monitoring period. As a result, SWC measured at this site was relatively lower compared to the other sites. In contrast to the fast responses that were observed in deep soil layers at the riparian sites, Spanjaardskloof's deep layer only exhibited the highest response during the May 2021 rainfall event, resulting in a change from 14 mm (2021/05/04) to 66 mm (2021/05/23), while the SWC in the shallow layers increased from 6 mm (2021/05/04) to 52 mm (2021/07/21) (Figure 5.8).

Despite Sandfontein's higher rainfall than other sites, shallow soil layers had a higher SWC than deeper soil layers for most periods, except from September to November 2020. The low soil water storage at the site coincided with the rock layer observed below the 40 cm depth, leading to a very shallow soil layer (Figure 5.8).

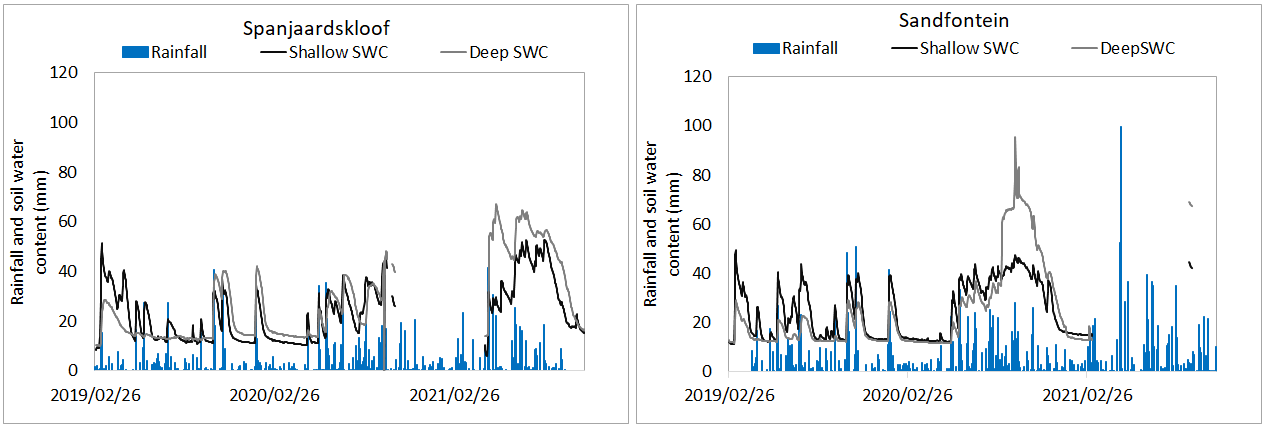

Figure 5.8: Spanjaardskloof and Sandfontein's daily soil water content response to rainfall in the shallow (0 – 50 cm, black) and deep (50 – 100 cm, grey) soil layers during February 2019 to November 2021 period.

5.3.3 Seasonal response of soil water to tree water use

The SWC in deep soil layers was higher than in shallow layers at riparian sites (Moddervlei and Jan Swartskraal) from July 2019, but transpiration patterns varied according to season, with increased rates during dry summers and a decline during winters (Figure 5.9). As a result of the missing data at Jan Swartskraal, these variations were not visible. On the 3rd of December 2019, a peak transpiration rate of 14.17mm/day was observed at Modddervlei, and the lowest rate of 0.39mm/day was measured on the 23rd of July 2019. As a result of having access to residual soil moisture stored in the deep soils, riparian trees' transpiration pattern followed the evaporative demand (represented by ETo) that increases during summer and declines during winter.

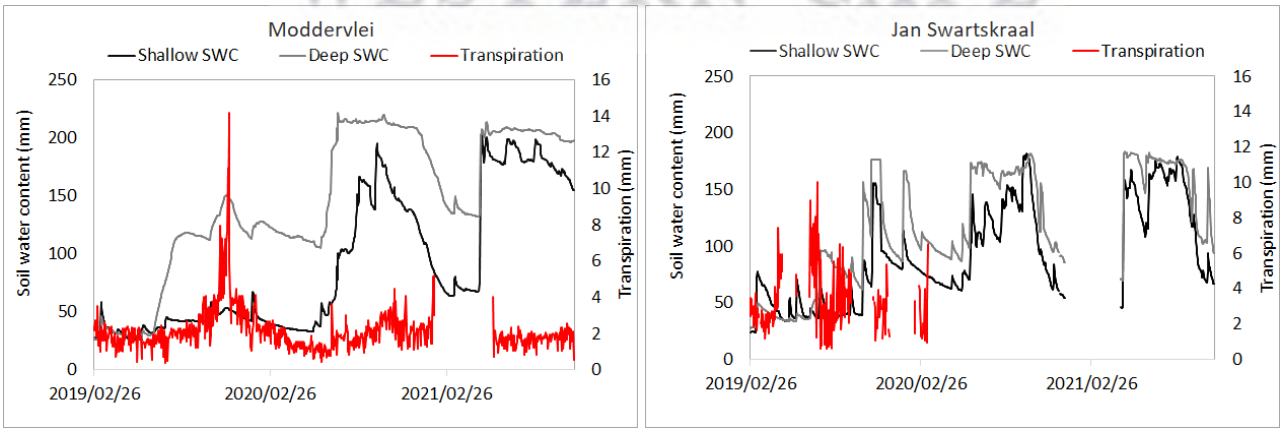

Figure 5.9: Moddervlei and Jan Swartskraal's seasonal response of soil water content to transpiration in the shallow (0 – 50 cm, black) and deep (50 – 100 cm, grey) soil layers during February 2019 to November 2021 period.

In comparison to other sites, Spanjaardskloof recorded the lowest SWC. There were shallow soil layers at Sandfontein, compared to other sites. When SWC was low during the summer season at both sites, low rates of transpiration were observed. This was observed during February-March 2020 when both sites experienced low transpiration rates and SWC (Figure 5.10). This means that although the atmospheric evaporative demand (ETo) was increasing during summer, the transpiration rates from non-riparian (mid-slope and upland) *A. longifolia* decreased as soil water content decreased. During October 2019, January 2020, and May 2021, deep soil layers responded to rainfall and had increased SWC (Figure 5.8). Accordingly, transpiration rates peaked at 4.3 mm/day on the 17th of August 2020 at Spanjaardskloof, and at 10.1 mm/day on the 21st of November 2019 at Sandfontein. Thus, suggesting that rainwater stored in the shallow soil layers was an important source of water for the non-riparian trees.

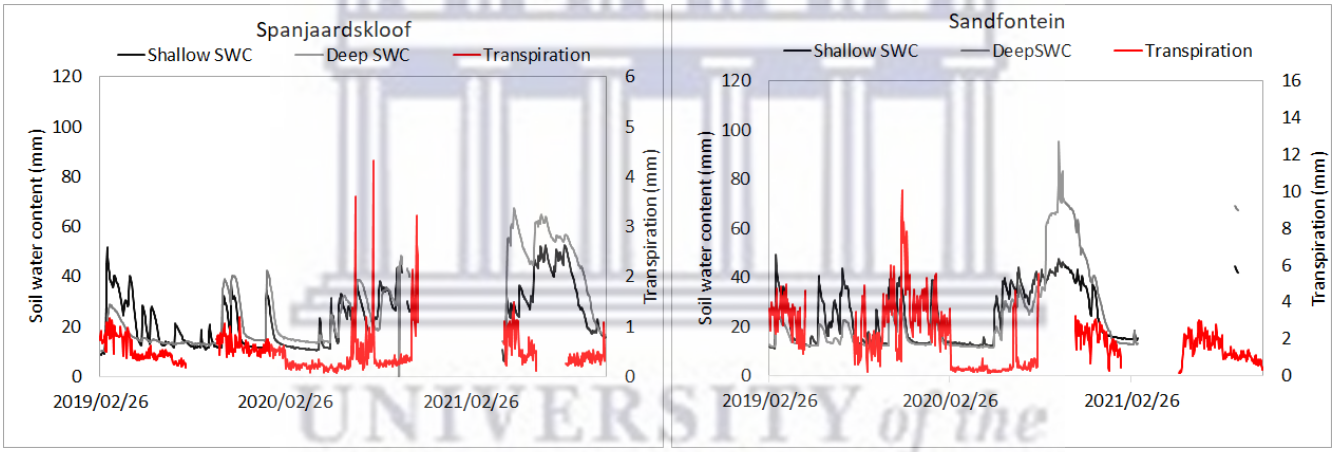

Figure 5.10: Spanjaardskloof and Sandfontein's seasonal response of soil water content to transpiration in the shallow (0 – 50 cm, black) and deep (50 – 100 cm, grey) soil layers during February 2019 to November 2021 period.

These results suggest that the riparian sites, Moddervlei and Jan Swartskraal had higher water use rates than non-riparian mid-slope and upland sites due to the prolonged wetting of deeper soil layers. In contrast, the mid-slope, and upland sites at Spanjardskloof and Sandfontein had increased rates of transpiration during periods when the deep soil layers had high SWC. Moreover, the magnitude of transpiration also differed among non-riparian sites, with higher rates of transpiration at Sandfontein (upland site) than the midslope site at Spanjaardskloof. Thus, suggesting the potential influence of other water sources i.e groundwater at both riparian and non-riparian sites.

5.3.4 The response of groundwater table to rainfall

The increasing annual rainfalls were also observed during June 2019 to October 2021 period, when depth to the water table was also monitored (Figure 5.11).

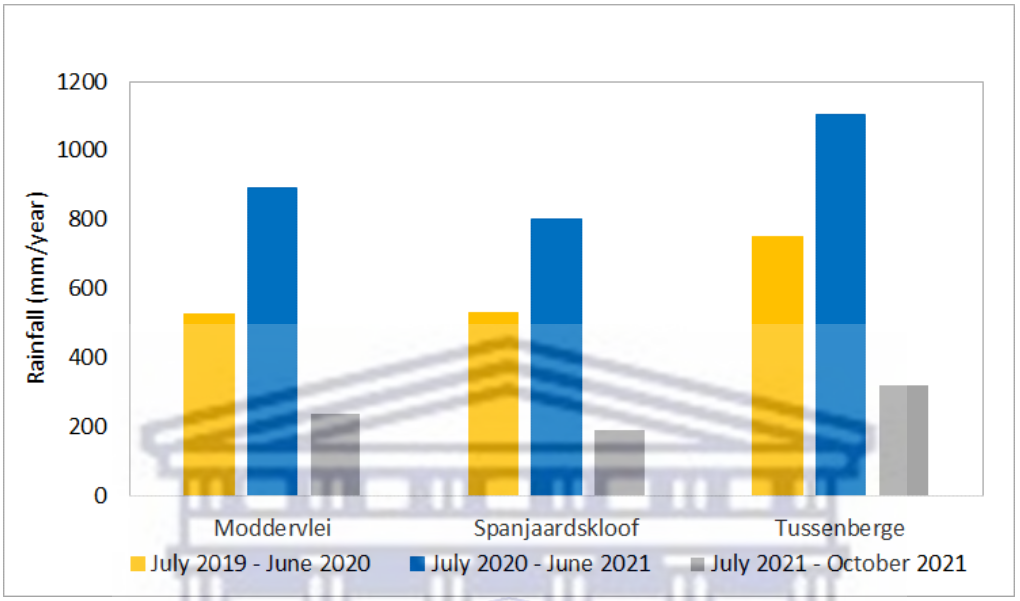

Figure 5.11: Total rainfall across the study sites during periods when depth to the water table, soil water content, and transpiration rates were monitored from June 2019 to October 2021.

As rainfall increased between June 2019 to October 2021, rising water tables were also observed (Figure 5.12). The rising water tables at the riparian sites were observed from late October 2019, and it is also evident that the water table responded to the high rainfall received during 2021, causing the water table to rise to the surface. As alluded to previously, May 2021 had the highest monthly rainfall across the sites. The 147 mm of rainfall received over three days in early May 2021 rose the water table from 1.45 to 0.37 m in Pz-3m and from 2.48 to 0.86 m in BH8-8m at Moddervlei (Figure 5.12). Similar responses were also observed at Jan Swartskraal, where the water table in the piezometer (Pz4-2.5m) ranged between 1.8 m and 0 (surface). The fast response in the water table at these riparian sites is likely responsible for the prolonged wetting of the deep soil layers at these sites (Figure 5.7).

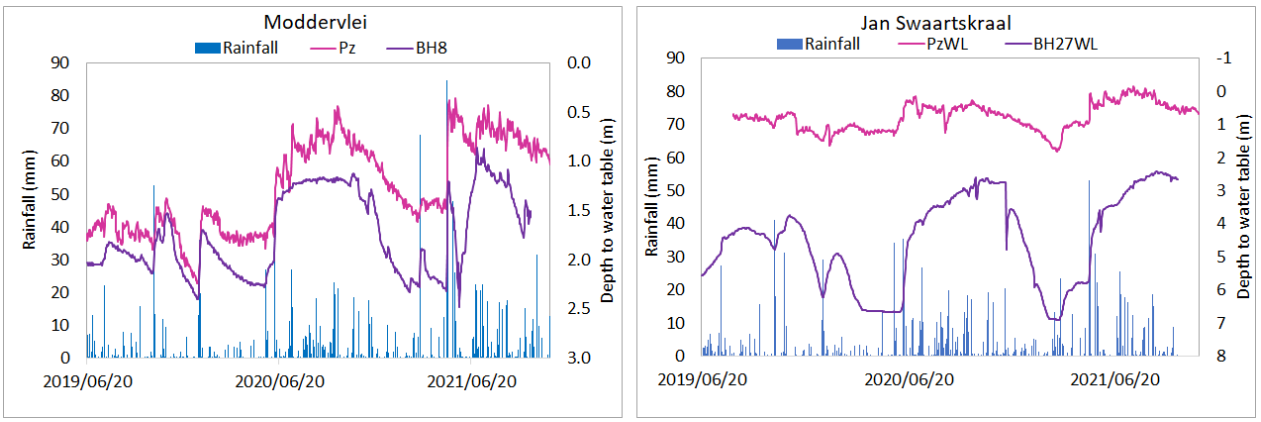

Figure 5.12: Moddervlei and Jan Swartskraal's daily groundwater table response to rainfall from June 2019 to November 2021.

At Spanjaardskloof, the water table in the BH9-60m responds to cumulative rainfall and not individual rainfall events (Figure 5.13). Thus, the response was gradual, the rising water table was mostly observed in early June 2020 from the 58 mm rainfall received over three days (10-12th June 2020) that resulted in a 0.5 m rise in the water table from 5.43 to 4.93 m in BH9-60m. During May 2021, the 123 mm of rainfall received over four days (5-8th May 2021) resulted in the water table rising from 4.75 to 4.31 m. In contrast, the water table in BH10 – 20 m rose rapidly as a response to rainfall greater than 20 mm/day which causes rapid downward preferential flow through fractured rock. A remarkable increase in the water table was observed during the Winter (June) seasons of 2020/2021. The gradual response of the water table during large rainfall events can also explain increased SWC in deep soil layers during large events (Figure 5.8).

The water table in the Sandfontein boreholes varied from about 0 to 1.8 m (Figure 5.13). This was an indicator of the water table's response to rainfall as the site received the highest rainfall among the studied stations. Borehole 28-50m, had a higher water table due to pressure from water flowing from an upslope recharge area (Mazvimavi et al., 2021). The water table in the boreholes declined from November/December to April/May annually, these are periods when transpiration rates were expected to increase. During the study period, the water table was at the surface from the 16th of September – the 9th of December 2020, and from the 25th of June to the 25th of September 2021. The ground surface was observed to be waterlogged during these periods. Thus, the areas that received the most rainfall during the study period, had shallow water tables sometimes

reaching the surface. While at Spanjaardskloof, the water table only reached 1.2 m during the wet seasons.

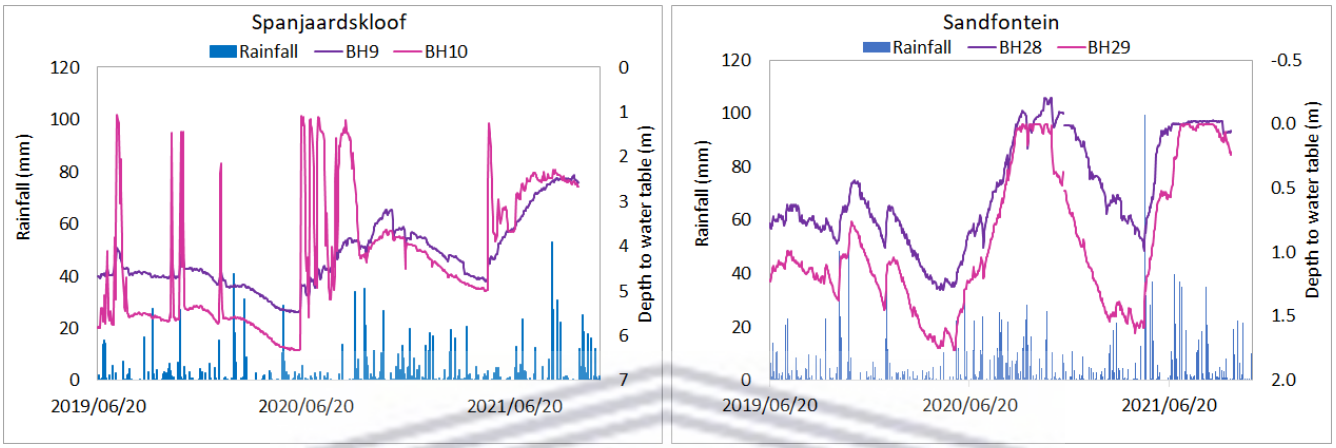

Figure 5.13: Spanjaardskloof and Sandfontein's daily groundwater table response to rainfall from June 2019 to November 2021.

5.3.5 Diurnal response of groundwater to tree water use

During the period of the study, transpiration rates across the study sites were relatively high in November 2019. Between the 20th to the 30th of November 2019 period, no significant rainfall was observed across the sites, only 0.3 mm/day was received at Modderlvei on the 27th of November 2019. This resulted in a 4 mm increase in SWC in shallow soil layers at Moddervlei, while SWC in the deep soil layers across the sites declined during this period. At Moddervlei, the water table and river depth showed 196- and 347-mm decline, respectively. The declining water table in the lowland was more than the 27- and 76-mm decline measured in BH28-50m and BH29-11m in the uplands at Sandfontein. The water table at Spanjaardskloof, was deep compared to the other sites. However, an unexpected 17 mm rise in the water table was observed during the 20th to the 30th of November 2019 period. The highest ETo rates across the sites were measured on the 28th of November 2019, with the highest at 7.1 mm in the headwaters followed by 6.9 mm at the mid-slope site (Spanjaardskloof) and 6.1 mm on the lowlands (Table 5.3).

Table 5.3: Summary of daily ETo, transpiration, soil water, and groundwater variations during the 20-30th of November 2019 period across the study sites. S shallow and S deep are soil water storages estimated for the shallow and deep soil layers using equations 5.2 and 5.3

Moddervlei

Date	ETo (mm)	Transpiration (mm)	Rainfall (mm)	$S_{shallow}$ (mm)	S_{deep} (mm)	DTW in Pz-3m (m)	DTW in BH8-8m (m)	Stream stage (m)
2019/11/20	4.8	4.0	0.0	49.8	142.2	1.392	1.526	1.538
2019/11/21	4.5	5.3	0.0	50.3	143.5	1.426	1.531	1.488
2019/11/22	5.5	4.2	0.0	51.1	145.3	1.465	1.540	1.439
2019/11/23	5.6	6.5	0.0	51.8	147.1	1.474	1.567	1.398
2019/11/24	5.5	7.0	0.0	52.5	148.5	1.474	1.586	1.355
2019/11/25	5.4	7.2	0.0	52.8	149.5	1.489	1.602	1.317
2019/11/26	5.8	5.2	0.0	53.0	150.0	1.513	1.618	1.278
2019/11/27	5.1	7.0	0.3	53.2	150.2	1.543	1.638	1.246
2019/11/28	6.1	7.6	0.0	53.3	150.2	1.597	1.655	1.224
2019/11/29	5.8	7.7	0.0	53.4	150.1	1.612	1.698	1.210
2019/11/30	5.4	11.2	0.0	53.4	149.9	1.588	1.742	1.191

Spanjaardskloof

Date	ETo (mm)	Transpiration (mm)	Rainfall (mm)	$S_{shallow}$ (mm)	S_{deep} (mm)	DTW in BH9-60m (m)	DTW in BH10-20m (m)
2019/11/20	5.2	0.8	0.0	30.5	39.5	4.507	5.324
2019/11/21	4.8	0.8	0.0	29.2	38.9	4.513	5.400
2019/11/22	5.8	0.8	0.0	27.4	38.1	4.511	5.407
2019/11/23	5.3	0.6	0.0	25.2	37.2	4.512	5.408
2019/11/24	5.3	0.6	0.0	22.9	36.1	4.515	5.414
2019/11/25	5.6	0.7	0.0	20.5	34.8	4.513	5.416
2019/11/26	6.1	0.6	0.0	18.6	33.4	4.510	5.414
2019/11/27	5.7	0.6	0.0	17.2	31.9	4.502	5.406
2019/11/28	6.9	1.2	0.0	16.2	30.3	4.488	5.392
2019/11/29	6.0	0.7	0.0	15.4	28.8	4.481	5.378
2019/11/30	4.9	0.6	0.0	14.8	27.2	4.490	5.384

Sandfontein

Date	ETo (mm)	Transpiration (mm)	Rainfall (mm)	$S_{shallow}$ (mm)	S_{deep} (mm)	DTW in BH28-50m (m)	DTW in BH29-11m (m)
2019/11/20	5.0	8.5	0.0	35.8	26.0	0.453	0.797
2019/11/21	4.8	10.1	0.0	34.6	25.2	0.446	0.796
2019/11/22	5.7	8.6	0.0	33.5	24.5	0.441	0.799
2019/11/23	5.4	7.2	0.0	32.1	23.7	0.452	0.814
2019/11/24	5.2	8.3	0.0	30.2	22.8	0.463	0.827
2019/11/25	5.3	7.4	0.0	28.1	21.9	0.462	0.833
2019/11/26	6.1	7.6	0.0	26.1	20.8	0.460	0.838
2019/11/27	5.5	7.1	0.0	24.1	19.9	0.458	0.842
2019/11/28	7.1	5.4	0.0	22.5	18.8	0.445	0.839
2019/11/29	5.8	4.4	0.0	20.7	17.8	0.458	0.854
2019/11/30	5.1	7.7	0.0	18.9	16.7	0.480	0.873

Groundwater abstraction by plants depends on the specific yield (Sy) of the subsurface material. Specific yield is the storage space available in the subsurface material for the loss or gain of groundwater as the water table fluctuates (rise and fall) (Lv et al., 2021; Said et al., 2005). It is an important parameter in the estimation of groundwater evapotranspiration (ETg) from diurnal water-level fluctuation readings (White, 1932; Chen et al, 2010). Thus, the error in the estimation of ETg comes from the uncertainty in determining Sy (Lv et al., 2021) as it varies spatially with soil texture, water table depth, and time (Chen et al, 2010). The lowest Sy was 0.05 and 0.08 estimated from BH28-50m and Pz-2.5m at Sandfontein and Jan Swartskraal, respectively. The low Sy values were explained by average water tables of 0.5 and 0.7 m.b.g.l, respectively. The highest Sy of 0.34 and 0.25 were observed in BH10-20m at Spanjaardskloof and BH24-50m at Jan Swartskraal, respectively (Figure 5.14). This range agreed with Loheide et al. (2005) who indicated a range of Sy from 0.01 to 0.30 in sandy environments, while the review by Lv et al. (2021) established a Sy estimate of 0.35 for sandy soils. Figure 5.14 shows the influence of geology on Sy, where Sy from BH9-60m was 0.12. This was rather unexpected for a deep aquifer system with a water table at 4.5 m.b.g.l. Based on the drilling profiles by Mazvimavi et al. (2021), BH9-60m was drilled on a fractured sandstone material which is highly permeable. This is the same for BH28-50m at Sandfontein which is located on a discharge zone indicated by a water table very close to the surface due to pressure from water flowing from an upslope recharge area.

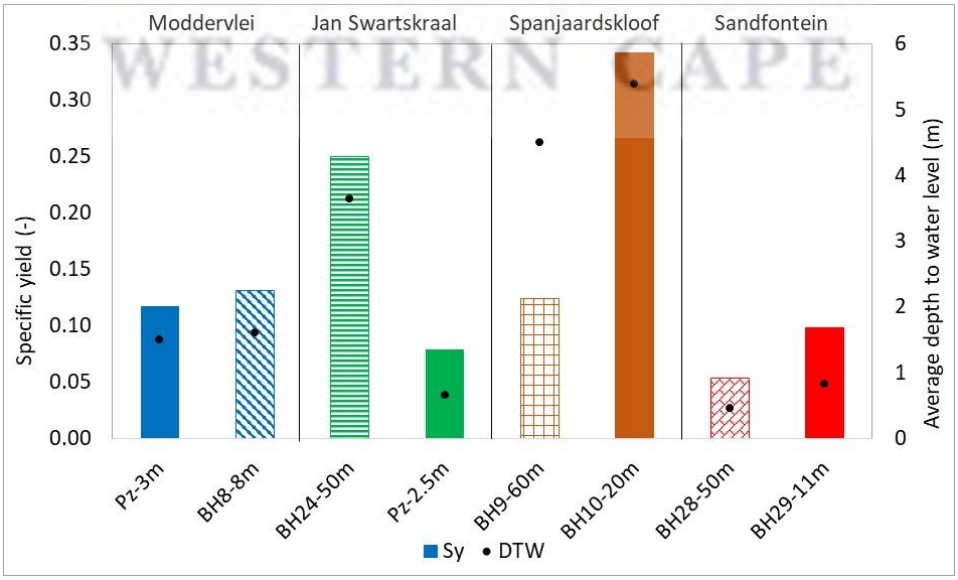

Figure 5.14: The specific yields (Sy) of the subsurface material in monitoring piezometers (Pz) and boreholes (BH) in the Nuwejaars Catchment.

Figure 5.15 to Figure 5.21 shows diurnal changes in the water table depth. This indicates that at each site, transpiration by *A. longifolia* affected groundwater. The decline during the day means that the rate of water abstraction by the plants was greater than the groundwater inflow to the site. If the groundwater inflow rate was greater than the rate of abstraction by trees, water abstracted would be replenished immediately, hence no decline would be observed in the water table. During the night without significant transpiration, the water table recovered due to groundwater inflow. Thus, resulting in diurnal variations observed in the water table.

On average, Moddervlei's water table in the piezometers declined by 21 mm between 08:00 and 16:00 when transpiration rates increased. As transpiration rates declined after 16:00, the water table rose by 13 mm (from 1.52 to 1.51 m) (Figure 5.15). The average decline in BH8 was 15 mm between 08:00 and 16:00 and a 1 mm rise was observed between 16:00 – 23:00. On average, transpiration rates increased by 4.5 mm/day.

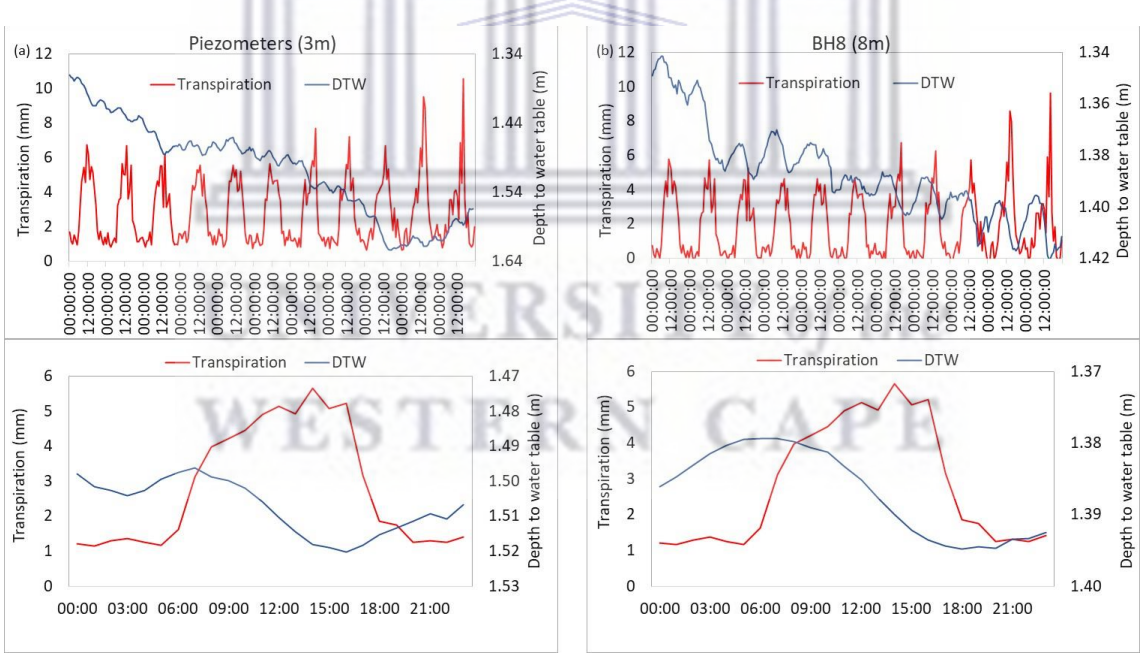

Figure 5.15: Moddervlei's diurnal variations in transpiration and depth to the water table from the 20th to the 30th of November 2019 in the Piezometers (a) and BH8 (b). The bottom figures illustrate the average hourly DTW and transpiration from 00:00 to 24:00 for the selected period.

The average groundwater decline was 21 mm during the 20th to the 30th of November 2019 period at Moddervlei, the highest estimated ET from groundwater (ET_g) was 5.4

mm/day observed in the piezometers (Pz-3m) at Moddervlei (Figure 5.16). This was almost equivalent to average transpiration rates of 4.5 mm during the same period.

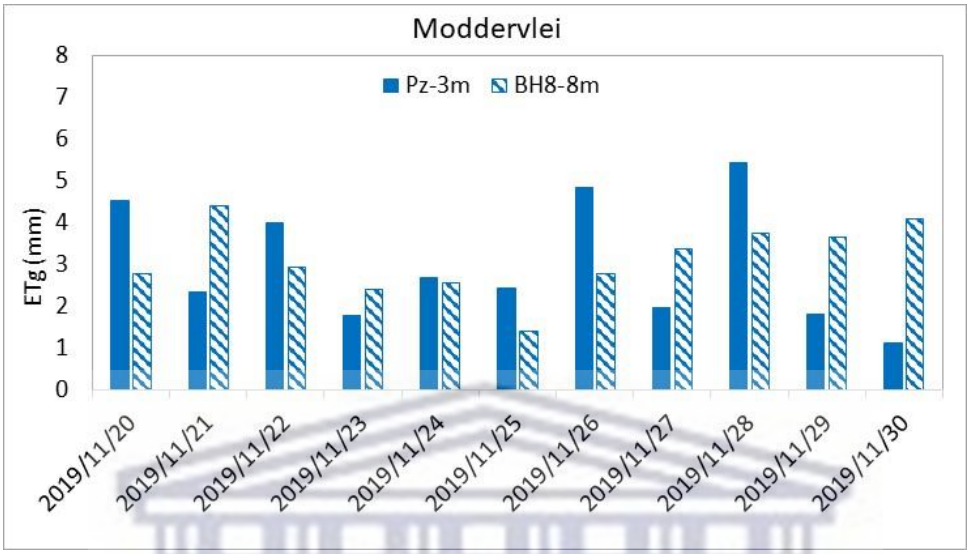

Figure 5.16: Moddervlei's daily evapotranspiration from groundwater (ETg) estimated from the monitoring piezometers (Pz, solid) and boreholes (BH, shaded).

In the mid-slope riparian, diurnal fluctuations differed between the shallow piezometer (Pz4-2.5m) and the deep borehole (BH24-50m) at Jan Swarskraal (Figure 5.17). In the shallow piezometer, the water table declined by 18 mm between 8:00 to 15:00, and then followed by a 23 mm rise between 15:00 to the next day. The water table in the deep aquifer measured from BH24-50m shows a 6 mm rise from 00:00 to 5:00 am. Thereafter, a 6 mm drop in the water table was observed between 05:00 and 13:00. After 13:00, the water table recovered by 5 mm between 13:00 and 17:00, and then followed by a 6 mm decline to the next morning (Figure 5.17). These results suggest groundwater inflow in the deep aquifer system at this site, resulting in a rise in the water table during the day. The average rate of 3.2 mm was observed from 5:00 to 16:00.

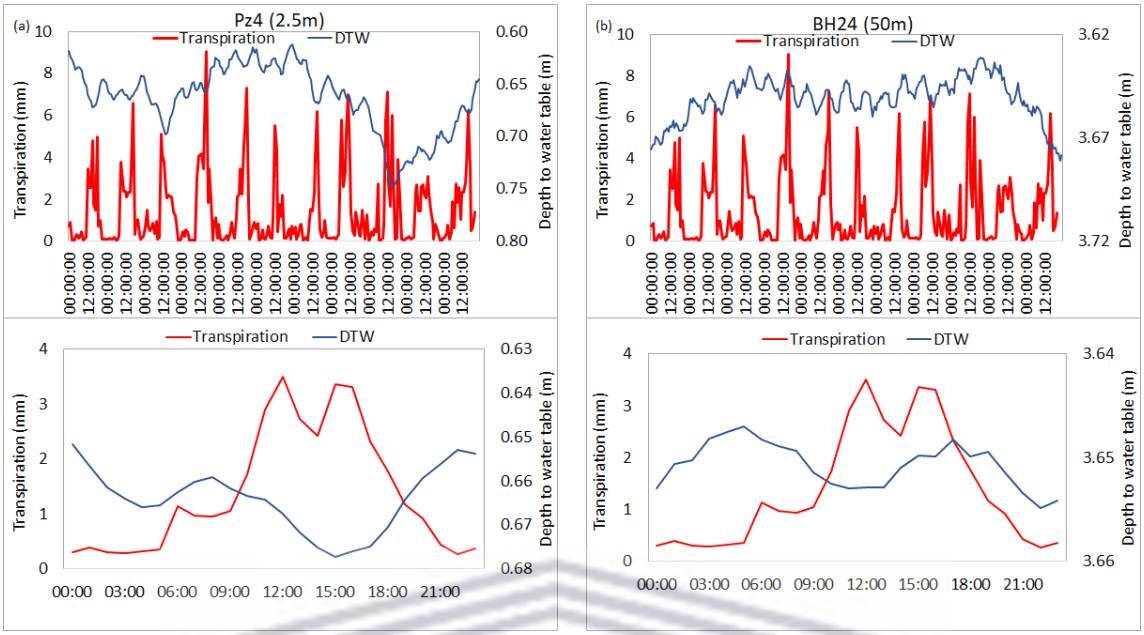

Figure 5.17: Jan Swartskraal's diurnal variations in transpiration and depth to the water table from the 20th to the 30th of November 2019 in the Piezometer (a) and BH24 (b). The bottom figures illustrate the average hourly DTW and transpiration from 00:00 to 24:00 for the selected period.

At Jan Swartkraal, ET_g ranged from 3.0 up to 7.1 mm/day. The highest ET_g were estimated in the shallow piezometer (Figure 5.18). As expected, ET_g was higher in shallow water tables measured in the piezometers at the riparian sites (Moddervlei and Jan Swartskraal).

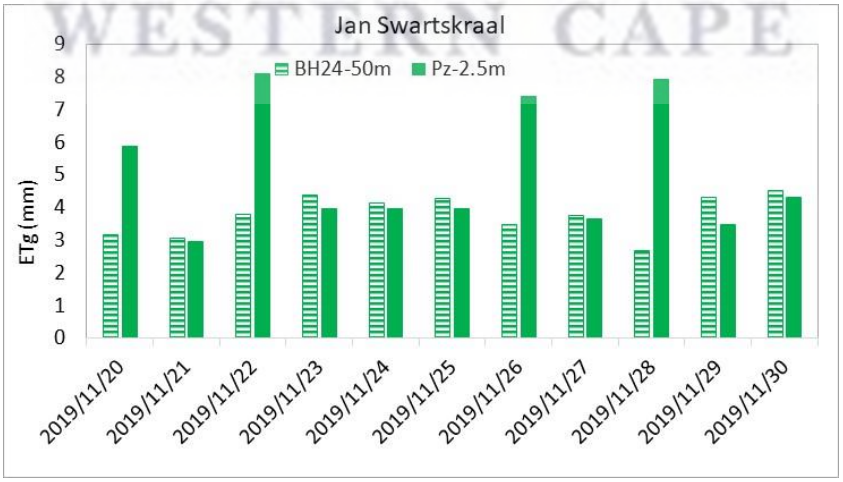

Figure 5.18: Jan Swartskraal's daily evapotranspiration from groundwater (ETg) estimated from the monitoring piezometers (Pz, solid) and boreholes (BH, shaded).

In the mid-slope non-riparian site at Spanjaardskloof, groundwater inflow into the deep aquifer was also observed in BH9 – 60 m. The water table in BH9 – 60 m rose from 4.51 to 4.49 m (~ 20 mm) between 00:00 and 05:00 am. This was followed by 23 mm decline from 05:00 to 12:00. Thereafter, a 12 mm rise was observed between 12:00 and 18:00. After 18:00, the water table declined by 12 mm. Daily average transpiration increase was 0.9 mm at Spanjaardskloof (Figure 5.19).

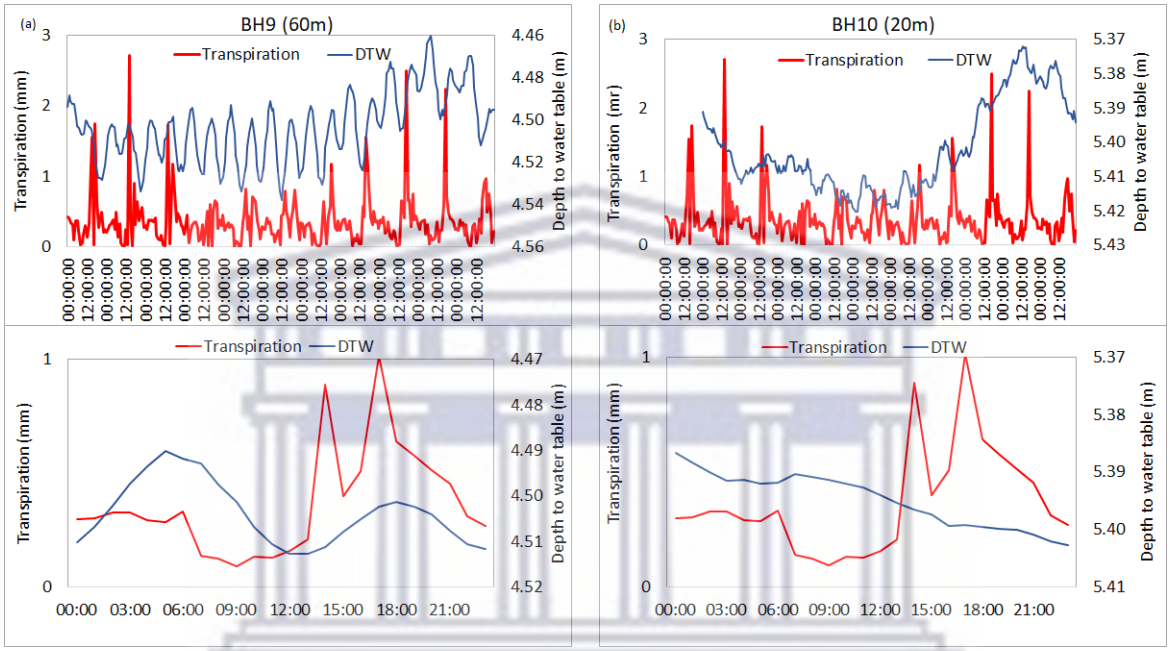

Figure 5.19: Spanjaardskloof's diurnal variations in transpiration and depth to the water table from the 20th to the 30th of November 2019 in the BH9 (a) and BH10 (b). The bottom figures illustrate the average hourly DTW and transpiration from 00:00 to 24:00 for the selected period.

Although low rates of transpiration were measured at Spanjaardskloof. However, ET_g estimates were higher in both shallow and deep aquifers. ET_g ranged between 2.9 and 7.0 mm/day (Figure 5.20). At Spanjaardskloof, higher ET_g estimates (7.0 mm/day) were observed in the deep borehole (BH9-60m) where the water table was ~ 4.5 m. This is the borehole where groundwater inflow was evident in the diurnal variations.

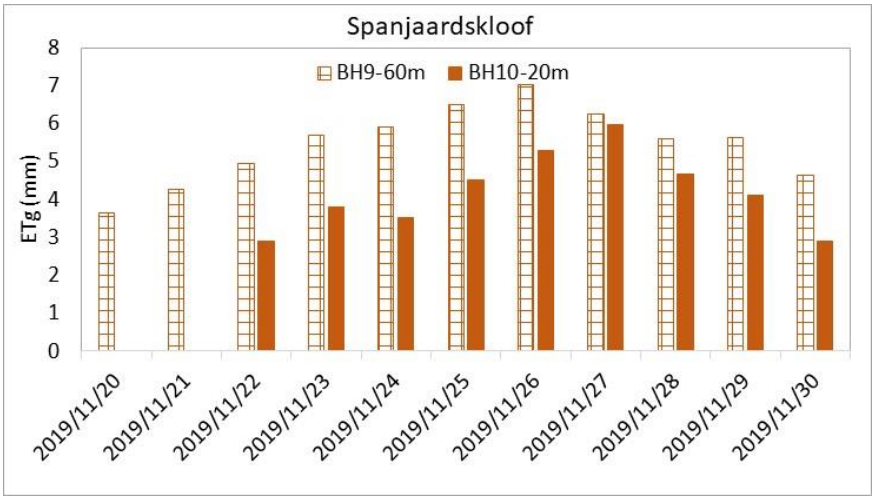

Figure 5.20: Spanjaardskloof's daily evapotranspiration from groundwater (ETg) estimated from the shallow (solid) and deep (shaded) boreholes (BH).

The downslope movement of water was observed in the deep aquifer system located in the uplands at Sandfontein. The water table in BH28-50 m rose by 16 mm between 00:00 and 07:00 and was followed by a 24 mm decline during the day between 07:00 and 14:00. Between 14:00 and 20:00, the water table rose by 18 mm. The shallow aquifer in BH29-11 m shows similar patterns (Figure 5.21). On average, daily transpiration rates increased by 4.1 mm between 08:00 am and 12:00 pm at this site. This was almost equivalent to the average transpiration rate of 4.5 mm measured at Moddervlei.

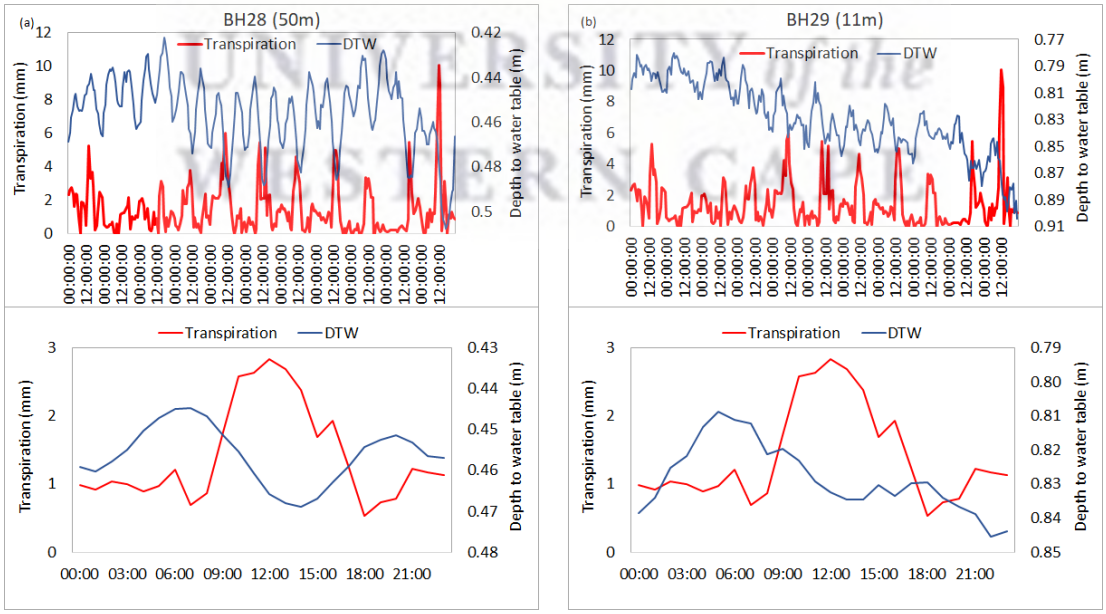

Figure 5.21: Sandfontein's diurnal variations in transpiration and depth to the water table from the 20th to the 30th of November 2019 in the BH28 (a) and BH29 (b) at Sandfontein. The bottom figures illustrate the average hourly DTW and transpiration from 00:00 to 24:00 for the selected period.

At the non-riparian sites, BH29 -11 m at Sandfontein in the uplands had the highest ET_g rate of 6.7mm/day (Figure 5.22). The water table in this borehole ranged between 0.4 and 0.5 m. These results provide evidence which suggests that transpiration by *A. longifolia* stands had a greater impact on shallower water tables in the riparian areas and on the headwaters of the catchment. The higher water table resulted in the capillary fringe having little to no storage capacity, hence the low specific yield observed at these sites.

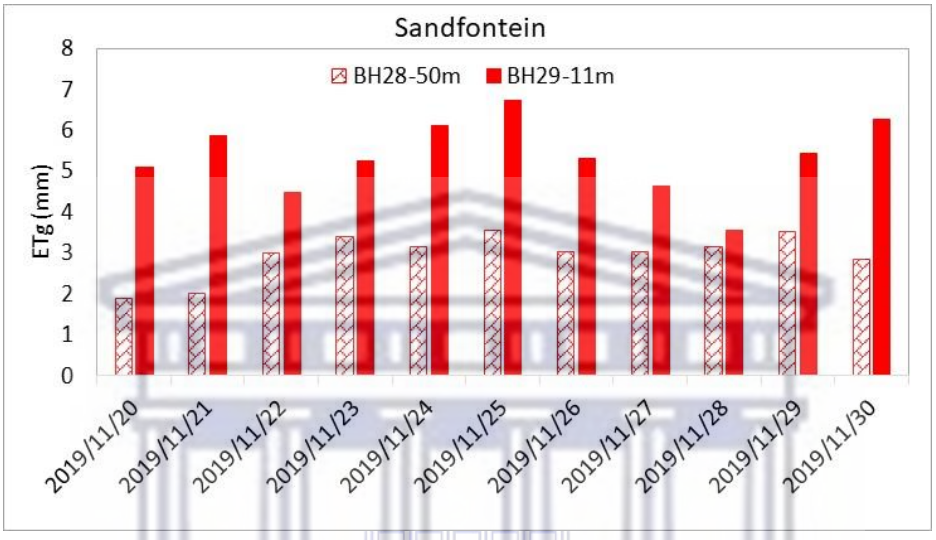

Figure 5.22: Sandfontein's daily evapotranspiration from groundwater (ETg) estimated from the shallow (solid) and deep (shaded) boreholes (BH).

5.3.6 Seasonal response of groundwater table to tree water use.

The rising water tables at the riparian sites were observed from late October 2019 (Figure 5.12). The water table at the riparian site was shallow, ranging between 2.4 m (January 2020) to 0.5m (May 2021) in the lowland, and between 6.6 m (April 2020) to 0 m (on the surface) during May 2021. Although, transpiration showed seasonal variations, with peaks during the dry summer period. At Moddervlei, transpiration peaks also coincided with the rising groundwater table (~ 1.4 m) observed during November 2019 (Figure 5.23). In the mid-slope non-riparian site, at Spanjaardskloof, the gradual response of the water table during large rainfall events was observed. At Spanjaardskloof, transpiration rates peaked at 3.2 mm/day during July 2020, when the water table was at 4.9 and 1.2 m in BH9-60 m and BH10-20 m, respectively. The water table showed a decline between February – March 2020, and transpiration rates were. On the uplands, at Sandfontein, transpiration peaked at 10.1 mm/day during November 2019. This period coincided with the period when the water table was at 0.5 m as a result of October 2019 rainfall (Figure

5.23). Thus, the shallow water table on the uplands explains the higher rates of transpiration compared to the mid-slope non-riparian site at Spanjaardskloof.

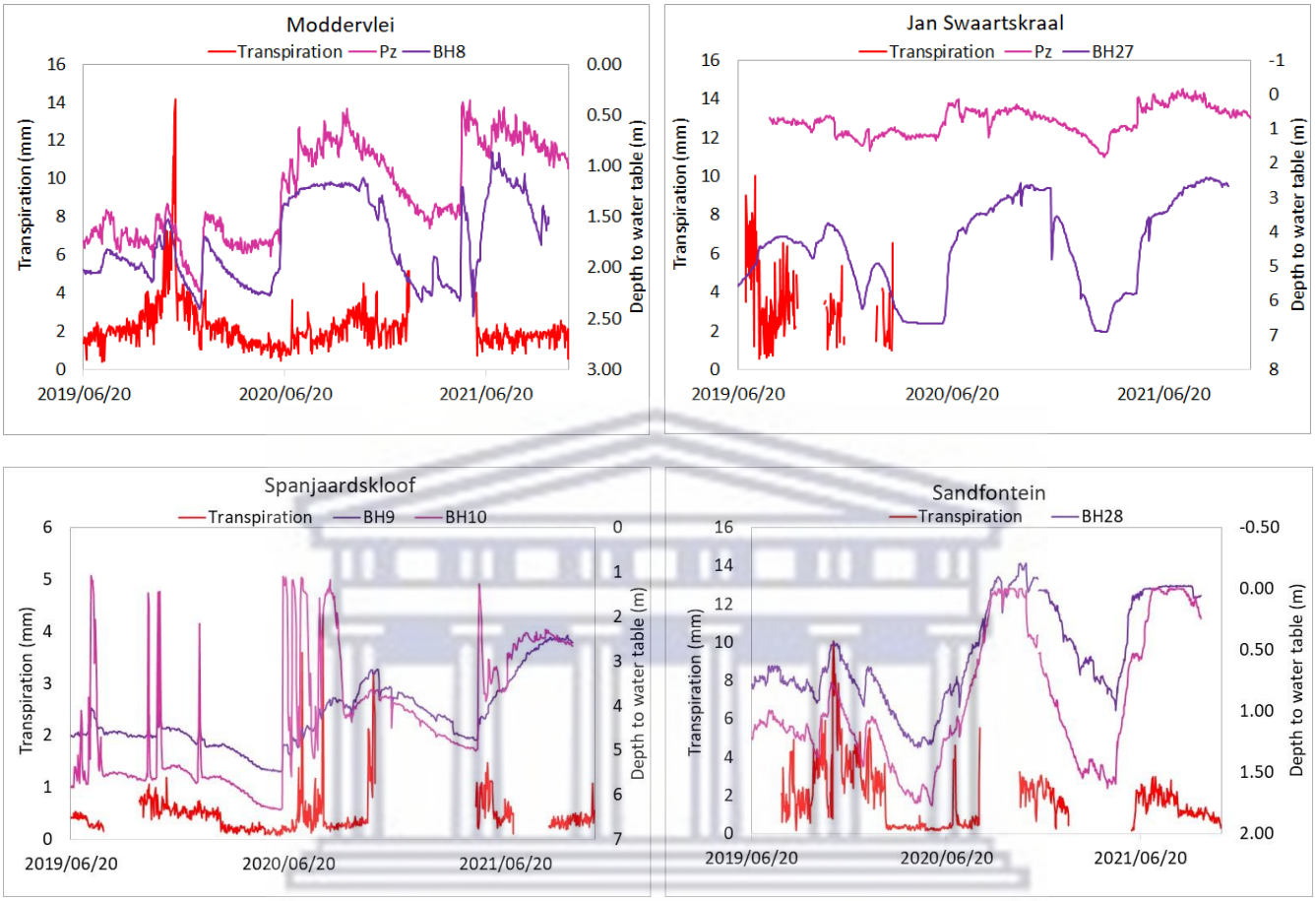

Figure 5.23: Daily response of groundwater to transpiration during February 2019 to November 2021 period.

Based on these results, it is therefore evident that the contrasting rates of water use by *A. longifolia* result from the differences in the water table across the sites in the Nuwejaars Catchment.

5.4 Discussion

The relationships between soil water, groundwater, and transpiration rates in areas that are invaded by *A. longifolia* on different topographic positions in the Nuwejaars Catchment were investigated in this chapter. Specifically, to determine the relationship between transpiration rates of *A. longifolia* stands and the variations in (a) soil water content and (b) depth to the groundwater table.

In the Nuwejaars Catchment, *A. longifolia* stands were mostly dense along the riparian zones and in mountainous parts of the catchment that receive higher rainfall than lowlands (Mtengwana et al., 2020), and in parts that are sandy with low holding capacity, high infiltration and hydraulic conductivity. This agreed with the findings by Morais & Freitas (2012) who demonstrated that *A. longifolia* tends to be abundant and more invasive in the wetter and high-rainfall regions, indicating that *A. longifolia* thrives in areas with moderate to low water stress.

The selected sites for this study all have a sandy soil texture. The responses of sandy soils to rainfall were similar at the riparian sites with SWC increasing gradually and remaining high in the deep soil layers. This suggests that the water table was rising into the deep soil layer at the riparian sites. It was also apparent that the wetting of deep soil layers at riparian sites resulted in higher rates of transpiration at these sites. Other researchers have made similar findings that demonstrated high rates of transpiration at riparian sites resulted from several factors including available soil water, and the ability of riparian vegetation to extract water from the water table (Dzikiti et al., 2013; Ping et al., 2006), especially in semi-arid and arid areas (Xu and Yu, 2020). Other studies found that the presence of shallow groundwater in riparian zones enhances the phreatic nature of riparian vegetation. When the water table is shallow enough, it becomes accessible for riparian vegetation to extract water through the capillary fringe and/or directly from groundwater (Pettit and Froend, 2018; Scott-Shaw et al., 2017; Smith and Allen, 1996). The direct impact of riparian *A. longifolia* trees on groundwater was also observed from the diurnal response of the water table to transpiration rates. High evapotranspiration from groundwater (ET_g) estimates were observed in the piezometers at Moddervlei and Jan Swaartkraal, as well as in the shallow BH29- 11m at Sandfontein.

In the mid-slope non-riparian site, at Spanjaardskloof, very high SWC were observed in the topsoil layer after rainfall events and this infiltrated. The water table at Spanjaardskloof responded gradually to cumulative rainfall received at the site. The weathered and fractured sandstone material at Spanjardskloof (Mazvimavi et al., 2021) explains the cumulative response of the water table at this site. During June – August 2020, the water table in BH10 – 20m increased to 1.2 m, which increased SWC in the deep soil layers. Consequently, high rates of transpiration were observed. The low bulk density and soil compaction at Spanjaardskloof compared to other sites enables high root

densities. Therefore, wetting of deep soils with high root density led to high rates of transpiration when moisture becomes available in deep soil horizons. Consequently, the high permeability of fractured aquifers resulted in high ET_g estimates despite the deep groundwater levels observed at Spanjaardskloof.

The higher rainfall in the headwaters at Sandfontein resulted in shallow water tables. This resulted in high rates of transpiration at this site. Transpiration rates measured from Sandfontein were almost equivalent to those measured from the riparian site, at Moddervlei. Therefore, the two non-riparian stands at Sandfontein and Spanjaardskloof had contrasting water use rates which were attributed to the differences in depths to the water table at these sites. The results presented in this chapter also show diurnal responses in groundwater at the non-riparian sites. This also confirms that *A. longifolia* trees across the sites were shallow-rooted and the hypothesis that transpiration patterns are mediated by depth to the water table across the sites (Grossiord et al., 2017; Ping et al., 2006; Xu and Yu, 2020; Zolfaghar et al., 2017). Water availability increased transpiration rates from the lowlands to the headwaters. These findings confirmed the statement by Nowell (2011) who highlighted that IAPs growing in deep sands, such as those observed in the riparian zones, can access groundwater and therefore their water use rates are mainly limited by climatic conditions than water availability. Moreover, Chapter 4 of this study illustrated higher rates of transpiration in the riparian zones (Moddervlei, Jan Swartskraal) and at Sandfontein, while Spanjaardskloof had the lowest rates of transpiration.

The findings in this study also support the assumption that IAPs act as groundwater pumps in areas they invade (Pettit and Froend, 2018; Snyder, 2000). Although *A. longifolia* stands occurred on different topographic positions, the differences in transpiration rates by *A. longifolia* across the sites correspond with differences in depth to groundwater, where high rates of transpiration and shallow water tables were observed in lowland and mid-slope riparian, as well as the upland sites, while the mid-slope non-riparian site had the lowest rates of transpiration and deeper groundwater levels compared to other sites.

5.5 Conclusions and recommendations

The study aimed to investigate how groundwater and soil water variations affect transpiration patterns by *A. longifolia* stands occurring in different topographic positions. The results show that the differences in transpiration patterns resulted from the differences in depth to the water table such that high rates of transpiration from *A. longifolia* trees at Moddervlei, Jan Swaartskraal, and Sandfontein were explained by the shallow water tables. The differences in transpiration patterns were also consistent with evapotranspiration from groundwater (ET_g), which was also high at Moddervlei, Jan Swartskraal, and Sandfontein. The low rates of transpiration at Spanjaardskloof were related to low rainfall, soil water content, and deeper groundwater table compared to other sites. This study confirms the assumption that IAPs act as groundwater pumps in areas they invade (Pettit and Froend, 2018; Snyder, 2000). For further validation of these findings, the use of tracer methods is recommended to confirm groundwater extraction from *A. longifolia* invasions and other IAP species.

Chapter 6

A comparative analysis of actual evapotranspiration from indigenous fynbos and invasive Acacia longifolia stands.

An Eddy covariance system and a borehole on a fynbos site, Tussenberge.

6.1 Introduction

The Cape Floristic Region (CFR) is an extremely important reservoir of biodiversity (Holmes et al., 2008). Fynbos is sclerophyllous shrubland dominated by species of the *Proteaceae*, *Ericaceae* and reed-like *Restionaceae*, and is the major indigenous vegetation in the CFR (Rebelo et al., 2006). The integrity of the CFR is adversely affected by habitat destruction caused by the increasing extent of invasive alien plants (IAPs), agriculture, urbanisation, dam construction, rural infrastructure, and climate change. These factors threaten the long-term biological diversity of the CFR (Joubert et al., 1997; Rebelo, 2006). The value of this biodiversity hotspot is recognized by the United Nations, which has awarded the region a World Heritage status. Therefore, the conservation of such a global heritage calls for an international effort (Araya and Walker, 2009).

South Africa's National Biodiversity Strategy and Action Plan (NBSAP, 2005) identified the CFR as a priority area and calls for further research and monitoring programmes to support integrated management of ecosystems. An improved understanding of the patterns and processes of the fynbos biome, including threatening processes, will promote better management of this biodiversity hotspot (Araya and Walker, 2009). Previous studies established that the ecosystem services of the fynbos biome are greatly affected by the expansion of IAPs (Blanchard and Holmes, 2008; Dzikiti et al., 2014). In areas where fynbos vegetation is displaced, the Australian acacias (e.g., *Acacia mearnsii*, *A. longifolia*, *A. saligna*) and *Eucalyptus* species (e.g., *E. camuldulensis)* were dominant (van Wilgen *et al.*, 2004; Forsyth et al., 2004). As a result, several studies have compared water use from IAPs with various indigenous species in South Africa (Dye et al., 2001, 2008; Dzikiti et al., 2016; Gush, 2018, p. 20; Mapeto et al., 2018; Scott-Shaw et al., 2017). These studies highlighted that the detrimental impacts of IAPs on water resources result from their high rates of water use and their ability to adapt and/or adjust water sources depending on their availability (Dzikiti et al., 2013; Ntshidi, 2015). The impacts are particularly severe for IAPs that occupy riparian zones (Le Maitre et al., 2015), where they tend to have dense thickets. The results from these studies and those presented in Chapter 4 of the current study support the idea that areas with dense invasions, should receive a high priority for alien plant clearing where water savings are assumed to be higher than in areas with sparse populations (Ntshidi, 2015).

The rapid population growth and economic development in the Western Cape region are placing increasing demands on water resources. Furthermore, future climate predictions for the Western Cape Province show a decrease in annual rainfall. This implies that the availability of water in the Western Cape will decrease over the next few decades. The increasing extent of IAPs in the Province will further exacerbate water shortages. Therefore, water resource management needs to focus on demand management involving regulations to control increased demand (Araya and Walker, 2009). South Africa enacted one of the largest government-funded programmes in the world aimed at managing IAPs, that is, the Working for Water Programme (WfW) (van Wilgen et al., 2012). This programme was initiated in 1995 with the objectives of clearing IAPs to increase water delivery, improve ecological integrity, and alleviate poverty by creating jobs (van Wilgen et al., 2004). However, research showed that clearing of IAPs can succeed or sometimes fail to facilitate indigenous vegetation recovery. Therefore, there is a need for understanding the effectiveness of clearing IAPs and control operations carried out by WfW (Holmes et al., 2008; Kraaij et al., 2017; van Wilgen et al., 2012). The development and implementation of monitoring programmes in areas where clearing was done were also recommended. Therefore, the current study aims to inform the effectiveness of clearing interventions taking place in the Nuwejaars Catchment, in the Western Cape Province of South Africa, by quantifying the potential benefits that can be achieved by clearing non-riparian settings that were previously overlooked and not prioritized.

Hydrological studies have focused on the effects of woody invasive vegetation as they generally have higher rainfall interception, higher transpiration rates, deeper roots, greater standing biomass, greater carbon sequestration, and longer growing seasons than the co-occurring herbaceous plants (Calder and Dye, 2001; Cavaleri et al., 2014; Enright, 2000). There is a lack of quantitative information on water use by indigenous vegetation at the community scale in the CFR (Holmes et al., 2008; van Wilgen et al., 2012). It was previously established that the potential water savings arising from clearing IAPs greatly depend on the water use characteristics of the indigenous vegetation that replaces the cleared vegetation (Doody et al., 2011; Dye et al., 2001; Dzikiti et al., 2014). Therefore, the lack of quantified information constrains the estimations of the hydrological benefits to be achieved by clearing IAPs and replacing them with indigenous vegetation.

The Nuwejaars Catchment is home to more than 1 750 plant species – mostly belonging to the fynbos biome (Nowell and Esler, 2011). Much of this fynbos vegetation is restricted mainly to the mountainous parts of the catchment. Lowland areas that were dominated by *Elim Asteraceous* fynbos and *Renoster* fynbos have largely been converted to croplands and vineyards. Large parts of the lowland riparian areas have also been encroached by IAPs dominated by *Acacia longifolia*, which displaced the endangered sand *proteoid* fynbos ('Alguhas-final brief report', no date). To improve the integrity of these ecosystems, alien plant clearing was introduced. The clearing is prioritized in the lowland riparian zones of the catchment and now has extended even to the mountainous parts of the catchment. The current study aims to quantify the potential benefits of clearing the invasive *A. longifolia* invasions by (i) quantifying actual evapotranspiration (AET) rates from a fynbos stand, and (ii) comparing the AET rates from fynbos with that of the invasive *A. longifolia* stand occurring in a similar environment.

6.2 Methods and materials

6.2.1 Approach of the study

Chapter 4 identified the sites invaded by *A. longifolia* in the Nuwejaars Catchment. The weather patterns across the sites were analysed and transpiration rates of *A. longifolia* stand at the different locations in the Nuwejaars Catchment were quantified. Chapter 5 investigated the relationships between transpiration patterns of *A. longifolia* trees, soil water, and groundwater variations at the invaded sites. The information on the weather patterns and soil water dynamics from the upland site, Sandfontein, was used to predict and/or simulate AET rates from the *A. longifolia* stand at Sandfontein (Figure 6.1). To achieve the objective for this chapter, the quantified rates of water use by the fynbos stand were critical in determining the incremental water gains that can be achieved by clearing *A. longifolia* stands occurring in a similar setting. The quantified incremental water use was estimated from the difference between the actual evapotranspiration rates from the indigenous fynbos stand and that of the invasive *A. longifolia* stand.

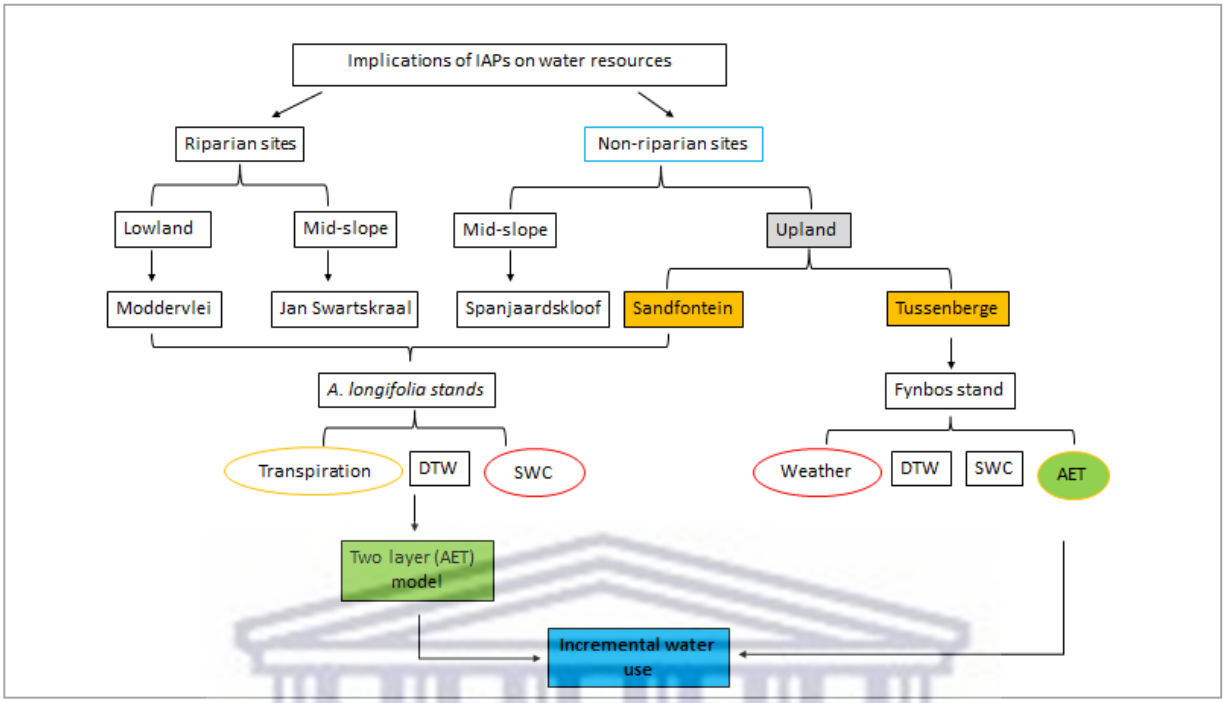

Figure 6.1: Summary of the research approach. The oval shapes show data that was used for model input (red) and validation (orange). DTW and SWC represent the measured depth to the water table and soil water contents, respectively.

6.2.2 Study site

This experiment was conducted on the mountainous parts of the Nuwejaars Catchment in the Cape Agulhas region of the Western Cape Province. The study area, site descriptions, and the criteria used for selecting sites are provided in Chapter 2. The location of the eddy covariance and sap flow systems used for tree water use monitoring on the headwaters of the catchment are illustrated in Figure 6.2.

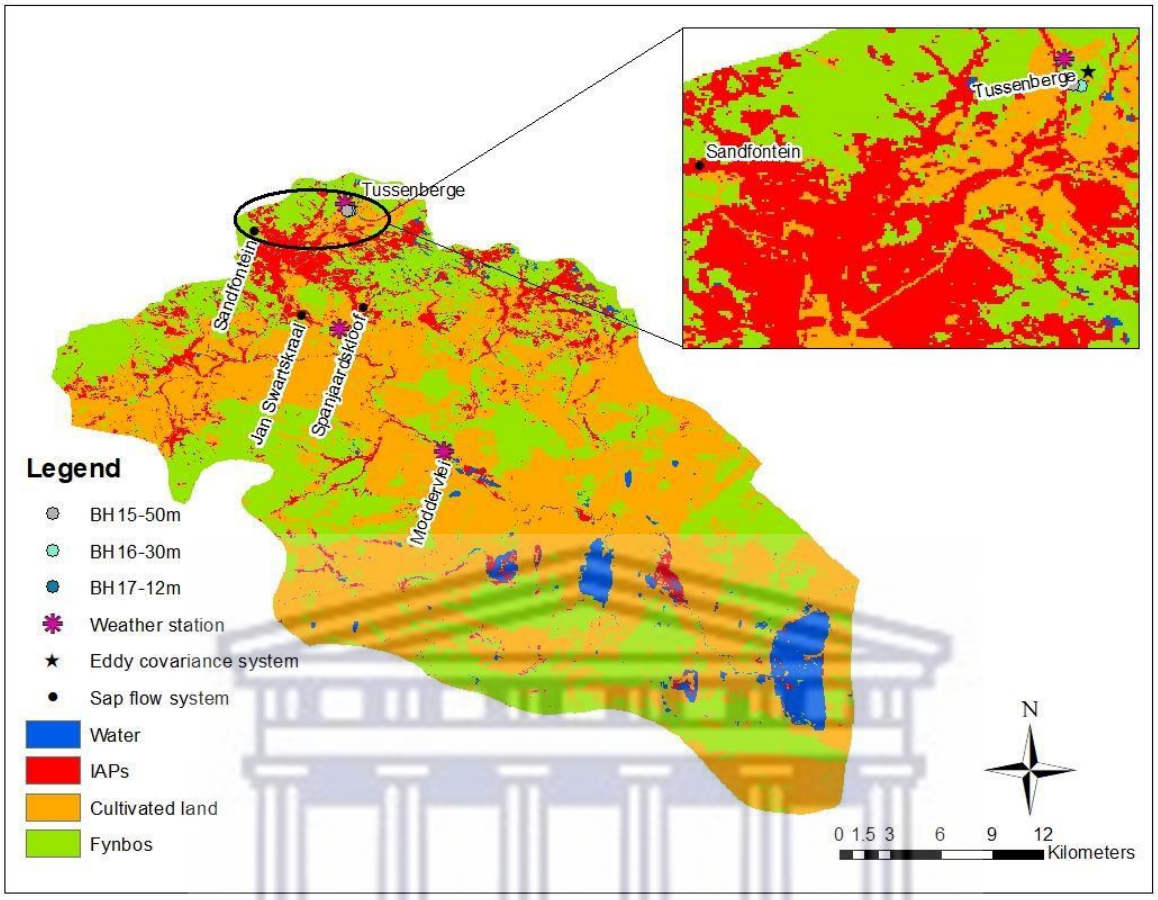

Figure 6.2: The location of tree water use monitoring systems under different land use/land covers in headwaters of the Nuwejaars Catchment (Image source: Landsat8, acquired on the 12th of November 2020).

The typical fynbos shrubs of Tussenberge include proteas, ericas, and restios. A weather station and boreholes had already been installed at this site for other components of an ongoing hydrological monitoring project carried out in the catchment. An eddy covariance system was located ~5km from the sap flow monitoring site at Sandfontein. The Sandfontein site represents the highest elevation at which *A. longifolia* trees were found in the Nuwejaars Catchment. This Chapter aims to monitor tree water use under different landcover types, and these sites were comparable (Table 6. 1).

Table 6.1: Comparison of Tussenberge and Sandfontein's tree water use monitoring sites.

Site Name	Cover Type	Species	Elevation (m.a.s.l)	Slope	Geology	Water table (m)
Tussenberge	Non-invaded area	Indigenous (Proteas, Ericas)	230	0.1	Sandstone	1.5 – 8.0
Sandfontein	Invaded area	Acacia longifolia	228	0.1	Sandstone	0.0 – 1.8

6.2.3 Monitoring of microclimate

The weather conditions of the site were monitored using a weather station located 300 m northwest of the flux tower. Chapter 4 explains in detail the location and description of the Tussenberge weather station relative to the sap flow monitoring site at Sandfontein.

6.2.4 Monitoring actual evapotranspiration rates from a fynbos stand

To estimate actual evapotranspiration on a fynbos patch, an eddy covariance system (IRGASON integrated CO2/H2O Open-Path Gas Analyzer and 3D Sonic Anemometer) was installed (Figure 6.3). The system comprised an infrared gas analyser (IRGA, Model LI-7500, LI-COR, Lincoln, NE, USA) which measured the concentration of atmospheric water vapour and carbon dioxide, a 3D sonic anemometer (Campbell Scientific Instrument-CSI, Logan, UT, USA) which measured the wind speed, and a pyranometer which measured solar radiation. These sensors were installed at ~ 8 m above ground. The system also included a relative humidity and temperature probe (model HMP45C- LC) at ~ 2 m height. The air temperature, relative humidity, water content of the air, the vertical component of wind speed, and sensible heat were measured every 60 minutes. The vapour flux measurements allow actual ET to be calculated. Below the tower, two clusters of Hukseflux soil heat flux plates (Delft, Netherlands) were installed horizontally at 8 cm depth below the ground to measure the soil heat fluxes. Soil averaging thermocouples (Model: TCAV, Campbell Sci. Inc., Utah, USA) were installed above the soil heat flux plates at 2 and 6 cm depths from the surface to correct the measured fluxes for the energy stored by the soil above the plates. The CS616 soil water content sensors (Campbell Scientific, Inc., Logan, UT) were also installed at 8 cm depth below the surface to monitor the volumetric soil water contents. These additional instruments allow the estimation of surface energy balance. The processed data collected was stored in a datalogger

(model CR6; Campbell Scientific Inc. Logan UT, USA) while high-frequency raw data were stored in an 8 gigabyte MicroSD card inserted in the data logger enclosed in a box installed at a height of 1.4 m above ground. The system was powered by a 105Ah- 12v battery charged by a solar panel.

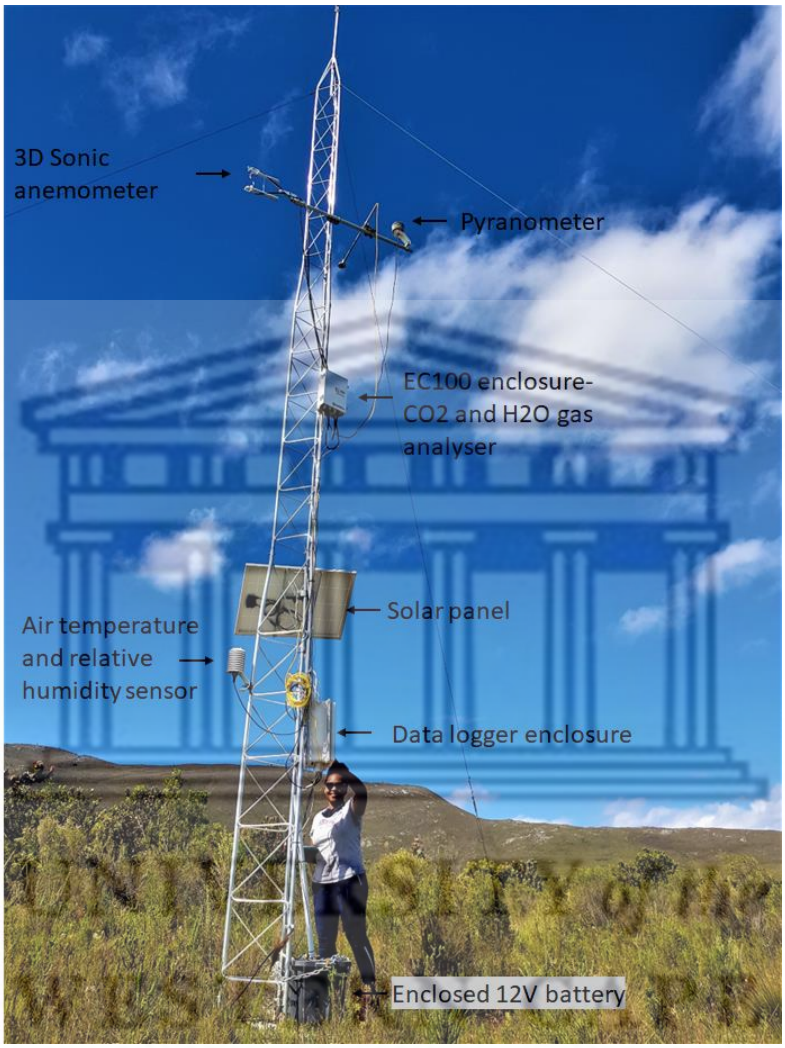

Figure 6.3: Eddy covariance system (eddy flux tower) installed at a site with fynbos shrubs.

i. Quality control of ET flux data

Technical malfunctions of the eddy covariance system were experienced during the monitoring period, such as the disconnection of cables due to windy conditions. Also, there were unexpected spikes in ET during rainy days, caused by the misalignment of sensors. Faulty data with poor quality were flagged with NAN (not a number), or unrealistically high values. The flagged values were removed, thus causing gaps in AET measurements.

6.2.5 Monitoring groundwater levels

Groundwater levels were monitored at ~ 250 m southeast of the eddy flux tower. The three boreholes drilled along a transect have depths of 50 (BH15), 30 (BH16), and 12 m (BH17) (Figure 2.11; Table 6.2). According to Mazvimavi et al. (2021), the Tussenberge boreholes were drilled into weathered sandstone. BH15-50m and BH17-12m are 6 meters apart, while BH16-30m is 128 meters away. To monitor groundwater levels at hourly intervals, Solinst water level data loggers (Model 3001, Georgetown, ON, Canada) were installed in the boreholes.

Table 6.2:The descriptions of the monitoring boreholes at Tussenberge.

Borehole ID	Depth (m)	Elevation (m)
BH15	50	202.03
BH16	30	209.01
BH17	12	202.42

6.2.6 Modelling actual evapotranspiration rates from Acacia longifolia stand.

A two-layer model was developed and successfully used by Dzikiti et al. (2013) to simulate actual evapotranspiration (AET) by riparian and non-riparian pines in the Western Cape. The selection of the model was based on its ability to partition AET into two layers namely, the upper transpiring layer (T_s) comprising the tree canopies and the below canopy layer in which soil evaporation (E_s) was assumed (Dzikiti et al., 2013) (Figure 6.4).

In this study, the model was used to simulate AET from the Sandfontein site invaded by *A. longifolia*. Using in-situ SWC measurements and microclimate data, a two-layer model was used to simulate daily AET rates from Sandfontein to allow the comparison between simulated AET rates from *A. longifolia* stand at Sandfontein and AET rates measured from the fynbos stand at Tussenberge. The simulation period was 9 months, from the 1st of February 2020 to the 31st of October 2020, to overlap with the period when AET data from the fynbos stand had no gaps.

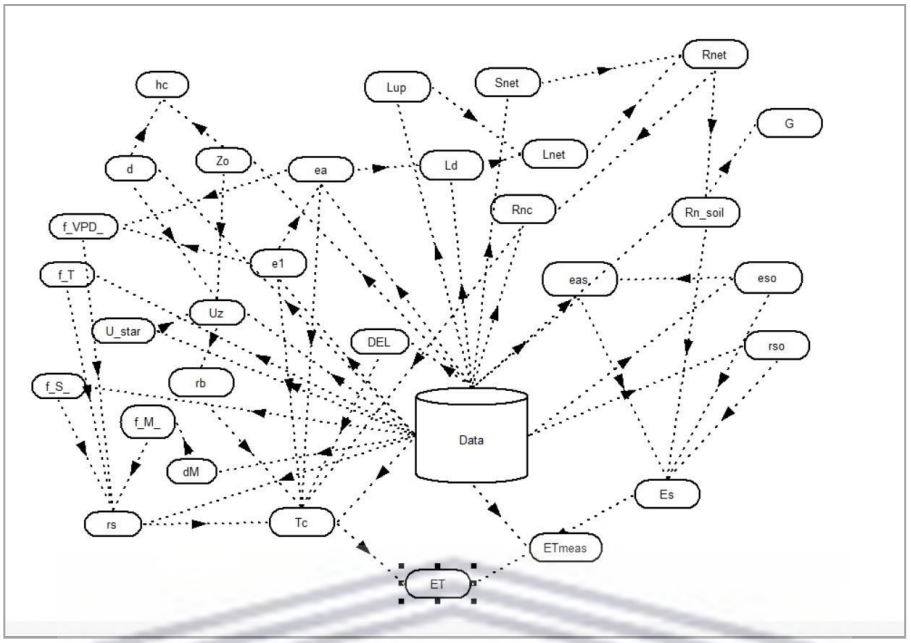

Figure 6.4: Structure of the two-layer AET model representation from Modelmaker software.

Transpiration (*Tc*) from the canopies is modelled using the following relationship (Zhang et al., 1997):

$$T_c = LAI\,\frac{\lambda[Rn_c * S + 0.93 * \rho c_p (e_1 - e_a) * r_b]}{(S + \gamma * 0.93\left(2 + \frac{r_b}{r_s}\right))} \qquad (6.1)$$

where *LAI* is the leaf area index of the canopy measured at the site using the LAI-2200C plant canopy analyser (PCA, LI-COR, Lincoln, Nebraska USA), λ is the latent heat of vaporisation of water (J/ kg), Rn_c is net radiation absorbed by the tree canopies (W/ m^2) modelled using the following Beer's law:

$$Rn_c = (1 - \exp(-k_e * LAI)\, R_{net} \qquad (6.2)$$

where *ke* is the extinction coefficient which was assumed as a constant with a value of 0.5 (Li et al., 2010), $R_{net}$is Net radiation on a grass reference surface (W/m^2) estimated from:

$$R_{net} = S_{net} + L_{net} \quad (6.3)$$

Net short (S_{net}) was estimated using the following:

$$S_{net} = S_0(1 - r) \quad (6.4)$$

Where S_0 is the measured solar radiation (W/m^2) and r is the surface reflectance (albedo). Net longwave radiation was calculated by combining the expressions by Ortega-Farias et al. (2000) and Brutsaert (1975) in which:

$$L_{net} = L_d + L_{up} \quad (6.5)$$

where,

$$L_d = 1.24 \frac{10 * \frac{e_a}{1000}}{(T_a+273)^{\frac{1}{7}}} * 5.67 * 10^{-8}(T_a + 273)^4 \quad (6.6)$$

$$L_{up} = 0.98 * 5.67 * 10^{-8} * (T_a + 273)^4 \quad (6.7)$$

$T_a$is the average air temperature in °C, actual and saturation vapour pressure (e_a and e_1) were estimated as:

$$e_a = e_1(\frac{RH}{100}) \quad (6.8)$$

$$e_1 = 610.8 * \exp(\frac{17.3 * T_a}{T_a+273}) \quad (6.9)$$

Δ is the slope of the saturation vapour pressure against the temperature curve (Pa /°C), ρ is the density of air (kg/ m^3), c_p is the specific heat of air at constant pressure (J/kg/ °C), $e_1 - e_a$ is the vapour pressure deficit (VPD) of the air (Pa), γ is the psychrometric constant (Pa/ °C), r_b nd r_s are the aerodynamic and canopy conductance (m/ s),

respectively. The aerodynamic conductance (r_b) was calculated using the equation for the leaf boundary layer resistance as explained by Dzikiti et al. (2013) and the canopy stomatal conductance (r_s) was estimated according to Zhang *et. al*. (1997) equation:

$$r_b = 0.01\sqrt{\left(\frac{U_z}{w_c}\right)} \quad (6.10)$$

Where w_c is the measured width of a leaf (m), U_z is the wind at canopy height (m/s) estimated from:

$$U_z = U^* * Ln\left(\frac{H-d}{Z_0}\right)/K_v \quad (6.11)$$

Where H is the average tree height (m), K_v is von Kármán's constant (0.4) of the logarithmic wind profile in the surface layer, U^* is the friction velocity modelled from:

$$U^* = K_v * u/Ln\left(\frac{2-0.63*2}{2*0.13}\right) \quad (6.12)$$

Where u is the measured wind speed (m/s) from the weather station.

Displacement plane, $d = 0.63H$ (6.13)

Roughness length, $Z_0 = 0.13H$ (6.14)

The leaf stomatal conductance of the plant species at the study site and this variable was determined from environmental factors according to Jarvis (1976) and Oren et al. (2001) wherein:

$$r_s = K_1(f\_S\_)\ (f\_VPD\_)\ (f\_M\_)\ (f\_T\_) \quad (6.15)$$

Where k_1 is the maximum stomatal conductance of the dominant plant species determined by model optimisation. *f(VPD), f(S), f(T),* and *f(M)* are stress functions derived from the

changes in atmospheric VPD, solar irradiance (*S*), air temperature, and soil water deficit *M* *as* described by Dzikiti *et al*. (2013):

Solar radiation stress function, $f\_S\_ = \frac{S_0}{K_r + S_0}$ (6.16)

Temperature stress function, $f\_T\_ = \frac{(T_a - T_l)}{(K_T - T_l)} * \frac{(T_h - T_a)^a}{(T_h - K_T)^a}$ (6.17)

Where T_l and T_h are maximum and minimum temperatures

$$a = \frac{T_h - K_T}{K_T - T_l} \quad (6.18)$$

VPD stress function, $f\_VPD\_ = \frac{1 - Kd_1 * (e_1 - e_a)}{1 + Kd_2 * (e_1 - e_a)}$ (6.19)

Soil water stress function, $f\_M\_ = 1 - Ks_1 * \exp(Ks_2 * SWD)$ (6.20)

Where *SWD* is soil water deficit estimated as:

$$SWD = \frac{(M_{max} - \vartheta)}{(M_{max} - M_{min})} \quad (6.21)$$

M_{max}, M_{min}, and ϑ are the maximum, minimum and measured volumetric soil water content (cm3/cm3). kd_1, kd_2, k_r, ks_1, ks_2 and K_T are parameters determined by model optimisation.

According to Shuttleworth and Wallace (1985), soil evaporation (E_s) can be simulated using the:

$$E_s = \frac{\rho c_p (es_o - ea_s)}{\gamma \lambda * rs_o} \quad (6.22)$$

where ρ is the density of air (kg/ m^3), c_p is the specific heat of air at constant pressure (J/ kg/°C), γ is the psychrometric constant (Pa/ °C), λ is the latent heat of vaporisation of water (J/ kg), rs_o is the soil/substrate surface resistance to water vapour transport modelled as:

$$rs_0 = b_1 \left(\frac{\vartheta}{\vartheta_{fc}}\right)^{b_2} \quad (6.23)$$

Where ϑ_{fc} is the field capacity (cm^3/cm^3) of the soil which was equivalent to the measured SWC (ϑ) 24 hours after heavy rain events that were adequate to wet the entire soil profiles. b_1 and b_2 are parameters determined by model optimisation.

Actual vapour pressure (ea_s) and saturation vapour pressure (es_o) at soil surface were simulated as:

$$ea_s = es_o \left(\frac{RH}{100}\right) \quad (6.24)$$

Where *RH* is the relative humidity.

$$es_o = 610.8\ exp\frac{(17.27 * T_s)}{(273.3 * T_s)} \quad (6.25)$$

Where T_s is surface or soil temperature (°C).

The daily evapotranspiration (*ET(t)*) by *Acacia longifolia* stands is then obtained by summing transpiration given by equation 6.1 and soil evaporation from equation 6.22:

$$ET(t) = T_C + E_S \quad (6.26)$$

The major limitation of the two-layer model described above is that canopy interception loss (I_s) from the *A. longifolia* stand is not accounted for. Interception depends on the atmospheric conditions that drive evaporation and rainfall characteristics, as well as the nature and density of the forest stand (Bulcock and Jewitt, 2010). The condition for canopy interception was then added to the model. Rainfall interception by vegetation canopy was simulated by calculating a maximum storage capacity (I_{max}), which is filled during rainfall. Previous studies indicate that interception capacity is linearly related to the plant leaf area index (LAI) (Pinto et a., 2013). Thus, the maximum interception loss (I_{max}) was estimated for

each site using the Von Hoyningen-Huene (1981) equation:

$$I_{max} = 0.935 + 0.498\ (LAI) - 0.0057(LAI^2) \qquad (6.27)$$

When rainfall received (P) on a particular day (t) is less than the maximum interception storage (I_{max}) of the canopy, then all the rainfall contributes to the interception loss (I_s). Therefore, the amount of rainfall reaching the ground (P_{net}) becomes zero. Thus, *Pnet* occurs when *P* is greater than I_{max}:

$$P_{net}(t) = max\ [P(t) - I_{max}; 0] \qquad (6.28)$$

The daily canopy interception loss ($I_s(t)$) is then estimated from the daily rainfall received ($P(t)$) and the amount of rainfall reaching the ground ($P_{net}(t)$):

$$I_s(t) = \frac{P(t) - P_{net}(t)}{LAI}, \qquad (6.29)$$

If P(t) < I_{max}:

$$I_s(t) = P(t) \qquad (6.30)$$

Actual evapotranspiration (*AET*) from *A. longifolia* stand at Sandfontein was simulated by summing evapotranspiration given by equation 6.26 and the daily evaporation from the canopy interception.

$$AET(t) = ET + I_s(t) \qquad (6.31)$$

6.2.7 Evaluation of model performance

Transpiration data from the sap flow system during the 1st of February to the 31st of October 2020 period at Sandfontein and the measured AET rates from the flux tower at Tussenberge during the same period, were used to evaluate the model simulation of daily transpiration (*Tc*) and AET rates. The following criteria were used to assess model performance:

a) The mean absolute error (MAE) measured the difference between the simulated and observed values.

b) The Nash-Sutcliffe efficiency (NSE) indicates how well the observed versus simulated data fits. NSE ranges between −∞ and 1, with NSE = 1 being a perfect fit. NSE lower than zero indicates that the mean value of the observed data would have been a better predictor than the model (poor model performance).

c) Percent bias (PBIAS) measures the underestimation and/or overestimation of the simulated data to the observed dataset. The best value of PBIAS is 0, with low-magnitude values indicating accurate model simulation. Positive values indicate model underestimation bias, and negative values indicate model overestimation bias.

6.2.8 Comparison of AET rates from fynbos and A.longifolia stands

To determine whether there were significant differences in AET rates by *A. longifolia* and fynbos stands occurring in a similar environment and/or setting, a paired t-test analysis was used to compare AET rates from Sandfontein (*A. longifolia*) and Tusssenberge (fynbos) using data from the 1st of February – the 31st of October 2020.

Monthly actual and reference ET data from Sandfontein and Tussenberge were used to estimate the ratio of actual evapotranspiration to reference evapotranspiration (AET/ETo). This was done to evaluate the impacts of water availability on vegetation water use. Given that ETo is the reference evapotranspiration (ET) for grass without shortages of water (Allen, 1998), likely to have higher rates than actual evapotranspiration that is prevailed by water stress at times. It was expected that the AET/ETo ratio may exceed 1 during wet periods when the vegetation at both sites was not experiencing water stress. The values lower than 1 show the period when AET was less than ETo, indicating the period when vegetation was water-stressed.

6.3 Results

6.3.1 Microclimate on the headwaters of the Nuwejaars Catchment

During the period August 2019 to November 2021, daily solar irradiance peaked during summer ranging between 31.1 - 34.1 MJ/m^2/day, while lower values ranging between 1.9 to 10.2 MJ/m^2/day were recorded in winter (Figure 6.5a). The minimum temperature recorded at Tussenberge was 7.1 °C in August 2021, while the maximum temperature was 28.0 °C in March 2020 (Figure 6.5b).

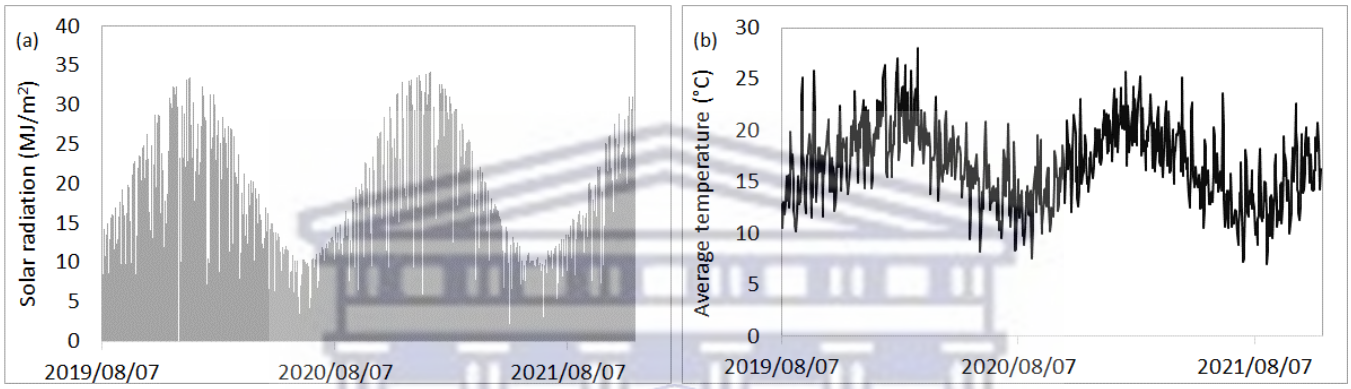

Figure 6.5: Daily variation in (a) solar radiation and (b) average temperatures at Tussenberge during the period from 7th August 2019 until 19th November 2021.

The daily vapour pressure deficit (VPD) of air peaked at about 2.9 Kpa in April 2021 with a minimum ranging between 0.5 to 1.7 KPa during winter, and 1.1 to 2.4 Kpa in summer (Figure 6.6a). The site is located on the mountainous part of the catchment that frequently experiences windy conditions, with wind speed reaching up to 6.7 m/s (June 2020), and the lowest wind speed recorded was 0.2 m/s in May 2020 (Figure 6.6b).

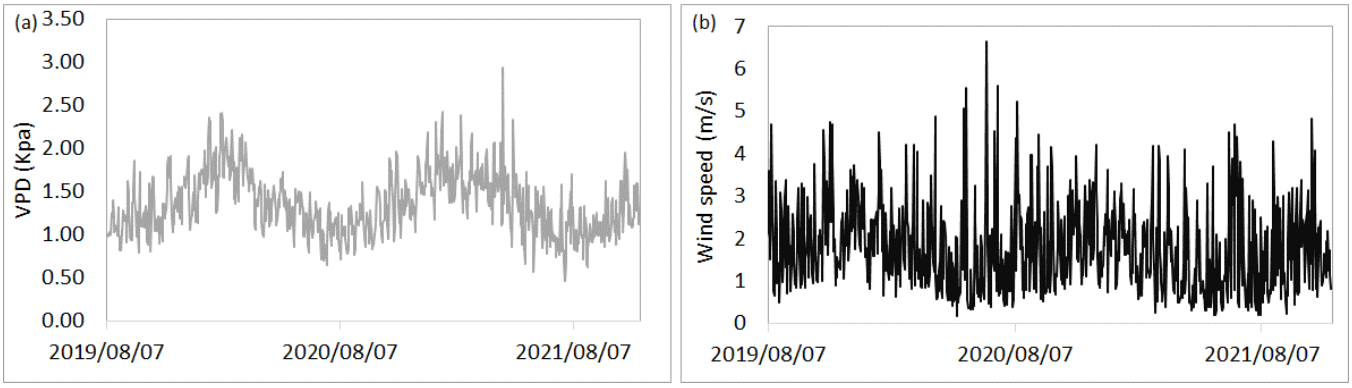

Figure 6.6: Daily variation in (a) Vapour pressure deficit (VPD) and (b) average Wind speed at Tussenberge during the period from 7th August 2019 until 19th November 2021.

High daily rainfall was received in October 2019 (48.6 mm/day), November 2019 (50.8 mm/day), January 2020 (41.6 mm/day), as well as May 2021 (99.6 mm/day) (Figure 6.7a). Tussenberge received an annual rainfall of 928 mm/year from January-December 2020 with the winter (June-August) rainfall making up 41% of this amount (Figure 6.7b). Although the data included in 2021 was only for 11.5 months, the total rainfall measured from January to November 2021 was 975 mm, which means that 2021 received 47 mm (~ 4.8 %) more rainfall than 2020. May 2021 recorded the highest rainfall of 273 mm/month during the study period (August 2019 – November 2021).

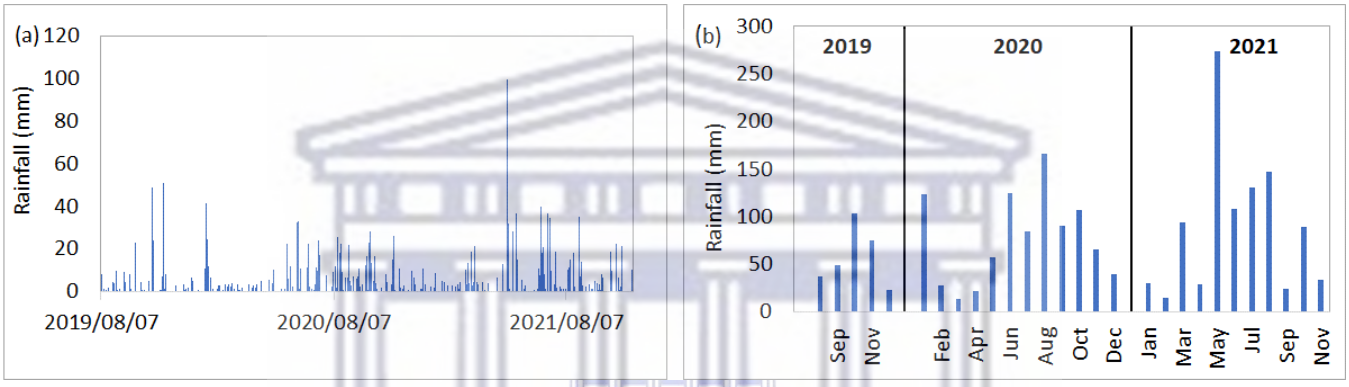

Figure 6.7: (a) Daily and (b) monthly rainfall variations at Tussenberge during the period from the 7th of August 2019 until the 19th of November 2021.

6.3.2 Soil water and groundwater variations

Generally, the groundwater table at Tussenberge and Sandfontein declined during November/December – May/June period, and then rose during the wet period from July to October. A notable rise in groundwater levels was observed between July and October 2020, when the water table rose by 3.80 m and 3.48 m in BH16-30 m and BH17-12m, respectively (Figure 6.8). At Sandftontein, the water table rose to the surface in October 2020. SWC also increased by 12 % (from 4.7 to 16.9 %) between June and October 2020. Although SWC was monitored in very shallow soil layers (8cm depth) at Tussenberge, the temporal variations at Tussenberge were similar to those at Sandfontein, where SWC was monitored down to 100 cm depth. At Sandfotein, SWC increased by 22 % (from 6.9 to 28.6 %) during June to October 2020 period (Figure 6.8b).

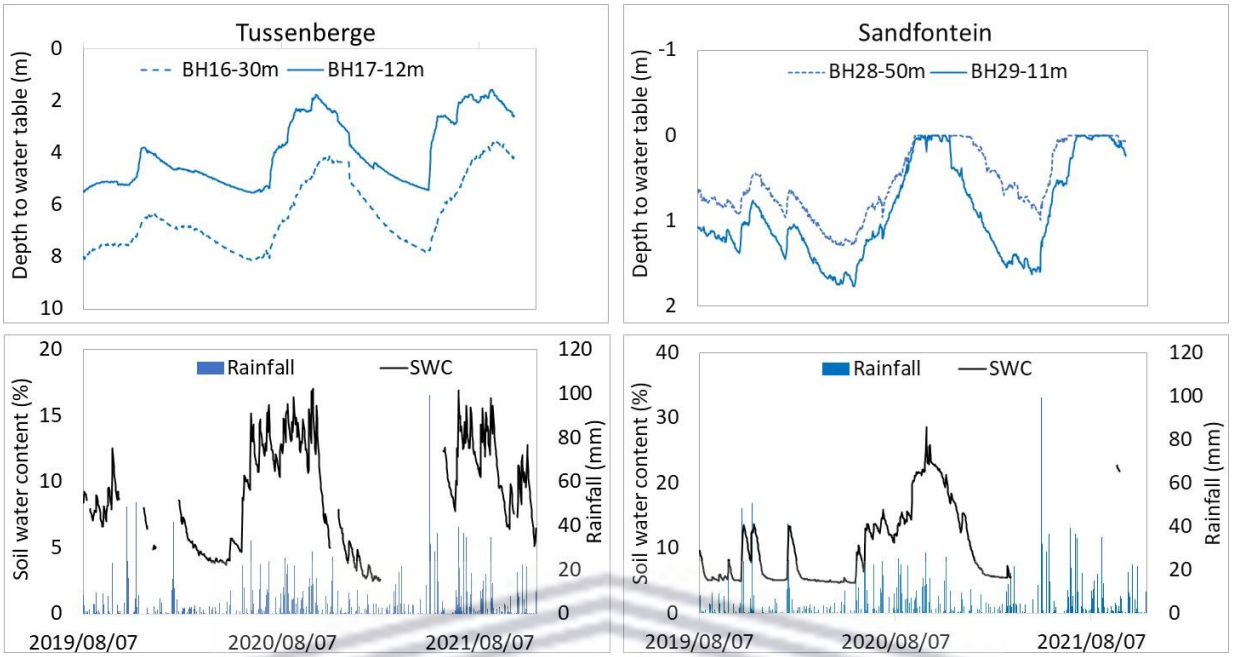

Figure 6.8: Tussenberge and Sandfontein's daily variation in groundwater levels (top) measured in shallow (solid line) and deep (dashed line) aquifer systems, and average soil water content (bottom).

6.3.3 Surface energy balance at Tussenberge

The energy fluxes measured from the eddy covariance system at Tussenberge were also used to estimate the energy available to evaporate water from the surface, known as surface energy balance. The seasonal changes in surface energy balance in Tussenberge are shown in Figure 6.9. The daily energy balance shows that net radiation and latent heat during a clear day in summer can reach up to 710 W/m^2 and 221 W/m^2, respectively (Figure 6.9a) and decline to 351 W/m^2 and 89 W/m^2, respectively during a clear day in winter (Figure 6.9c). Throughout the seasons, available energy (Rn-G) was mostly converted to sensible heat (H) used to warm the air and very little was converted to latent heat (LE) which is the energy equivalent of evapotranspiration. This means that minimal available energy was used as evapotranspiration by fynbos.

The differences between H and LE fluxes varied between the dry and wet seasons. During summer, the difference between H and LE fluxes was 139 W/m^2 in February 2020 (Figure 6.9a) and increased to 182 W/m^2 during October 2020 (Figure 6.9d). The partitioning of the available energy was almost equal during May 2020 (Figure 6.9b) and June 2020 (Figure 6.9c) when the solar radiation and temperatures were lower.

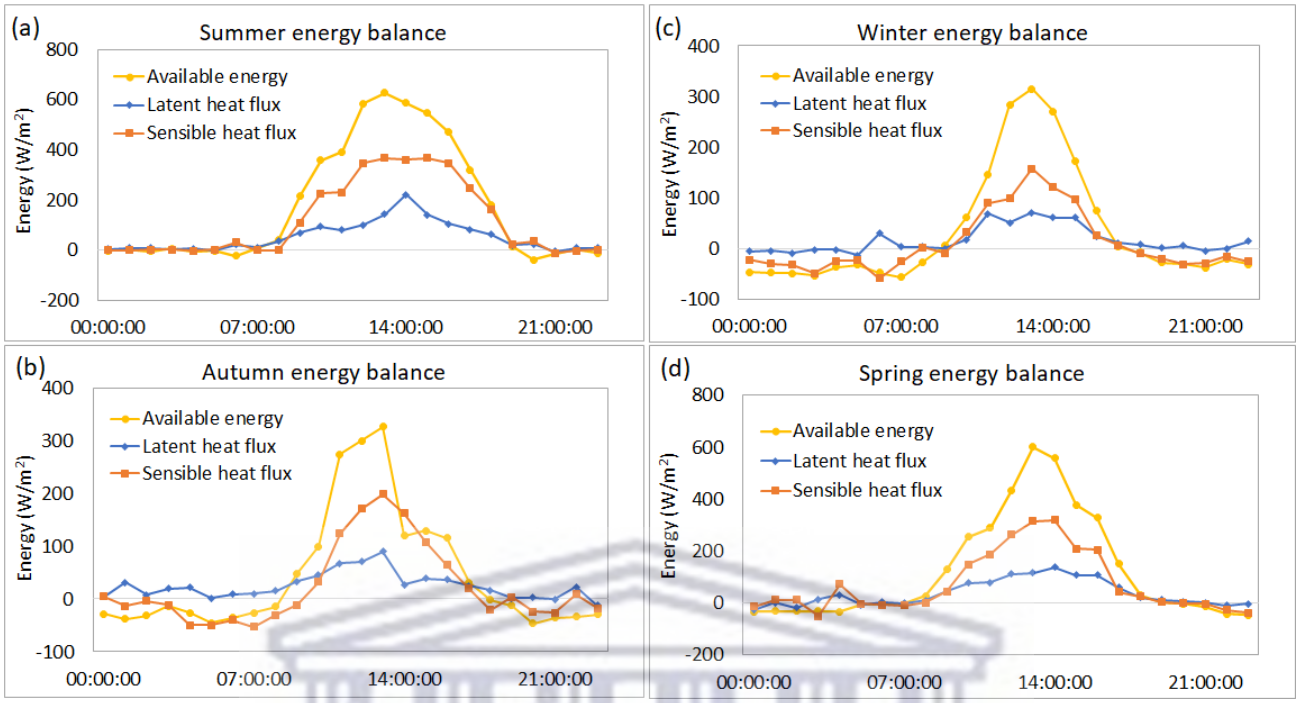

Figure 6.9: Typical surface energy balance for fynbos stand on a clear day in (a) summer (12th February 2020), (b) autumn (13th May 2020), (c) winter (20th June 2020), and (d) spring (October 2020).

A very strong linear relationship (R^2 = 0.9) was observed in the conversion of available energy (Rn-G) to turbulent fluxes (LE+H) during a dry day in February 2020 (Figure 6.10a). The relationship weakened as the wet winter season approached. As a result, there was no relationship observed between the available energy (Rn-G) and turbulent fluxes (LE+H) during the wet season in June 2020 (R^2 = 0, Figure 6.10c). This was attributed to the low VPD during rainy and wet conditions which suppress ET.

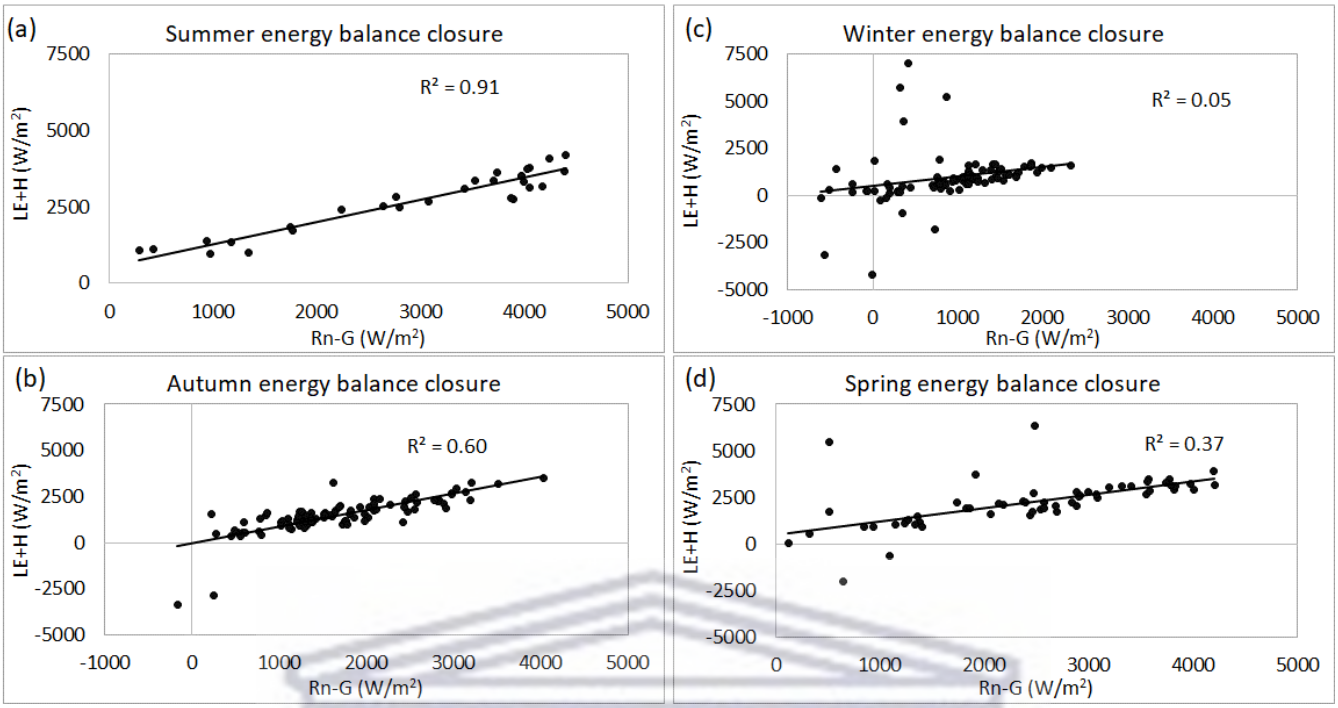

Figure 6.10: Energy balance closure for the fynbos stand in (a) summer (1st - 29th of February 2020), (b) autumn (1st of March - 30th of May 2020), (c) winter (1st of June - 31st of August 2020), and (d) spring (1st of September - 30th of October 2020)

6.3.4 AET rates measured from fynbos stand.

The reference evapotranspiration (ETo) rates at Tussenberge peaked at 7.9 mm/day on a summer day in January 2021, while the lowest rate of 0.1 mm/day was recorded in May 2021. The actual evapotranspiration (AET) rates were lower than ETo, peaking at 6.5 mm/day in November 2021, and a low AET of 0.1 mm/day was measured in October 2021 (Figure 6.11a). The peak AET rate of 6.5 mm/day exceeded the ETo of 5.4 mm/day, thus showing AET rates can exceed ETo when there is sufficient water and energy available. The relationship between ETo and AET was described linearly with $R^2 = 0.39$ and as expected increased with increasing ETo rates (Figure 6.11b).

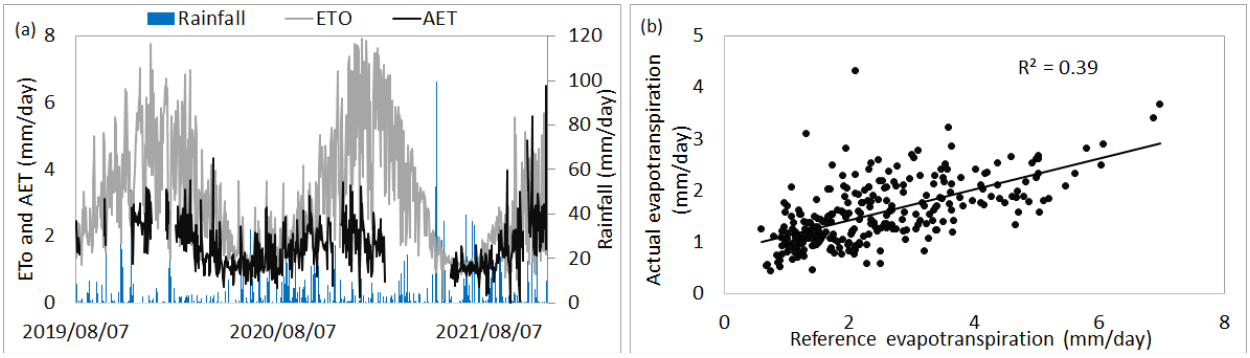

Figure 6.11: (a) Tussenberge daily rainfall, reference, and actual evapotranspiration from August 2019 to November 2021. (b) Relationship between reference ET and actual ET measured at the site.

6.3.5 Drivers of actual evapotranspiration at the fynbos site

Statistically, the microclimate at Tussenberge significantly influenced AET rates by fynbos vegetation ($p<0.05$) (Table 6.3). Much of the variation in AET by fynbos shrubs was accounted for by the available energy (Rn-G, 58%), rainfall (24%), and wind speed (14%).

Table 6.3: Statistical regression between weather variables and AET rates at Tussenberge

	Sig		
Regression	0.00		
Residual			
Coefficients	Standardized Coefficients	t	Sig.
	Beta		
Rn-G (W/m^2)	**0.58**	10.03	0.00
VPD (Kpa)	**-0.08**	-1.26	0.21
Tmean (°C)	**0.04**	0.56	0.58
Wind speed (m/s)	**0.14**	2.75	0.01
Rainfall (mm)	**0.24**	4.28	0.00

Although rainfall accounted for 24% of the variation in AET (Table 6.3), there was no relationship observed between variations in SWC measured at 8 cm depth and AET (Figure 6.12d). It is apparent in Figure 6.12e, that there is a very weak relationship between AET rates and changes in DTW from BH16-30 m than in BH17-12 m measured ~250 m away from the flux tower (Figure 6.12f). This implies that the AET rates had a relationship with groundwater tables below 4 m below the surface.

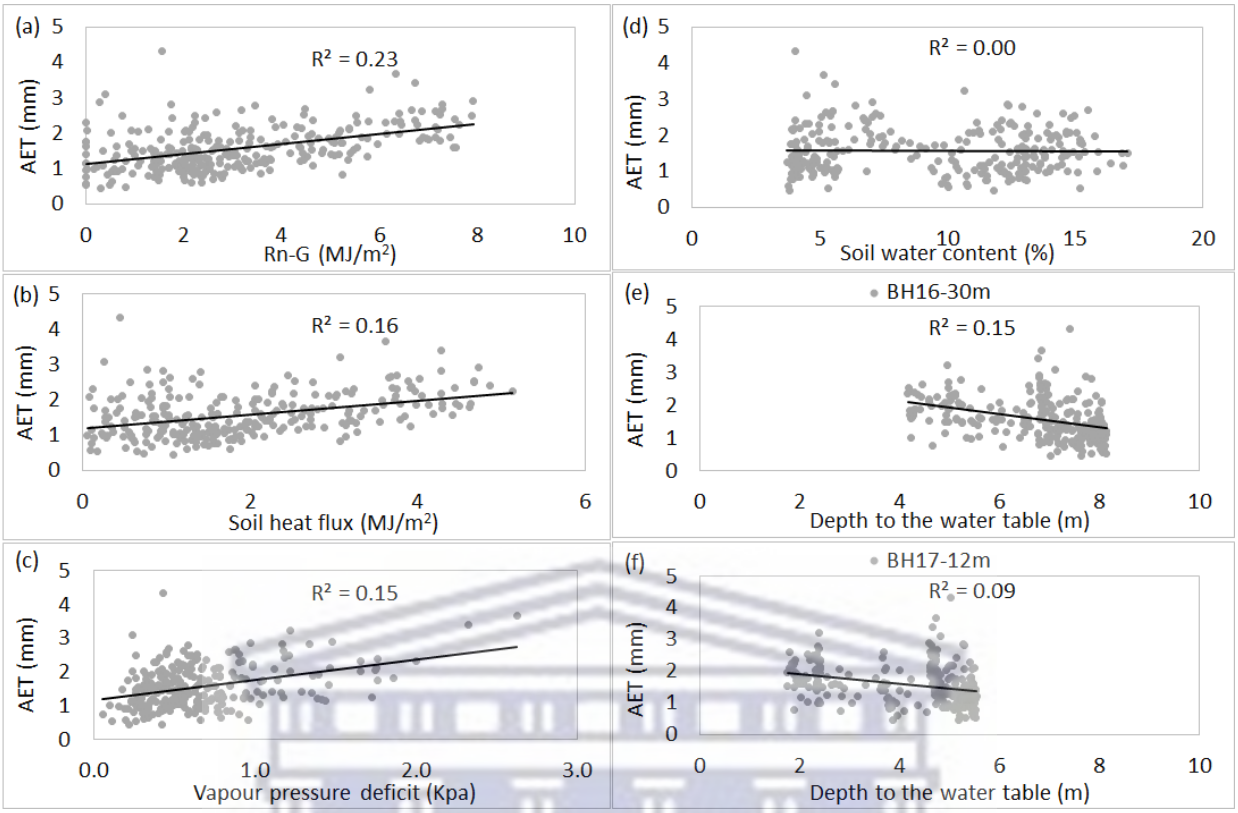

Figure 6.12: Tussenberge daily AET responses to environmental drivers. Rn-G represents the available energy.

6.3.6 Simulated AET rates for A. longifolia stand at Sandfontein.

i. Validation

AET rates from *A. longifolia* stand were simulated using a two-layer model. The model prediction on stand transpiration (*Tc*) was fairly accurate ($R^2 > 0.5$). The fair performance of the model in simulating transpiration was also confirmed statistically by MAE and NSE values. The simulated *Tc* was 129 mm for the 9 months (February to October 2020) period, which underestimated the measured transpiration rates of 143 mm (by 10 %) during the same period (February to October 2020) at Sandfontein (Figure 6.13).

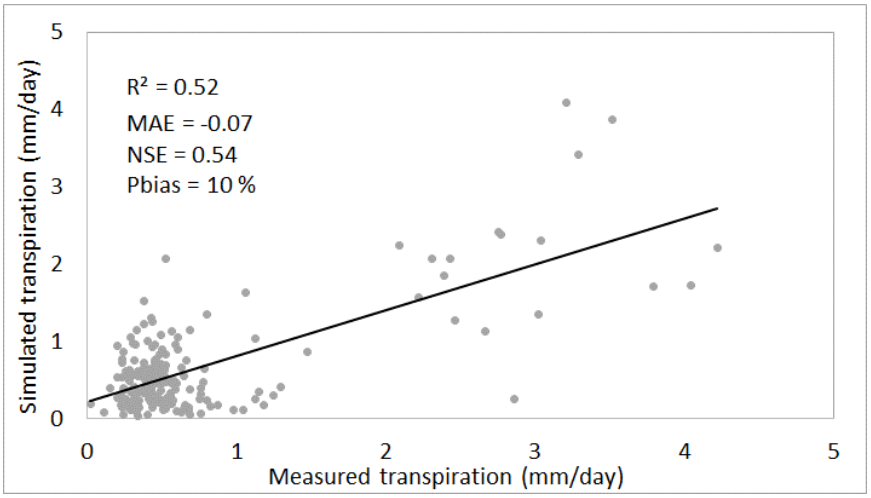

Figure 6.13: Validation of the AET model using simulated (Tc) and measured transpiration rates at Sandfontein from the 1st of February until the 31st of October 2020 period.

To validate the model further, the two-layer AET model was used to simulate AET by fynbos vegetation using the parameters calibrated for the Tussenberge site (Table 6.4).

Table 6.4:Calibration parameters for AET simulations for A. longifolia and fynbos at Sandfontein and Tussenberge sites, respectively.

Parameter	*A. longifolia* (Sandfontein)	*Fynbos (Tussenberge)*
b1	0.002	0.004
b2	0.141	-0.176
K_1 (mm/s)	9.720	1.405
K_{d1} (KPa)	-0.002	-0.002
K_{d2} (Kpa)	0.029	0.029
K_r (W/m^2)	937 845	852 032
K_T (°C)	20.300	19.404
K_{s1}	0.00	0.000
K_{s2}	13.892	13.892
r	0.160	0.200

The model performance was assessed using AET rates measured from fynbos using the flux tower at Tussenberge. Figure 6.14 shows R^2 = 0.30 between the simulated and measured AET rates at Tussenberge. This was rather expected as the AET model simulations are derived from the Penman-Monteith equation (6.1). This equation (6.1) was also to estimate the ETo rates, in which R^2 = 0.39 between measured AET and ETo rates were observed in Figure 6.11. The good model performance was also confirmed by MAE

between the simulated and measured AET which was close to 0 (Figure 6.14). The simulated AET rates from Tussenberge during the 9 months (February – October 2020) was 424 mm, which was 1 % less (underestimation) than the 429 mm AET measured from the flux tower. Suggesting that the two-layer AET model can realistically predict AET rates.

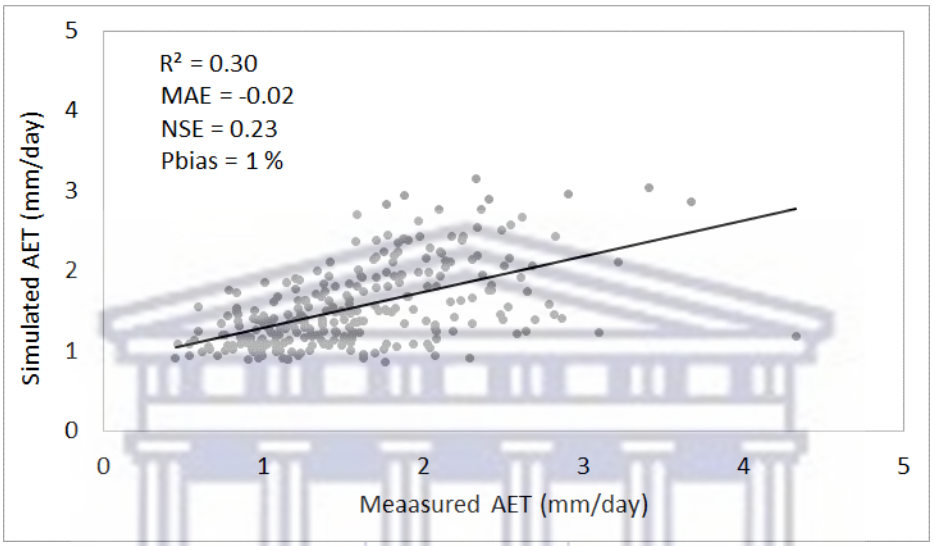

Figure 6.14: Validation of the AET simulations using the measured AET rates at Tussenberge from the 1st of February until the 31st of October 2020 period.

ii. Simulated AET rates from A. longifolia

During the simulation period of 9 months (from February to October 2020), actual evapotranspiration by *A. longifolia* at Sandfontein was 742 mm, peaking at 6.3 mm/day in February 2020 and a low rate of 0.8 mm/day was estimated in July 2020 (Figure 6.15a). Generally, the simulated AET rates varied seasonally, with high AET rates during the dry months (February – May 2020 and September – October 2020) and low AET during the wet period (June – August 2020). The seasonal variation in simulated AET rates corresponded with reference evapotranspiration (ETo) rates. Notably, the daily and monthly AET rates of *A. longifolia* from April to September 2020 exceeded ETo rates (Figure 6.15 a&b). These differences were associated with the canopy interception of rainfall that the model accounted for during rainy days. Interception loss from the model accounted for 14 % of AET simulations over the 9 months. Furthermore, the periods when AET exceeded ETo coincided with months when the groundwater table rose and high SWC were observed as explained in Figure 6.8. Conversely, during the dry summer period

(February – March 2020), ETo rates were higher than the simulated AET rates. This means the dry summer conditions, associated with lower water tables and SWC (Figure 6.8) constrained AET rates, while the wet winters increased the water use rates by *A. longifolia*.

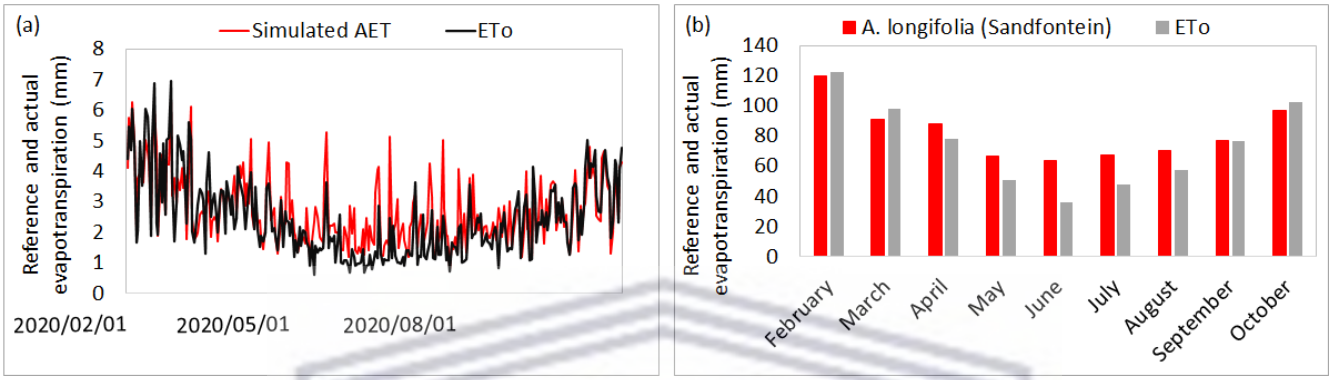

Figure 6.15: Sandfontein's (a) daily and (b) monthly AET simulations and ETo rates during the 1st of February to 31st October 2020 period.

6.3.7 Comparison of actual evapotranspiration rates by A. longifolia and a fynbos stand

The simulated rate of AET from *A. longifolia* at Sandfontein during the 9 months (February to October 2020) period was 742 mm, while measured AET from the fynbos stand at Tussenberge was 429 mm during the same period. This suggests that the AET rates from *A. longifolia* were significantly ($p<0.05$,) higher than AET rates from the fynbos stand. This was also confirmed by higher maximum stomatal conductance (K1) in *A. longifolia* compared to fynbos (Table 6.4).

Table 6.5: Paired t-test between AET rates from A. longifolia and fynbos.

	A.longifolia (Sandfontein)	*Fynbos (Tussenberge)*
Mean	2.71	1.57
Observations	274	274
Pearson Correlation	0.59	
P(T<=t) two-tail	0.00	

Generally, AET rates from both sites showed seasonal variation. The daily AET rates ranged between 0.8 – 6.3 mm/day for *A. longifolia*, while AET rates for the fynbos stand were between 0.5 – 4.3 mm/day (Figure 6.16 a&b). Notably, between May – September

2020, daily AET rates from the fynbos stand were almost equal to the AET rates from the *A. longifolia* stand (Figure 6.16a). This coincides with the period with increased SWC and rising groundwater table in Tussenberge (Figure 6.8).

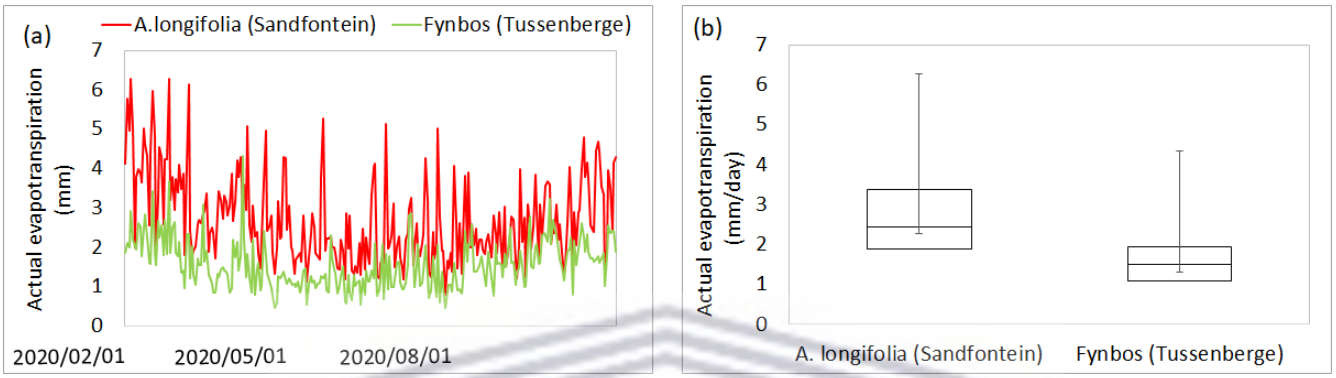

Figure 6.16: Daily AET rates by A. longifolia and fynbos stands from 1st February to 31st October 2020.

Monthly AET rates for *A. longifolia* were significantly higher than AET rates for fynbos, such that from April to August 2020, AET for *A. longifolia* were higher than rates of water use by fynbos and the reference grass (Figure 6.17a). Higher rates of water use for *A. longifolia* were also evident from the ratio of the monthly AET to ETo rates that peaked at 1.76 and 0.94 for *A.longifolia* and fynbos, respectively (Figure 6.17b).

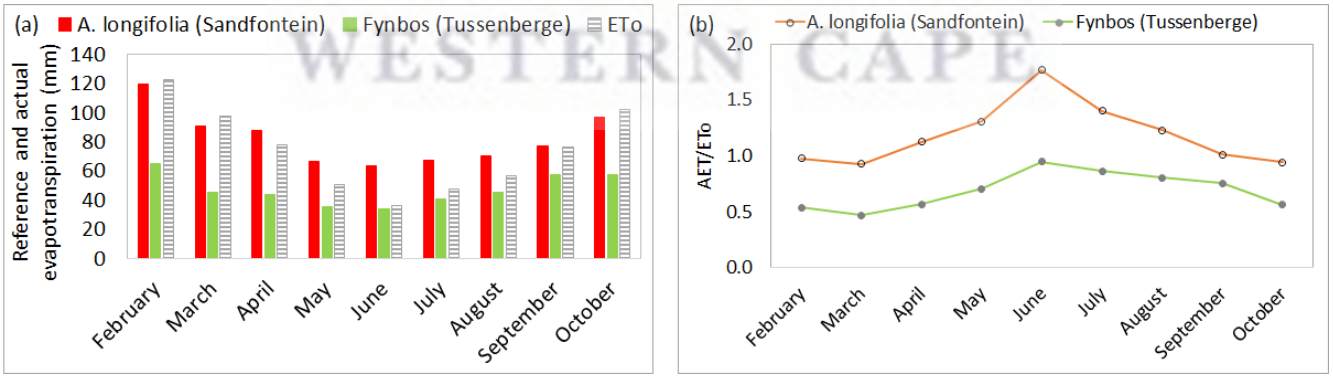

Figure 6.17: (a) Monthly AET rates and (b) changes in the ratio between the AET and ETo rates by A. longifolia and fynbos stands from 1st February to 31st October 2020.

6.4 Discussion

The clearing of invasive alien plants (IAPs) was identified as an option to minimise their impact on-catchment water yields; especially along the riparian zones that tend to have increased moisture which promotes the rapid growth rates of IAPs, enabling them to outgrow, over-shadow, or quickly displace the indigenous vegetation (Fourie et al., 2013). Previous research associated the fast growth rate of IAPs with increased water use rates compared to the indigenous vegetation (Calder and Dye, 2001; Dye et al., 2001; Everson et al., 2016; Scott-Shaw, Everson and Clulow, 2017; Gush, 2018). Large-scale funding by both the government and the private sector continues in support of the Working-for-Water (WfW) Programme which is active in many regions of the country. An important justification for this programme is the potential hydrological benefits that are believed to follow the replacement of dense IAPs stands with indigenous vegetation, largely herbaceous or shrub-dominated plant communities (Calder and Dye, 2001; Dye et al., 2001).

6.4.1 Microclimate, soil water, and groundwater patterns at Tussenberge

The comparative analysis of weather characteristics from the headwaters to the lowlands in the Nuwejaars Catchment showed that the Tussenberge site located in the headwaters received more rainfall than other parts of the catchment (Chapter 4). Humid conditions were also observed in the headwaters compared to the lowlands and mid-slope, thus resulting in ETo rates increasing from the headwaters to the lowlands. This explained the significant differences that were observed in transpiration rates by *A. longifolia* invasions monitored across the catchment. During the August 2019 to November 2021 period, seasonal variations in solar irradiance, temperatures, and VPD were observed, with peak values observed during the summer periods. The wet winter conditions resulted in low solar irradiance, temperatures, and VPD. These are variables that affect the surface energy balance and thus the water use patterns by vegetation. The surface energy balance at Tussenberge provided independent evidence of the low water use rates from the fynbos stand, where a significant proportion of the available energy was converted to sensible heat with a very small proportion used to evaporate the water (latent heat) across all the seasons. In this context, this implies that at times when energy was available, AET was constrained by other factors such as VPD and water availability.

During the study period (August 2019 – November 2021), much of the rainfall was received during the winter months (June – August), where August 2020 and May 2021 had high rainfall. The wet winters resulted in increased SWC and raising groundwater tables from July to October, followed by a decline during November/December in Tussenberge. The declining SWC and groundwater tables during November/December can affect water availability for vegetation.

6.4.2 AET rates from fynbos

There is a widespread belief in South Africa that indigenous vegetation, in contrast to the IAPs, is water efficient and should be used in land restoration programmes due to their slower growth rates that are generally translated to less water-use consumption compared to IAPs (Everson et al., 2016). AET rates of fynbos during the study period reached a peak of 6.5 mm/day during November 2021, while lower rates were observed during the winter season. Although higher rainfalls translate to water available for plants, it was evident in this study that the wet conditions during 2021 resulted in lower VPD which suppressed AET rates than in the year 2020. These observations were also confirmed statistically, whereby the available energy (Rn-G) was the major driver for AET by fynbos stand. AET rates from the fynbos stand from February to October 2020 were 429 mm. This rate was close to the annual actual ET of 551 mm that was measured from the dryland sandstone fynbos in a study by Dzikiti et al. (2014). In the study by Dzikiti et al. (2014), the annual AET by dryland sandstone fynbos was lower compared to what was measured from the riparian sandstone fynbos (which was 1 460 mm/year). The differences were attributed to the shallow, rocky, and coarse-sand characteristics of the soils at the Montane site at Kogelberg Nature Reserve. This implies that the fynbos vegetation can potentially use considerable volumes of water when conditions are favourable. This was also confirmed in a study in the Western Cape by Dye (2008) who established an annual AET of 757 mm from the fynbos stand at Helderberg, while 1332 mm/ year was simulated at Jonkershoek. The differences in AET rates at these sites were also attributed to the permanent wet conditions at the Jonkershoek mountains and a depth to the water table of 1.1 m during the period of simulation (Dye et al., 2008).

At Tussenberge, AET rates by fynbos showed no relationship with SWC. This was attributed to soil water contents at Tussenberge that were being monitored at very

shallow layers (~ 8 cm depth). Therefore, it is probable that the fynbos vegetation growing at Tussenberge has a deeper rooting system as was previously observed that non-riparian hillslope vegetation tends to expand their root systems where the most growth-limiting resource is abundant until water demands are met (Brantley et al., 2017; Eliades et al., 2018). The protea shrubs in the mountainous Jonkershoek site, with similar climate characteristics and geological formations as the Tussenberge site, reportedly have deep tap roots extending beyond 3-m below the surface (Dye, 2008). This explains the weak relationship between AET and groundwater fluctuations in BH16-30m (with DTW ranging between 8.0 and 3.6 m) at Tussenberge. Although this was contrary to long-standing assumptions that vegetation growing in uplands uses water mainly from rain or stored in the soil (Tromp-van Meerveld and McDonnel, 2006; Sun et al., 2008), Dzikiti et al. (2014) also confirmed that indigenous fynbos vegetation has a wide range of water use rates depending on access to water. A study by Scott and Le Maitre (1998) also highlighted that most renosterveld shrubs are likely to develop deep roots where possible, but the interaction with groundwater may be minimal in fynbos sites that are underlain by shale formation. However, for weathered sandstone aquifers such as the one at Tussenberge, groundwater extraction may be important and a reliable source of water for the fynbos stand.

6.4.3 Simulated AET rates of A. longifolia stand at Sandfontein

In a list of research recommendations for enhancing our understanding of the impacts of alien invasions, Versfeld et al. (1998) expressed the need for improved measurement of ET from invading species. It was also recommended that research be initiated to provide a modelling framework to permit rapid assessment of the annual water use of a wide range of vegetation types occurring in areas of the country invaded by alien invasive plants (Dye et al. 2001). In this study, a two-layer ET model was used to quantify ET by invasive *A. longifolia* stands. The dual-source model that partitions evapotranspiration into different components was observed to produce the best predictions in non-homogenous ecosystems (Shuttleworth and Wallace, 1985). The model performed well and produced realistic AET rates that were validated with the measured transpiration rates at Sandfontein and AET rates from fynbos at Tussenberge. The simulated AET rates from the *A. longifolia* stand on the headwaters (Sandfontein) during the 9 months (February – October 2020) was 742 mm.

6.4.4 Comparing AET rates between indigenous fynbos and invasive A. longifolia stands.

AET rates from *A. longifolia* stand at Sandfontein were 742 mm, which was significantly higher than the measured AET rates of 429 mm from the fynbos stand at Tussenberge. The differences in AET rates were high during the dry summer seasons, with differences of up to 45 %. Although AET rates were lower during winter (June – August), *A. longifolia* exhibited higher rates of AET than fynbos. Therefore, the results of this study validate the previous assumption of potential water savings assumed to follow the clearing of IAPs and restoring the cleared land with indigenous vegetation. This study confirms that incremental water gains can be achieved by clearing *A. longifolia* stands occurring in non-riparian settings. These findings also agree with the ecological rationale for the WfW programme (Calder and Dye, 2001; Doody et al., 2011; Sebinasi Dzikiti et al., 2013; Holmes et al., 2008).

Although AET rates by riparian fynbos were not measured in the current study, the conclusions made previously by Dye et al. (2008) and Dzikiti et al. (2014) implied that the benefits of replacing IAPs with fynbos may differ and significantly decrease in areas that are not water stressed, since both studies highlighted that fynbos vegetation can also use considerable volumes in situations where water is readily available. Consequently, the alien clearing programme has prioritized such areas and thus has been believed to strongly improve catchment yields of the invaded sites (Dye et al., 2001). The potential benefits of clearing IAPs occurring in the non-riparian setting have been overlooked. This study has made a useful contribution in this direction, by providing the first assessment and comparative analysis of daily and monthly actual ET rates between an indigenous fynbos stand and invasive *Acacia longifolia* stand occurring in a non-riparian setting with similar climate and elevations in the Nuwejaars Catchment, Western Cape Province of South Africa.

6.5 Conclusion

The high AET rates from the invasive *A. longifolia* stand in Sandfontein compared to the indigenous fynbos at Tussenberge have illustrated that hydrological benefits can be achieved by clearing *A. longifolia* stands in non-riparian settings, as they consumed substantially more water than the indigenous fynbos vegetation. Thus, the clearing of *A.*

longifolia stands will significantly reduce annual AET rates in the Nuwejaars Catchment, resulting in potential water savings that were previously confirmed only from the clearing of IAPs occurring in the riparian zones.

This study recommends further work on the monitoring of water use of fynbos vegetation. There is a need for more accurate long-term measurements of AET in various fynbos ecosystems as well as the field measurement of AET rates by IAPs to better understand the implications of IAPs on catchment water balance, land use management and rehabilitation strategies.

Chapter 7
The catchment scale impacts of IAPs on water resources

Alien clearing project taking place in the Nuwejaars Catchment.

7.1 Introduction

Evapotranspiration (ET) is the essential component of the water cycle that accounts for 59 % of land surface precipitation and more than 50 % of the solar radiation absorbed by the land surface (Jiang and Liu, 2021), thus considered the second largest flux of the hydrological cycle (Ward and Robinson, 2000; Mu et al., 2011; Le Maitre, 2015). Evapotranspiration can be estimated using various methods and techniques such as lysimeters, eddy covariance, Bowen ratio, scintillometer, and model simulations (Jiang and Liu, 2021; Turk et al., 2021). The limitations of using field observations include that in-situ measurements provide only point- or field-scale measurements (Jiang and Liu, 2021). Although they are accurate, they cannot be used for catchment scale ET mapping (Turk et al., 2021). Field measurements are rarely repeated for large areas, making it difficult to establish the temporal dynamics (He et al., 2011) and are useful for the verification of large-scale ET estimations (Gibson et al., 2013). They are not only time-consuming but are only representative of the site selected for monitoring and may lead to the misrepresentation of ET variations (Reyes-Acosta and Lubczynski, 2013).

Over the last few decades, the introduction of satellite remote sensing has offered robust, instantaneous, and efficient spatio-temporal ET estimations (Li et al., 2009). Satellite remote sensing techniques have become attractive because of their ability to provide repetitive and synoptic views without any disturbance and site accessibility (Liou and Kar, 2014). Consequently, remote sensing has been used to observe and monitor the spatial and temporal variation of hydro-meteorological fluxes over large areas (Schmugge *et al.,* 2002). The information can therefore be used for improved management of water resources (Li et al., 2009; Liou and Kar, 2014). For this reason, there is a growing interest and innovative ideas for advanced technologies that can be used to estimate ET (Nouri *et al.,* 2013). Courault et al. (2003) classified these satellite-based methods into empirical direct methods, residual methods of the energy budget, deterministic methods, and vegetation index methods. These methods generate surface parameters at a pixel scale and are suitable for the spatial modelling of ET (Revollo, 2010).

The MODerate Resolution Imaging Spectroradiometer (MODIS) MOD16 algorithm developed by Mu et al. (2007, 2011) is one of the commonly used remote sensing products to provide global estimates of ET (Ramoelo et al., 2014). MOD16 is a remotely sensed ET model based on the Penman-Monteith approach with some modifications to account for

parameters not estimated from remote sensing images (Mu et al., 2011; Wang et al., 2012). ET estimations include evaporation from wet and moist soil, rainwater intercepted by the canopy before reaching the ground, water vapour, and transpiration through plants (Mu et al., 2011). A major limitation of MOD16 ET is the coarse spatial resolution of 1 km^2 (Ramoelo et al., 2014). Coarse spatial resolution imagery can be useful for routine monitoring and estimation of ET due to its high temporal resolution (Mohammadian et al., 2017). However, the spatial resolution associated with coarse images is generally too low to provide beneficial information for hydrological applications, as pixel sizes often exceed the size of the area under observation (Mohammadian et al., 2017). The inconsistency of the spatial resolution in the input data sets, especially for regions with strong climatic gradients can introduce errors (Ramoelo et al., 2014). Even though this product has been validated on several parts in North and South America, Europe, Asia, and Australia, there are still concerns about over- or underestimation (Ramoelo et al., 2014). Ndara (2017) used MOD16 ET to investigate ET variations on different land cover in the Heuningnes catchment, Western Cape Province of South Africa. The results showed that MOD 16 could distinguish the spatial variation of ET over different land cover types. The study revealed that the forests in the catchment had higher ET rates than other land covers. This is in agreement with the well-established finding that evapotranspiration is generally higher in forested than non-forested catchments.

The Surface Energy Balance Algorithm over Land (SEBAL) (Bastiaanssen et al., 2005) and the Surface Energy Balance System (SEBS) (Su, 2002) are examples of models that estimate ET from the combination of empirical relationships and physical components (Courault et al., 2003; Revollo, 2010). They generate atmospheric variables from remote sensing data and assume semi-empirical relations to estimate emissivity and surface roughness. To estimate the sensible heat flux, an area must be divided into wet and dry land (Courault et al., 2003). Although the advantages of using remote sensing models for spatial coverages are generally known. Nonetheless, some parameters have been reported to be difficult to estimate, such as the stomatal resistance and temperature which can lead to model errors. Other limitations include the limited availability of high-spatial and temporal resolution thermal infrared imagery needed for the energy balance approach, the scattering, and the absorption of radiation by clouds (Jarmain, 2010). The availability of good-quality imagery is another major constraint for the running of ET

models (Gokool et al., 2016). This at times limits the number of images that can be used due to cloudy conditions which affect ET estimations. While moderate and fine spatial resolution imagery can be obtained to overcome the limitations given by coarse remote sensing imagery, their limited temporal resolution does not allow for operational monitoring and estimation of ET (Gokool et al., 2016). It is in this light that other researchers used Landsat 8 images for the estimation of ET. This includes the study by Mohammadian et al. (2017) who estimated daily ET using Landsat 8 datasets based on the Surface Energy Balance System (SEBS) algorithm over the Zayanderud Dam area in central Iran. SEBS ET showed variation across the different land cover types.

In South Africa, Ramjeawon (2016) developed a method to estimate ET for the natural vegetation of South Africa using remote sensing. This was also done using the SEBS model in conjunction with Landsat 7 ETM+ and 8 OLI/TRS images which showed that the ET estimates from SEBS compared well to the in-situ ET measurements and followed the seasonal trend. A study by Mengistu et al. (2014) showed that Landsat images provided better ET estimates from agricultural fields in KwaZulu-Natal, South Africa when compared to MODIS imagery and that was attributed to the differences in spatial resolution. A general conclusion from studies that mapped the spatial variation of ET highlighted a need to determine the effect of different land cover types and their contributions to catchment evapotranspiration (Shoko, 2014). Chemura et al. (2020) also highlighted the need to understand the impacts of land cover change on aspects of the water balance in a catchment. In conjunction with point measurements of actual evapotranspiration rates (AET) from fynbos and the modelled AET from a site invaded by *A. longifolia,* this study aims to estimate catchment scale AET and to determine the landcover/land use that contributes most to the catchment AET in the Nuwejaars Catchment. The main objective of the study was to quantify the catchment scale volume of water that can potentially be saved by clearing IAPs in the Nuwejaars Catchment.

7.2 Methods and materials

Catchment-scale estimations of actual evapotranspiration were derived using the Surface Energy Balance Systems (SEBS) model. The SEBS model developed by Su (2002) was used to estimate the actual ET using satellite earth observation data (Landsat 8 imagery),

in combination with the weather data acquired from the automatic weather stations in the catchment. The model has been tested and validated on a variety of landscapes (Gibson et al., 2013; Mohammadian et al., 2017; Ramjeawon, 2016).

7.2.1 Surface Energy Balance System (SEBS)

The estimation of ET as a residual of the shortened energy balance is a commonly applied technique for both operational and scientific research purposes (Gokool et al., 2016b). SEBS model has been applied extensively for the estimation of regional fluxes and ET (Yang et al., 2009; Zhou et al., 2013). SEBS is available as a pre-packaged tool in various software packages, originally coded in interactive data language (IDL), and implemented in ILWIS. The model is based on the energy balance approach:

$$R_{net} = G + H + \lambda E \quad (7.1)$$

R_{net} is net radiation at the surface (W/m^2), G is soil heat flux (W/m^2), H is the sensible heat (W/m^2), and λE is the latent heat (W/m^2).

Remote sensing data were used to estimate heat fluxes in the SEBS model. Remote sensing images were pre-processed for the conversion and correction of radiance and reflectance bands using the equations in Figure 7.1.

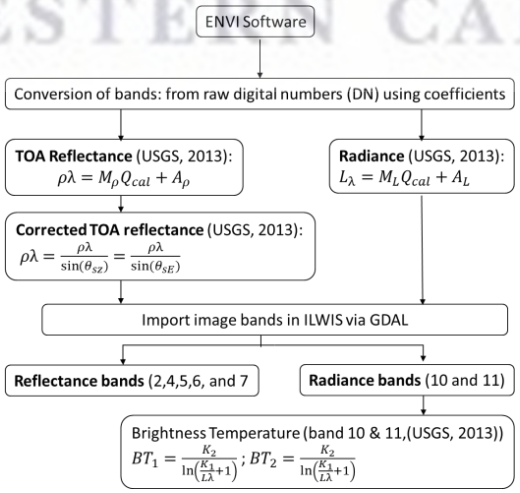

Figure 7.1: Landsat 8 image pre-processing (adopted from Shoko, 2014).

Radiance bands were used for the estimation of land surface temperature (LST), while reflectance bands were used to estimate the albedo, emissivity, fractional vegetation cover (FVC), leaf area index (LAI), normalised difference vegetation index (NDVI), and emissivity of the area. The model also uses meteorological data (*i.e.,* temperature, humidity, wind speed and pressure) measured from the weather stations established across the catchment as input (Figure 7.2).

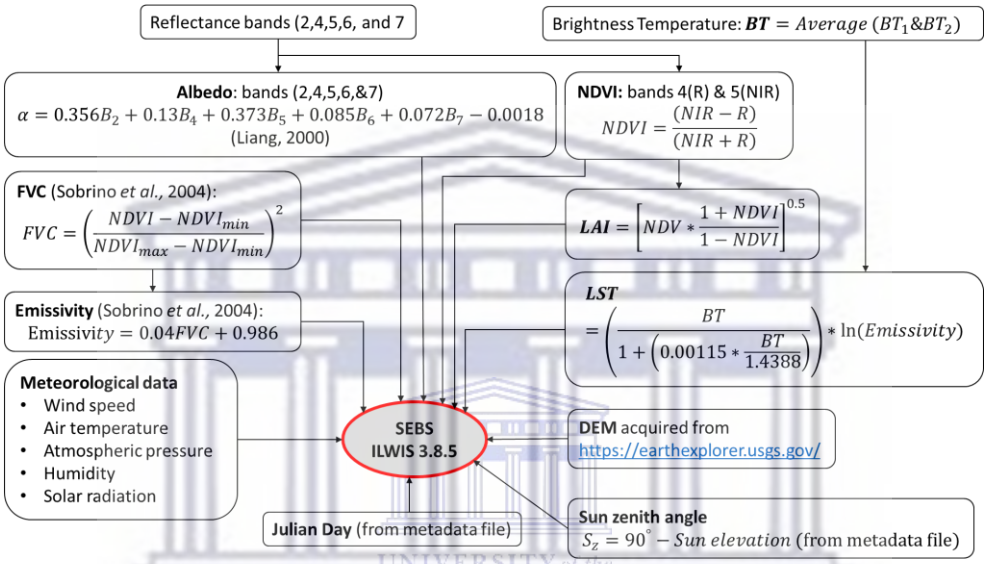

Figure 7.2: SEBS Computation using Landsat 8 Images (adopted from Shoko, 2014).

7.2.2 Remote sensing inputs

Remotely sensed inputs for the model were derived from the 30 m resolution Landsat 8 images for the period 2018 to 2021 (Table 7.1). The period was chosen to overlap with the AET measured from the flux tower and based on the availability of Landsat 8 images. The study also intended to cover the wet and dry seasons. Therefore, four Landsat 8 images covering the study area for four different dates shown in Table 7.1 were used. Landsat 8 images are available at the USGS data centre at a 16-day temporal resolution and these images were acquired using the bounding coordinates of the study area. The image scenes which covered the Nuwejaars Catchment were obtained and used images with less than 1% cloud cover (http://landsat.usgs.gov/).

Table 7.1: Description of Landsat 8 images used in SEBS.

Date	Number of bands	Spatial resolution (m)	Image scene (path/row number)	Scene cloud cover (%)
2018/12/25	11	30	174/084	0.80
2019/07/21	11	30	174/084	0.05
2020/03/01	11	30	174/084	0.36
2021/07/10	11	30	174/084	0.95

The Thermal Infrared Sensor (TIRS) in Landsat 8 dataset consists of band numbers 10 and 11. These bands were used to retrieve the land surface temperature (LST). The raw bands were converted from raw digital numbers (DN) using coefficients from the metadata file into reflectance (2, 4, 5, 6 and 7) and radiance (10 and 11) bands using ENVI 4.3 version software (Figure 7.1).

7.2.3 Meteorological inputs

Meteorological data used in the SEBS model included daily mean temperature, wind speed, humidity, pressure, and solar radiation from three weather stations located in the Nuwejaars Catchment. The description of the sites/locations of the weather station catchment are included in Chapter 4.

7.2.4 Validation of SEBS AET estimations

AET estimates from SEBS were validated using AET data from the eddy covariance system at Tussenberge. AET estimates from the 1st of March 2020 and the 10th of July 2021 images were used for validation since the eddy covariance system was installed in August 2019 in the Nuwejaars Catchment.

Daily AET rates from the eddy covariance system were compared to SEBS AET estimates acquired from the location of the flux tower on the map.

To validate the spatial variation of AET, the simulated AET was compared to reference evapotranspiration (ETo) rates across the different sites with weather stations in the catchment.

7.3 Data analysis

The contributions of different land cover types on catchment water losses were estimated by overlaying the land-use/landcover map with SEBS AET map. Thereafter, the AET rates for each pixel land cover were extrapolated and multiplied by pixel area (30 m x 30 m) to get the total AET rate from each land cover. This was done for March 2020 (representing the dry season) and July 2021 (representing the wet season) images.

The hydrological benefits of clearing alien-invaded areas and restoring them with fynbos vegetation were calculated as the difference in the volume of water loss between invaded and non-invaded (fynbos vegetation) areas.

7.4 Results

The headwater (upland) and mid-slope sites had slightly higher mean temperatures, humidity, and windspeed than the lowland sites, except on March 1st, 2020, when the lowland site had marginally higher mean temperatures, humidity, and windspeed than other parts of the catchment (Table 7.2).

Table 7.2: Meteorological data measured on weather stations and used to map AET on SEBS.

Date	Station name	Tmean (°C)	Tmax (°C)	Tmin (°C)	Solar radiation (W/m^2)	Windspeed (m/s)	Pressure (Kpa)	Humidity (%)
2018/12/25	Moddervlei	22.4	29.1	15.7	418.6	3.94	101	63
	Spanjaardskloof	23.0	31.6	14.5	369.4	0.94	100	63
	Tussenberge	-	-	-	-	-	-	-
2019/07/21	Moddervlei	11.9	20.9	2.9	158.3	0.99	102	58
	Spanjaardskloof	11.7	21.8	1.5	159.8	0.82	101	61
	Tussenberge	12.2	19.4	5.0	141.0	1.31	99	59
2020/03/01	Moddervlei	21.1	26.0	16.2	288.0	3.94	101	76
	Spanjaardskloof	20.6	27.7	13.5	303.6	3.16	101	73
	Tussenberge	20.9	27.1	14.7	288.2	2.40	99	73
2021/07/10	Moddervlei	11.5	18.3	4.8	140.3	0.90	102	72
	Spanjaardskloof	12.5	19.4	5.6	150.8	1.90	101	68
	Tussenberge	12.0	15.7	8.2	144.1	1.60	100	64

7.4.1 Remote sensing inputs during a wet and dry period

SEBS inputs were derived from remotely sensed datasets using equations outlined in Figure 7.2 for 1st March 2020 (representing the dry season) and 10th July 2021 (representing the wet season). These figures show the spatial variations of the SEBS inputs for the two selected days representing a dry (March 2020) and wet (July 2021) period.

Higher LST estimates of up to 290K were obtained during the dry season compared to 282K estimated during the winter season. During the dry season, the upper part of the catchment showed lower LST estimates than in the lowland. This agrees with low temperatures observed in the headwaters than in the lowlands (Table 7.2). During the winter season, both the uplands and lowland areas had lower LST estimates compared to the mid-slopes. This is attributed to the high rainfall received in the uplands and lowlands parts of the catchment which cools the area compared to the mid-slopes.

During dry and wet seasons, albedo shows low values (0.03 – 0.15) in the headwaters and lowland parts of the catchment. On the headwaters, these are areas with dense IAPs canopies, which are also present along the rivers and floodplains. The rivers were shown with high albedo (reflectance) during both seasons. This also agrees with the low emissivity estimations on the water bodies which implies that the surface water bodies had low absorption ability of incoming radiation and thus low evaporation compared to areas where IAPs were found.

The LAI and FVC show similar patterns. On uplands and along riparian zones, LAI and FVC of 2.43 and 0.87, respectively, were observed, while on water bodies, LAI and FVC observed were close to zero (0.43 and 0.36, respectively). This illustrates the capability of the SEBS model to distinguish between land cover types. NDVI estimates also show variation across the different land covers. The uplands and riparian zones had high NDVI values of up to 0.8 while lower values (-0.4 to 0) were observed on water bodies, in the rivers and wetlands. Lower NDVI estimates were observed during 2020 compared to 2021, this is attributed to the drought that was experienced in the Western Cape Province between 2017 – 2019. This has a potential effect on the derived total evaporation estimates and energy fluxes. The wet season during 2021, was characterized by higher rainfall, temperature and thus vegetation development, hence NDVI had higher estimates.

It is evident from the spatial variation of input variables (meteorological and remote sensing) that the SEBS model can distinguish the different types of land cover.

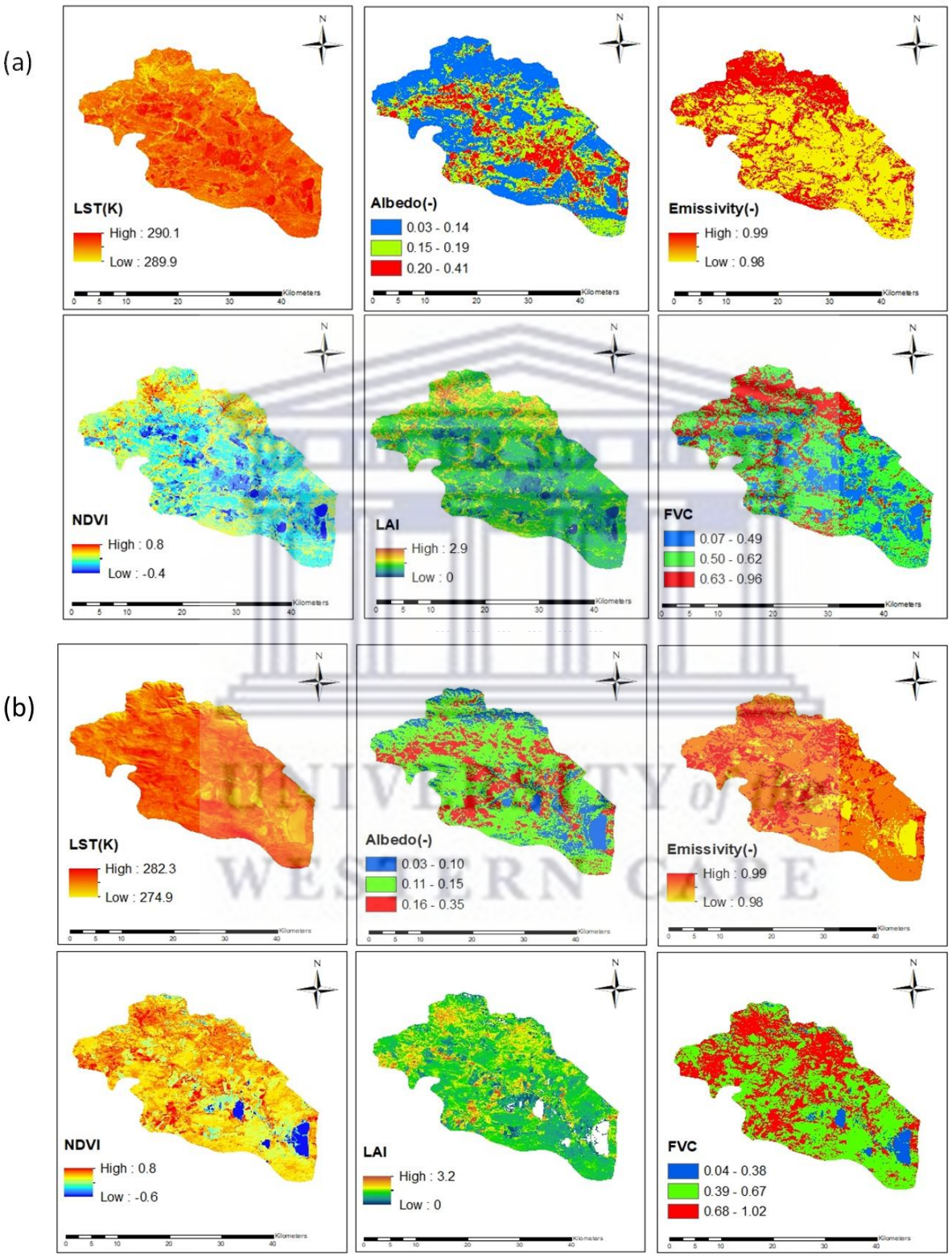

Figure 7.3: SEBS remote sensing inputs for (a) 1st March 2020 (dry season) and (b) 10th July 2021 (wet season).

7.4.2 Comparing AET rates from sites dominated by fynbos and IAPs.

The variation in input variables for the estimation of SEBS AET resulted in the variation in AET between areas dominated by IAPs and fynbos (Figure 7.4). During the wet period, represented by July 2019 and 2021 images, AET rates sites dominated by IAPs and fynbos both ranged between 0.1 - 1.4 mm/day (Figure 7.5). During the dry period, December 2018, and March 2020, AET rates showed slight variations, with higher rates in the northern part of the catchment and lower rates in the low-lying areas including the rivers (Figure 7.4). AET from IAPs ranged between 5.0 – 7.1 mm/day on the 25th of December 2018, while AET rates from fynbos were between 5.1 – 6.9 mm/day on the same day (Figure 7.5). These results suggest that the daily rates from fynbos and IAPs were in the same order of magnitude and these results coincided with the findings in Chapter 6 which illustrated that on some days, daily AET rates from the fynbos stand were almost equal to the AET rates from the *A. longifolia* stand.

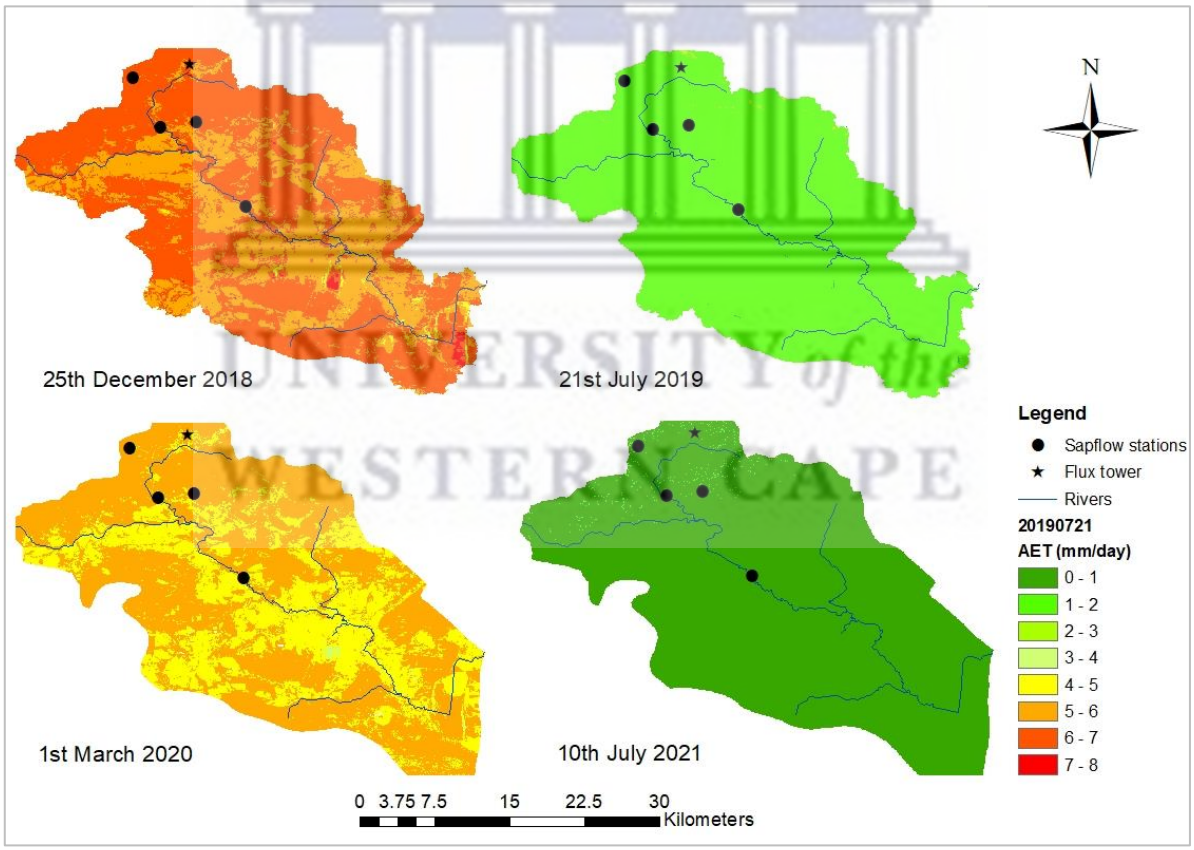

Figure 7.4: SEBS AET across the catchment for four selected days, 25th December 2018, 1st March 2020 (representing dry season), and 21st July 2019, 10th July 2021 (representing wet season).

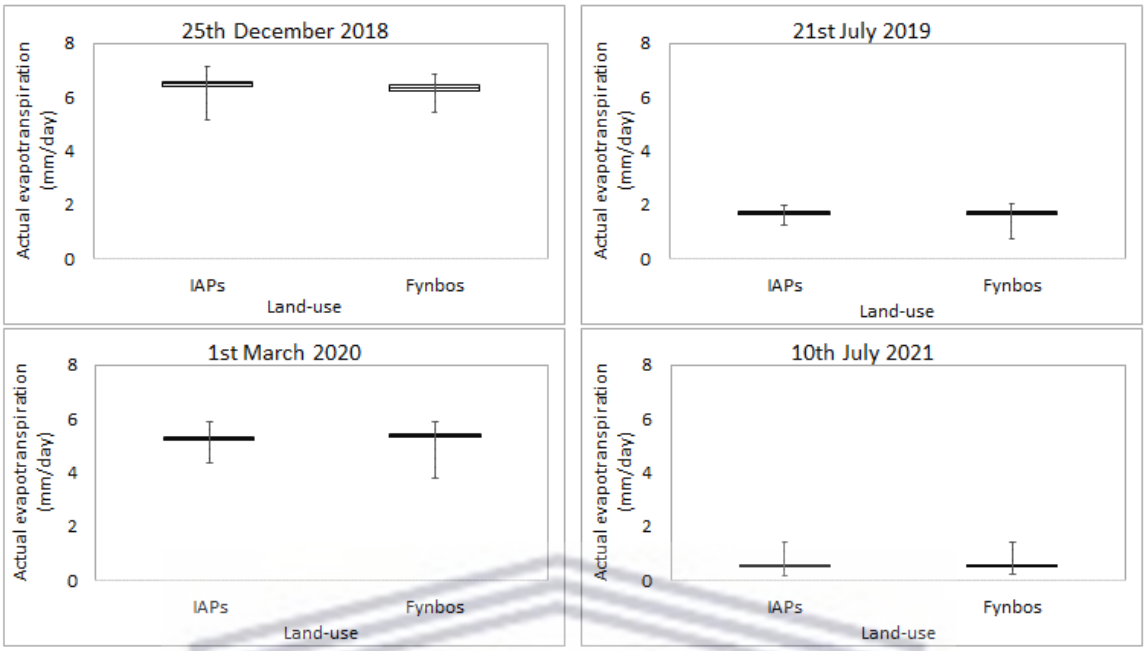

Figure 7.5: SEBS daily AET rates from IAPs and fynbos land covers during four selected days, representing dry season (25th December 2018, 1st March 2020), and wet season (21st July 2019, 10th July 2021).

7.4.3 Comparing AET and ETo rates across the Nuwejaars Catchment

The daily AET estimates from SEBS daily AET rates were validated using reference evapotranspiration (ETo) estimated from the weather stations and measured AET from the flux tower installed in the catchment (Figure 7.6). The comparison between SEBS daily AET and ETo rates show variation across the sites and different seasons. The lowland riparian (Moddervlei) and headwaters (Tussenberge) characterised by high rainfall and shallow water tables showed an overestimation of AET during the dry summer period (2018 and 2020 images). During summer, SEBS AET was higher than the reference and measured (from fynbos) AET. This was expected as ETo is estimated for short grass, while SEBS AET was estimated from IAP trees and fynbos shrubs at Moddervlei and Tussenberge, respectively. The overestimation of SEBS AET was also observed when compared with the measured AET, especially during the summer period. The overestimation of SEBS during summer was also previously observed by Gokool et al. (2016) and Gibson et al. (2013). In the mid-slope, at Spanjaardskloof, the differences in SEBS AET and reference ET were not as pronounced as the sites on the lowland and upland. During winter, the July 2019 image shows that SEBS AET estimations were close

to the reference ET measured across all the sites. This shows that the model estimations were realistic, especially during the wet winter season.

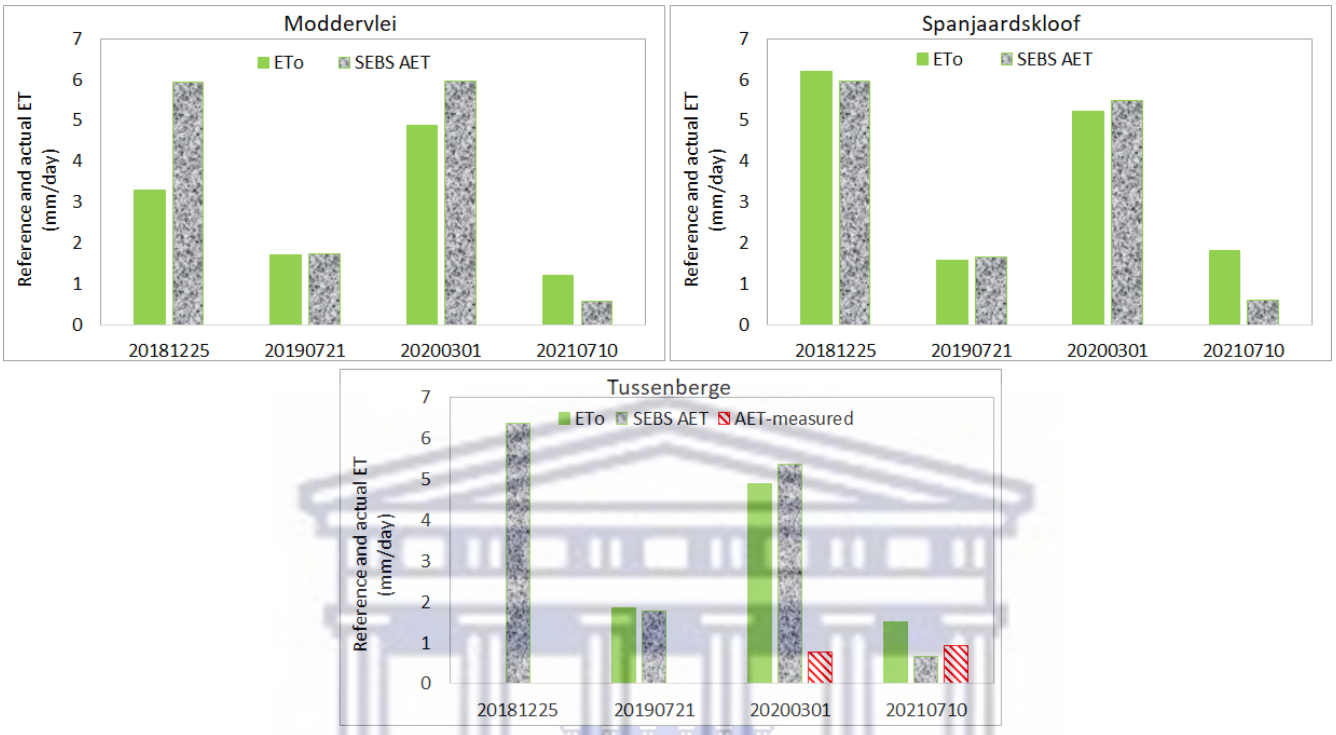

Figure 7.6: Comparison of SEBS AET to the reference ETo and measured AET across the sites.

7.4.4 Contributions of landcover on catchment scale AET during wet and dry seasons

AET varied seasonally, higher daily rates were observed during summer, while the wet winter season had lower rates. Table 7.3 shows that during summer (March 2020), daily AET was 90 % (5.8 mm/day) more that the daily AET during winter (0.6 mm/day). Accordingly, different land cover types contributed differently to AET rates. Despite the lower AET rates during winter, AET contributions from IAPs and fynbos increased from 9 to 17 % during summer and from 38 to 50 % during winter (Table 7.3). The higher contributions from fynbos land cover are explained by greater area coverage (48%) than IAPs (11%). Increased contributions from IAPs and fynbos land covers during winter were consistent with higher NDVI estimates observed in Figure 7.3 during winter (July 2021). These were attributed to SWC increases and rising groundwater tables during the wet winter period, which enhances vegetation growth and therefore increases AET estimates.

Table 7.3: Contribution of landcover types on daily AET rates (mm/day) during the dry (March 2020) and wet (July 2021) seasons

Landcover/land-use	Area (hectare)	1st Mar-20	10th Jul-21
		AET mm/day	
Water	4465	0.0	0.0
IAPs	8348	**0.5**	**0.1**
Cultivated land	26721	3.1	0.2
Fynbos	36466	**2.2**	**0.3**
Total	76000	**5.8**	**0.6**

The headwaters of the Nuwejaars Catchment make up ~ 38 % of the catchment area. According to Mazvimavi et al. (2021), these headwaters contribute significantly to mean annual surface water flows during both wet and dry seasons. These are parts of the catchment with elevations greater than 200 m.a.s.l. Upland areas that generate substantial amounts of mean annual runoff and sustain lowland areas downstream are defined as strategic water source areas (SWSAs) and are also known as 'water towers' (Nel et al., 2013). In the Nuwejaars Catchment, Tussenberge and Sandfontein sites at 230 and 228 m.a.s.l, respectively, are both located in water source areas and therefore were used as a case study to quantify the hydrological benefits of clearing IAPs in the Nuwejaars Catchment. Although the previous Chapters showed contrasting water use rates along the topographic gradient, with high rates of water use in the lowland and headwaters of the catchment, the rates of water use by IAPs at Sandfontein were similar to those used by riparian IAPs at Moddervlei and Jan Swartskraal. Moreover, water consumed by IAPs occurring in these 'water towers' has the potential to affect and reduce the overall availability of water resources downstream and in the lowlands of the Nuwejaars Catchment (Mazvimavi et al, 2021). This provides justifications to use the water use rates from Sandfontein (representative of IAPs) and at Tussenberge (representing fynbos) to estimate the incremental water use.

7.4.5 Quantifying the impacts of clearing IAPs in the Nuwejaars Catchment.

About 11 % of the Nuwejaars Catchment was invaded by IAPs, and annual water use rates from the dominant *A. longifolia* stand were 742 mm/year, while 429 mm/year were measured from the fynbos stand. Under the assumption that 100% density cover is present in these invaded areas and that all alien species transpire at similar rates to

A. *longifolia* trees. Table 7.4 shows that at the catchment scale, the volume of water lost through AET by IAPs was equivalent to 61.94 Mm^3. Also, if the areas occupied by IAPs (~11 %) in the catchment were cleared and replaced by fynbos, the water loss would decrease by 43 % (26.73 Mm^3).

Table7.4: Potential water savings that may be achieved by clearing IAPs in the Nuwejaars Catchment.

	IAPs	Fynbos
Actual evapotranspiration (mm/year)	742	429
Total area (ha)	8348	
The volume of water loss (m^3)	61 942 160	35 812 920
	61.94 Mm^3	**35.21 Mm^3**

7.5 Discussion and Conclusion

The previous estimates of actual evapotranspiration in Chapter 6 were site-specific. AET data at a catchment scale are presented in this chapter. The data used in SEBS to estimate AET at a spatial resolution of 30 m x 30m is sufficient for management at a catchment scale (Nowell, 2011). The purpose of this chapter was to provide quantifiable benefits of clearing IAPs in the Nuwejaars Catchment that leases with the previous estimates by Nowell, (2011) that can be used to inform clearing organizations and motivate ecosystem services payments.

The seasonal variation in actual ET illustrated high AET rates during the dry season and low AET during the wet season in the catchment. Spatial variations in AET rates were particularly observed during the dry season, where high AET rates were observed on the upland/headwaters of the catchment and along the corridors of the rivers. These were associated with corridors of IAPs that were observed along the riparian zones. These results agreed with findings from previous chapters that showed high rates of water use in areas invaded by the dominant *A. longifolia* trees. The site-specific results from the previous chapters showed that clearing *A. longifolia* trees would potentially result in water savings in the Nuwejaars Catchment. This was also confirmed by increased contributions of AET from IAPs during the wet season which signifies the impact of IAPs on water resources.

The occurrence of IAPs on the headwaters and 'water towers' of the catchment affects the water availability in the Nuwejaars Catchment. The amount of water lost through AET by IAPs in the Nuwejaars Catchment was estimated at 61.94 Mm^3/year. However, if these areas were cleared and replaced by fynbos vegetation, the volume of water lost would be 35.81 Mm^3/year. Therefore, the estimated water salvages through clearing IAPs and restoring with fynbos was 26.13 Mm^3/year. This equals 43 % of the current water losses. Based on the WR2012 Water Resources Assessment (Mazvimavi, 2021) this is two times the estimated mean annual runoff (MAR) for quaternary catchment G50B. Additionally, this benefit was greater than the 17 Mm^3/year potential water savings estimated by Mkunyana et al. (2019). According to Mkunyana et al. (2019), 2016/2017 was a very dry year, so an above-average rainfall year such as 2020/2021 might have higher benefits.

The current study is the third to quantify the benefits of removing IAPs and replacing them with indigenous fynbos vegetation in the Nuwejaars Catchment, following Nowell (2011) and Mkunyana et al. (2019). This study, along with that of Mkunyana et al. (2019), agrees with Nowell (2011) who indicated that IAP clearing could save 36 Mm^3/year of water on the Agulhas Plain. Other researchers have also shown that IAPs have detrimental effects on water resources in invaded catchments (Le Maitre, 2004; van Wilgen et al., 2004; Dzikiti et al., 2013; Le Maitre, Gush and Dzikiti, 2015; Everson, 2016). Increasing groundwater levels and increased surface water runoff/flow were the hydrological responses that were observed following the clearing of IAPs in previous studies. The increased catchment water yields that will be achieved following the clearing of IAPs in the Nuwejaars Catchment will be beneficial for domestic use, agriculture, and/or ecosystem services.

7.6 Implications of the findings

The current study supports previous studies in identifying alien clearing as the first option for improving water supply in invaded catchments. Additionally, the clearing of IAPs should not be limited to riparian areas but should be prioritized in areas where dense thickets are present. Nowel (2011) also suggested that an increased water supply would contribute to the restoration of a wide range of wetlands and estuaries that attract and support the biodiversity in this catchment.

Chapter 8: Conclusions

This study quantified transpiration rates and the catchment-scale hydrological benefits of clearing IAPs existing in semi-arid riparian and non-riparian environments in the Nuwejaars Catchment. The conclusions from each study objective are summarised below.

8.1 The spatial distribution of IAPs.

The focus of this Chapter was to map the extent and distribution of IAPs and landcover changes in the Nuwejaars Catchment between the 1973 – 2021 period using Landsat imagery.

- IAPs were most evident in the catchment's headwaters and riparian zones. These were areas with high NDVI indicative of plants that are actively growing and consuming water.
- It was illustrated that the governmental interventions employed to combat the spread and impact of IAPs resulted in the declining spatial extent of IAPs in the Nuwejaars Catchment. The decline was from 25% in 1973 to 11% in 2021.

8.2 Water use rates of *A. longifolia* occurring at different positions/elevations.

Acacia longifolia was identified as the dominant invader in the Nuwejaars Catchment. This Chapter compared water use (transpiration) rates of *A. longifolia* stands occurring in different locations, from headwaters to lowlands in the Nuwejaars Catchment.

- The headwaters of the Nuwejaars Catchment received more rainfall than the other parts.
- Accordingly, *A. longifolia* stands on the headwaters (at Sandfontein) had high rates of water use similar to those observed in the lowland (Moddervlei) and mid-slope (Jan Swartskraal) riparian sites.
- The mid-slope non-riparian site at Spanjaardskloof had the lowest rates of transpiration compared to other sites.

The result from this study supports the hypothesis that riparian invasions use more water than invasions occurring in a non-riparian setting. Moreover, this study also revealed that high tree densities occur in both riparian and non-riparian settings depending on moisture availability and/or rainfall that accelerates plant growth. Therefore, dense invasion should be flagged as high-priority areas for alien plant clearing regardless of whether the area is in a riparian or non-riparian setting. It is recommended that further work be done on monitoring tree water use on different IAP species occurring in the Nuwejaars Catchment.

8.3 The influence of transpiration by *A. longifolia* on soil water and groundwater variations.

The relationship between transpiration and water availability can be explained in two ways; (i) to improve our understanding of how spatial variation in water availability affects tree water use patterns, or conversely, (ii) how transpiration influences soil water and groundwater variability in different topographical positions. This chapter analysed the relationships between transpiration patterns by *A. longifolia* stands, soil water and groundwater variations.

- The sites invaded by *A. longifolia* had a sandy soil texture.
- The response of soils to rainfall shows the water table's wetting front moving up into the deep soil layer at the riparian areas. Resulting in higher SWC in the deep layers at riparian sites (Moddervlei and Jan Swartskraal). In the mid-slope (Spanjaardskloof) and upland (Sandfontein) sites, high SWC was observed in the topsoil layer.
- As expected, the groundwater table was very shallow at riparian sites, explaining the prolonged wetting of the deep soil layers at Moddervlei and Jan Swartskraal.
- The differences in depth to water tables (DTW) were evident between non-riparian (mid-slope and upland hillslope) sites. The water table at Spanjaardskloof was deeper and responded gradually to cumulative rainfall. Such that, high rates of transpiration were observed during periods when the water table rose. On the other hand, the higher rainfall in the headwaters at Sandfontein resulted in the

shallow and sometimes raised water table to the surface. Thus, increasing the rates of transpiration at Sandfontein.

- The sites with shallow water tables, Moddervlei, Jan Swartskraal, and Sandfontein had higher transpiration rates compared to Spanjaardskloof, where the water table was deeper.
- Accordingly, evapotranspiration from groundwater (ET_g) was higher in piezometers and boreholes with shallow water tables.

These results suggested that the differences *A. longifolia* across the sites resulted from the differences in the groundwater water table from the headwaters to the lowlands. These results also support the assumption that IAPs act as groundwater pumps in areas they invade.

Further validation of these findings, the use of tracer methods is recommended to confirm groundwater extraction from *A. longifolia* invasions and other IAP species.

8.4 Actual evapotranspiration rates of *A. longifolia* and indigenous fynbos.

Previous studies hypothesised the detrimental impacts of IAPs on water resources as a result of their high rates of water use compared to the indigenous species. This chapter aimed to test this hypothesis by comparing the water use rates of fynbos vegetation with that of the invasive *A. longifolia* stand occurring in a similar environment.

- The measured actual evapotranspiration (AET) during February to October 2020 period was 429 mm from the fynbos stand at Tussenberge.
- The cross-validation of the two-layer model showed the ability of the model to realistically simulate AET rates across the two sites.
- The model simulations show *A.longifolia* had significantly high rates of actual evapotranspiration (742 mm) compared to the indigenous fynbos (429 mm) occurring in a similar setting.

These results confirm that the clearing of *A. longifolia* stands will significantly reduce annual actual evapotranspiration in the Nuwejaars Catchments, resulting in potential water savings. Thus, validating the previous assumption of land restoration and

potential water savings that were assumed by clearing IAPs and replacing them with indigenous vegetation. This study recommends further work on the monitoring of water use of fynbos vegetation. The study recommends accurate long-term measurements of AET in various fynbos ecosystems as well as the field measurement of AET rates by IAPs to better understand the implications of IAPs on catchment water balance, land use management and rehabilitation strategies.

8.5 The catchment scale impacts of clearing IAPs.

The objective of this Chapter was to estimate AET at a catchment scale and to determine which land cover contributed the most to AET. This was done to estimate the water losses (through AET) from IAPs and how much water the Nuwejaars Catchment could potentially save by clearing IAPs.

- High AET rates were observed on the upland/mountainous parts of the catchment, and the lowland, along the rivers. These are areas associated with corridors of IAPs.
- At a catchment scale, the amount of water lost through AET from IAPs was estimated at 61.94 Mm^3/year, while the volume of water lost would be 35.81 Mm^3/year if areas with invasions were replaced with indigenous vegetation.
- Meaning, the estimated water salvages through clearing IAPs and restoring with fynbos was 26.13 Mm^3/year. This equals 43 % of the current water losses.

This study, therefore, supports previous studies that identified alien clearing as an effective method of improving water supply in invaded catchments. These water savings will be beneficial for domestic use, agriculture, and/or ecosystem services.

References

Ahring, T.S., Steward, D.R., 2012. Groundwater surface water interactions and the role of phreatophytes in identifying recharge zones. Hydrol. Earth Syst. Sci. 16, 4133–4142. https://doi.org/10.5194/hess-16-4133-2012

Albano Pérez, E., Coetzee, J.A., Ruiz Téllez, T., Hill, M.P., 2011. A first report of water hyacinth (Eichhornia crassipes) soil seed banks in South Africa. South African Journal of Botany 77, 795–800. https://doi.org/10.1016/j.sajb.2011.03.009

Allen, R.G., Pereira, L.S., Raes, D. and Smith, M., 1998. Crop evapotranspiration-Guidelines for computing crop water requirements-FAO Irrigation and drainage paper 56. *Fao, Rome*, *300*(9), p.D05109.

Araya, Y. and Walker, N., 2009. Understanding how water resources shape our flora. *flora*, *88*(2), pp.70-72.

Banks, E.W., Simmons, C.T., Love, A.J., Shand, P., 2011. Assessing spatial and temporal connectivity between surface water and groundwater in a regional catchment: Implications for regional scale water quantity and quality. Journal of Hydrology 404, 30–49. https://doi.org/10.1016/j.jhydrol.2011.04.017

Bastiaanssen, W.G.M., Noordman, E.J.M., Pelgrum, H., Davids, G., Thoreson, B.P., Allen, R.G., 2005. SEBAL Model with Remotely Sensed Data to Improve Water- Resources Management under Actual Field Conditions. Journal of Irrigation and Drainage Engineering 131, 85–93. https://doi.org/10.1061/(ASCE)0733-9437

Bell, J.E., Sherry, R., Luo, Y., 2010. Changes in soil water dynamics due to variation in precipitation and temperature: An ecohydrological analysis in a tallgrass prairie: soil water dynamics in a tallgrass prairie. Water Resour. Res. 46. https://doi.org/10.1029/2009WR007908

Blanchard, R., Holmes, P.M., 2008. Riparian vegetation recovery after invasive alien tree clearance in the Fynbos Biome. South African Journal of Botany 74, 421–431. https://doi.org/10.1016/j.sajb.2008.01.178

Brantley, S.L., Eissenstat, D.M., Marshall, J.A., Godsey, S.E., Balogh-Brunstad, Z., Karwan, D.L., Papuga, S.A., Roering, J., Dawson, T.E., Evaristo, J., Chadwick, O., McDonnell, J.J., Weathers, K.C., 2017. Reviews and syntheses: on the roles trees play in building and plumbing the critical zone. Biogeosciences 14, 5115–5142. https://doi.org/10.5194/bg-14-5115-2017

Bulcock, H.H., Jewitt, G.P.W., 2010. Spatial mapping of leaf area index using hyperspectral remote sensing for hydrological applications with a particular focus on canopy interception. Hydrol. Earth Syst. Sci. 14, 383–392. https://doi.org/10.5194/hess-14-383-2010

Burgess, S.S.O., Adams, M.A., Turner, N.C., Beverly, C.R., Ong, C.K., Khan, A.A.H., Bleby, T.M., 2001. An improved heat pulse method to measure low and reverse rates of sap flow in woody plants. Tree Physiology 21, 589–598. https://doi.org/10.1093/treephys/21.9.589

Butler, J.J., Kluitenberg, G.J., Whittemore, D.O., Loheide, S.P., Jin, W., Billinger, M.A., Zhan, X., 2007. A field investigation of phreatophyte-induced fluctuations in the water table: phreatophyte-induced fluctuations. Water Resour. Res. 43. https://doi.org/10.1029/2005WR004627

Calder, I.R. and Dye, P., 2001. Hydrological impacts of invasive alien plants. *Land use and water resources research*, *1*(1732-2016-140259).

Cavaleri, M.A., Ostertag, R., Cordell, S. and Sack, L., 2014. Native trees show conservative water use relative to invasive trees: results from a removal experiment in a Hawaiian wet forest. *Conservation Physiology*, *2*(1), p.cou016.https://doi.org/10.1093/conphys/cou016

Cavaleri, M.A., Sack, L., 2010. Comparative water use of native and invasive plants at multiple scales: a global meta-analysis. Ecology 91, 2705–2715. https://doi.org/10.1890/09-0582.1

Chamier, J., Schachtschneider, K., Le Maitre, D., Ashton, P., Van Wilgen, B., 2012. Impacts of invasive alien plants on water quality, with particular emphasis on South Africa. WSA 38, 345–356. https://doi.org/10.4314/wsa.v38i2.19

Chen, B.-M., Gao, Y., Liao, H.-X., Peng, S.-L., 2017. Differential responses of invasive and native plants to warming with simulated changes in diurnal temperature ranges. AoB Plants 9, plx028. https://doi.org/10.1093/aobpla/plx028

Chen, L., Zhang, Z., Ewers, B.E., 2012. Urban Tree Species Show the Same Hydraulic Response to Vapor Pressure Deficit across Varying Tree Size and Environmental Conditions. PLoS ONE 7, e47882. https://doi.org/10.1371/journal.pone.0047882

Chen, L., Zhang, Z., Zha, T., Mo, K., Zhang, Y., Fang, X., 2014. Soil water affects transpiration response to rainfall and vapor pressure deficit in poplar plantation. New Forests 45, 235–250. https://doi.org/10.1007/s11056-014-9405-0

Chen, X., Song, J. and Wang, W., 2010. Spatial variability of specific yield and vertical hydraulic conductivity in a highly permeable alluvial aquifer. *Journal of Hydrology*, *388*(3-4), pp.379-388. https://doi.org/10.1016/j.jhydrol.2010.05.017

Chinchio, E., Crotta, M., Romeo, C., Drewe, J.A., Guitian, J., Ferrari, N., 2020. Invasive alien species and disease risk: An open challenge in public and animal health. PLOS Pathogens 16, e1008922. https://doi.org/10.1371/journal.ppat.1008922

Courault, D., Seguin, B., Olioso, A., 2003. Review to estimate Evapotranspiration from remote sensing data: some examples from the simplified relationship to the use of mesoscale atmospheric models. 19.

Dawson, T.E., Burgess, S.S.O., Tu, K.P., Oliveira, R.S., Santiago, L.S., Fisher, J.B., Simonin, K.A., Ambrose, A.R., 2007. Nighttime transpiration in woody plants from contrasting ecosystems. Tree Physiology 27, 561–575. https://doi.org/10.1093/treephys/27.4.561

Doody, T., Benyon, R., 2011. Quantifying water savings from willow removal in Australian streams. Journal of Environmental Management 92, 926–935. https://doi.org/10.1016/j.jenvman.2010.10.061

Doody, T.M., Nagler, P.L., Glenn, E.P., Moore, G.W., Morino, K., Hultine, K.R., Benyon, R.G., 2011. Potential for water salvage by removal of non-native woody vegetation from dryland river systems: water salvage from removal of non- native riparian species. Hydrol. Process.25, 4117–4131. https://doi.org/10.1002/hyp.8395

Dye, P. and Jarmain, C., 2004. Water use by black wattle (Acacia mearnsii): implications for the link between removal of invading trees and catchment streamflow response: working for water. South African Journal of Science, 100(1), pp.40-44.

Dye, P., Moses, G., Vilakazi, P., Ndlela, R., Royappen, M., 2001. Comparative water use of wattle thickets and indigenous plant communities at riparian sites in the Western Cape and KwaZulu-Natal. Water SA 27,529–538. https://doi.org/10.4314/wsa.v27i4.4967

Dye, P.J., Naiken, V., Clulow, A., Prinsloo, E., Crichton, M., Weiersbye, I., 2017. Sap flow in Searsia pendulina and Searsia lancea trees established on gold mining sites in central South Africa. South African Journal of Botany 109, 81–89.

https://doi.org/10.1016/j.sajb.2016.12.016
Dye, P.J., Jarmain, C., Le Maitre, D., Everson, C.S., Gush, M. and Clulow, A., 2008. Modelling vegetation water use for general application in different categories of vegetation. Water Research Commission Report, 1319(1), p.08.
Dzikiti, S., Gush, M.B., Le Maitre, D.C., Maherry, A., Jovanovic, N.Z., Ramoelo, A. and Cho, M.A., 2016. Quantifying potential water savings from clearing invasive alien Eucalyptus camaldulensis using in situ and high-resolution remote sensing data in the Berg River Catchment, Western Cape, South Africa. *Forest Ecology and Management*, *361*, pp.69-80. https://doi.org/10.1016/j.foreco.2015.11.009
Dzikiti, S., Jovanovic, N.Z., Bugan, R., Israel, S., Le Maitre, D.C., 2014. Measurement and modelling of evapotranspiration in three fynbos vegetation types. Water SA 40, 189–198.
Dzikiti, S., Ntshidi, Z., Le Maitre, D.C., Bugan, R.D.H., Mazvimavi, D., Schachtschneider, K., Jovanovic, N.Z., Pienaar, H.H., 2017. Assessing water use by Prosopis invasions and Vachellia karroo trees: Implications for groundwater recovery following alien plant removal in an arid catchment in South Africa. Forest Ecology and Management 398, 153–163. https://doi.org/10.1016/j.foreco.2017.05.009
Dzikiti, Sebinasi, Schachtschneider, K., Naiken, V., Gush, M., Le Maitre, D., 2013. Comparison of water-use by alien invasive pine trees growing in riparian and non-riparian zones in the Western Cape Province, South Africa. Forest Ecology and Management 293, 92–102. https://doi.org/10.1016/j.foreco.2013.01.003
Dzikiti, S., Schachtschneider, K., Naiken, V., Gush, M., Moses, G., Le Maitre, D.C., 2013. Water relations and the effects of clearing invasive Prosopis trees on groundwater in an arid environment in the Northern Cape, South Africa. Journal of Arid Environments 90, 103–113. https://doi.org/10.1016/j.jaridenv.2012.10.015
Eliades, M., Bruggeman, A., Lubczynski, M.W., Christou, A., Camera, C., Djuma, H., 2018. The water balance components of Mediterranean pine trees on a steep mountain slope during two hydrologically contrasting years. Journal of Hydrology 562, 712– 724. https://doi.org/10.1016/j.jhydrol.2018.05.048
Enright, W.D., 2000. The effect of terrestrial invasive alien plants on water scarcity in South Africa. Physics and Chemistry of the Earth, Part B: Hydrology, Oceans and Atmosphere 25, 237–242. https://doi.org/10.1016/S1464-1909(00)00010-1
Fan, J., Oestergaard, K.T., Guyot, A., Lockington, D.A., 2014. Estimating groundwater recharge and evapotranspiration from water table fluctuations under three vegetation covers in a coastal sandy aquifer of subtropical Australia. Journal of Hydrology 519, 1120–1129. https://doi.org/10.1016/j.jhydrol.2014.08.039
Forster, M., 2017. How Reliable Are Heat Pulse Velocity Methods for Estimating Tree Transpiration? Forests 8, 350. https://doi.org/10.3390/f8090350
Forsyth, A.T., 2012. Identifying and mapping invasive alien plant individuals and stands from aerial photography and satellite images in the central Hawequa conservation area.
Fourie, H., De Wit, M.P., Van der Merwe, A., 2013. The role and value of water in natural capital restoration on the Agulhas Plain. SAJEMS 16, 83–95. https://doi.org/10.4102/sajems.v16i1.252
Fricke, W., 2019. Night-time transpiration–favouring growth?. *Trends in Plant Science*, *24*(4), pp.311-317. https://doi.org/10.1016/j.tplants.2019.01.007
Gibson, L.A., Jarmain, C., Su, Z., Eckardt, F.E., 2013. Estimating evapotranspiration using remote sensing and the Surface Energy Balance System - A South African perspective. Water SA 39, 00–00.

Gokool, S., Chetty, K.T., Jewitt, G.P.W. and Heeralal, A., 2016. Estimating total evaporation at the field scale using the SEBS model and data infilling procedures. *Water SA*, *42*(4), pp.673-683.https://doi.org/10.4314/wsa.v42i4.18

Grossiord, C., Sevanto, S., Borrego, I., Chan, A.M., Collins, A.D., Dickman, L.T., Hudson, P.J., McBranch, N., Michaletz, S.T., Pockman, W.T., Ryan, M., Vilagrosa, A., McDowell, N.G., 2017. Tree water dynamics in a drying and warming world: Future tree water dynamics. Plant, Cell & Environment 40, 1861–1873. https://doi.org/10.1111/pce.12991

Gush, M.B., 2018. Measurement of water-use by *Jatropha curcas* L. using the heat-pulse velocity technique. WaterSA 34, 579. https://doi.org/10.4314/wsa.v34i5.180655

Hamada, Y., Stow, D.A., Coulter, L.L., Jafolla, J.C., Hendricks, L.W., 2007. Detecting Tamarisk species (Tamarix spp.) in riparian habitats of Southern California using high spatial resolution hyperspectral imagery. Remote Sensing of Environment 109, 237–248. https://doi.org/10.1016/j.rse.2007.01.003

Hassler, S.K., Weiler, M. and Blume, T., 2018. Tree-, stand-and site-specific controls on landscape-scale patterns of transpiration. *Hydrology and Earth System Sciences*, *22*(1), pp.13-30.

Hawthorne, S., Miniat, C.F., 2018. Topography may mitigate drought effects on vegetation along a hillslope gradient. Ecohydrology 11, e1825. https://doi.org/10.1002/eco.1825

He, K.S., Rocchini, D., Neteler, M., Nagendra, H., 2011. Benefits of hyperspectral remote sensing for tracking plant invasions: Plant invasion and hyperspectral remote sensing. Diversity and Distributions 17, 381–392. https://doi.org/10.1111/j.1472-4642.2011.00761.x

Henderson, L., 2007. Invasive, naturalized and casual alien plants in southern Africa: a sum-mary based on the Southern African Plant Invaders Atlas (SAPIA). Bothalia 37, 215–248. https://doi.org/10.4102/abc.v37i2.322

Henderson, L., Wilson, J.R.U., 2017. Changes in the composition and distribution of alien plants in South Africa: An update from the Southern African Plant Invaders Atlas. Bothalia 47. https://doi.org/10.4102/abc.v47i2.2172

Herdien, E.L., Petersen, C., Reed, C., Impson, D., Belcher, A., Ndiitwani, T., Buthelezi, S., Matoti, A., 2010. Ecological Status for Rivers of the Overberg Region 2004/2005 252.

Hoekstra, T. and Waller, L., 2014. De Mond Nature Reserve Complex: Protected Area Management Plan. *CapeNature: Cape Town, South Africa*.

Holden, P.B., Rebelo, A.J., New, M.G., 2021. Mapping invasive alien trees in water towers: A combined approach using satellite data fusion, drone technology and expert engagement. Remote Sensing Applications: Society and Environment 21, 100448. https://doi.org/10.1016/j.rsase.2020.100448

Holmes, P.M., Esler, K.J., Richardson, D.M. and Witkowski, E.T.F., 2008. Guidelines for improved management of riparian zones invaded by alien plants in South Africa. *South African Journal of Botany*, *74*(3), pp.538-552.

Hou, R., Ouyang, Z., Han, D., Wilson, G.V., 2018. Effects of field experimental warming on wheat root distribution under conventional tillage and no-tillage systems. Ecol Evol 8, 2418–2427. https://doi.org/10.1002/ece3.3864

Huddle, J.A., Awada, T., Martin, D.L., Zhou, X., Pegg, S.E. and Josiah, S.J., 2011. Do invasive riparian woody plants affect hydrology and ecosystem processes?. *Great Plains Research*, pp.49-71.

Jiang, Y., Liu, Z., 2021. Evaluations of Remote Sensing-Based Global Evapotranspiration Datasets at Catchment Scale in Mountain Regions. Remote Sensing 13, 5096. https://doi.org/10.3390/rs13245096

Joubert, A.R., Leiman, A., de KLERK, H.M., Katua, S. and Aggenbach, J.C., 1997. Fynbos (fine bush) vegetation and the supply of water: a comparison of multi-criteria decision analysis and cost-benefit analysis. *Ecological economics*, *22*(2), pp.123-140.

Kanso, T., Gromaire, M.-C., Ramier, D., Dubois, P., Chebbo, G., 2020. An Investigation of the Accuracy of EC5 and 5TE Capacitance Sensors for Soil Moisture Monitoring in Urban Soils-Laboratory and Field Calibration. Sensors 20, 6510. https://doi.org/10.3390/s20226510

Klaus, R., Dourado-Neto, D., Schwantes, A.P. and Timm, L.C., 2013. Soil Water Storage as Related to Water Balance. *International Centre for Theoretical Physics*, pp.1-12.

Kotzé, I., Beukes, H., Van den Berg, E. and Newby, T., 2010. National invasive alien plant survey. *Report number: gw/a/2010/21*, pp.1-55.

Kraaij, T., Hanekom, N., Russell, I.A. and Randall, R.M., 2009. Agulhas National Park-State of Knowledge. South African National Parks. *Unpublished Internal Report*, p.51.

Kraaij, T., Baard, J.A., Rikhotso, D.R., Cole, N.S., van Wilgen, B.W., 2017. Assessing the effectiveness of invasive alien plant management in a large fynbos protected area. Bothalia - African Biodiversity & Conservation 47, 1–11. https://doi.org/10.4102/abc.v47i2.2105

Le Maitre, D.C., 2004. Predicting invasive species impacts on hydrological processes: the consequences of plant physiology for landscape processes. *Weed Technology*, pp.1408-1410. https://doi.org/10.1614/0890037X(2004)018[1408:PISIOH]2.0.CO;2

Le Maitre, D.C., Gaertner, M., Marchante, E., Ens, E.-J., Holmes, P.M., Pauchard, A., O'Farrell, P.J., Rogers, A.M., Blanchard, R., Blignaut, J., Richardson, D.M., 2011. Impacts of invasive Australian acacias: implications for management and restoration: Australian acacias: linking impacts and restoration. Diversity and Distributions 17, 1015–1029. https://doi.org/10.1111/j.1472-4642.2011.00816.x

Le Maitre, D.C., Gush, M.B., Dzikiti, S., 2015. Impacts of invading alien plant species on water flows at stand and catchment scales. AoB PLANTS 7, plv043. https://doi.org/10.1093/aobpla/plv043

Le Maitre, D.C., van Wilgen, B.W., Gelderblom, C.M., Bailey, C., Chapman, R.A., Nel, J.A., 2002. Invasive alien trees and water resources in South Africa: case studies of the costs and benefits of management. Forest Ecology and Management 160, 143–159. https://doi.org/10.1016/S0378-1127(01)00474-1

Li, Q., Zhu, Q., Zheng, J., Liao, K., Yang, G., 2015. Soil moisture response to rainfall in forestland and vegetable plot in Taihu Lake Basin, China. Chin. Geogr. Sci. 25, 426–437. https://doi.org/10.1007/s11769-014-0715-0

Li, Z., Yu, P., Wang, Yanhui, Webb, A.A., He, C., Wang, Yanbing, Yang, L., 2017. A model coupling the effects of soil moisture and potential evaporation on the tree transpiration of a semi-arid larch plantation. Ecohydrology 10, e1764. https://doi.org/10.1002/eco.1764

Li, Z.-L., Tang, R., Wan, Z., Bi, Y., Zhou, C., Tang, B., Yan, G., Zhang, X., 2009. A Review of Current Methodologies for Regional Evapotranspiration Estimation from Remotely Sensed Data. Sensors 9, 3801–3853. https://doi.org/10.3390/s90503801

Liou, Y.-A., Kar, S.K., 2014. Evapotranspiration Estimation with Remote Sensing and Various Surface Energy Balance Algorithms—A Review. Energies 7, 2821–2849.

https://doi.org/10.3390/en7052821
Loheide, S.P., Butler, J.J., Gorelick, S.M., 2005. Estimation of groundwater consumption by phreatophytes using diurnal water table fluctuations: A saturated-unsaturated flow assessment: groundwater use by phreatophytes. Water Resour. Res. 41. https://doi.org/10.1029/2005WR003942
Lubczynski, M.W., Chavarro-Rincon, D.C., Rossiter, D.G., 2017. Conductive sapwood area prediction from stem and canopy areas—allometric equations of Kalahari trees, Botswana. Ecohydrology 10, e1856. https://doi.org/10.1002/eco.1856
Lv, Meizhao, Xu, Z., Yang, Z., Lu, H., Lv, Meixia, 2021. A Comprehensive Review of Specific Yield in Land Surface and Groundwater Studies. J Adv Model Earth Syst 13. https://doi.org/10.1029/2020MS002270
Magona, N., Richardson, D.M., Le Roux, J.J., Kritzinger-Klopper, S. and Wilson, J.R., 2018. Even well-studied groups of alien species might be poorly inventoried: Australian Acacia species in South Africa as a case study. *NeoBiota*, *39*, pp.1-29. https://doi.org/10.3897/neobiota.39.23135
Makoni, M., 2020. Africa's invasive species problem. The Lancet Planetary Health 4, e317–e319. https://doi.org/10.1016/S2542-5196(20)30174-1
Mapeto, T., Gush, M., Louw, J., 2018. Single-tree water use and water-use efficiencies of selected indigenous and introduced species in the Southern Cape region of South Africa. Southern Forests: a Journal of Forest Science 80, 85–93. https://doi.org/10.2989/20702620.2016.1274861
Marchante, E., Kjøller, A., Struwe, S., Freitas, H., 2008. Short- and long-term impacts of Acacia longifolia invasion on the belowground processes of a Mediterranean coastal dune ecosystem. Applied Soil Ecology 40, 210–217. https://doi.org/10.1016/j.apsoil.2008.04.004
Mazvimavi, D. 2018. *Finding "new" water to address conflicting and competing water demands in the Nuwejaars Catchment, Cape Agulhas.* WRC Report No 2324/1/18 Water Research Commission, South Africa. http://www.wrc.org.za/wp-content/uploads/mdocs/2324_final.pdf
Mazvimavi, D., Clarke, S., Day, J., Dube, T., Kanyerere, T., Machingura, J., Malijani, E., Mkunyana, Y.P. and Swartbooi, E., 2021. Understanding of Surface Water-Groundwater Interactions from Headwaters to Lowlands or Catchment Scale Sustainable Water Resources Management. https://www.wrc.org.za/wp-content/uploads/mdocs/2855%20final.pdf
Meijninger, W., Jarmain, C., 2014. Satellite-based annual evaporation estimates of invasive alien plant species and native vegetation in South Africa. Water SA 40, 95. https://doi.org/10.4314/wsa.v40i1.12
Metzen, D., Sheridan, G.J., Benyon, R.G., Bolstad, P.V., Griebel, A., Lane, P.N.J., 2019. Spatio-temporal transpiration patterns reflect vegetation structure in complex upland terrain. Science of The Total Environment 694, 133551. https://doi.org/10.1016/j.scitotenv.2019.07.357
Meyerson, L.A., Simberloff, D., Boardman, L., Lockwood, J.L., 2019. Toward "Rules" for Studying Biological Invasions. Bull Ecol Soc Am 100. https://doi.org/10.1002/bes2.1607
Mkunyana, Y.P., Mazvimavi, D., Dzikiti, S., Ntshidi, Z., 2019. A comparative assessment of water use by Acacia longifolia invasions occurring on hillslopes and riparian zones in the Cape Agulhas region of South Africa. Physics and Chemistry of the Earth, Parts A/B/C 112, 255–264. https://doi.org/10.1016/j.pce.2018.10.002
Mohammadian, M., Arfania, R., Sahour, H., 2017. Evaluation of SEBS Algorithm for

Estimation of Daily Evapotranspiration Using Landsat-8 Dataset in a Semi-Arid Region of Central Iran. OJG 07, 335–347. https://doi.org/10.4236/ojg.2017.73023

Morais, M.C., Freitas, H., 2015. Phenological dynamics of the invasive plant *Acacia longifolia* in Portugal. Weed Res 55, 555–564. https://doi.org/10.1111/wre.12177

Morais, M.C., Freitas, H., 2012. The acclimation potential of Acacia longifolia to water stress: Implications for invasiveness. Plant Science 196, 77–84. https://doi.org/10.1016/j.plantsci.2012.08.007

Morais, M.C. and Pereira, H., 2007. Heartwood and sapwood variation in Eucalyptus globulus Labill. trees at the end of rotation for pulpwood production. *Annals of Forest Science*, *64*(6), pp.665-671.

Morris, T.L., Esler, K.J., Barger, N.N., Jacobs, S.M. and Cramer, M.D., 2011. Ecophysiological traits associated with the competitive ability of invasive Australian acacias. *Diversity and Distributions*, *17*(5), pp.898-910.

Mtengwana, B., Dube, T., Mkunyana, Y.P., Mazvimavi, D., 2020. Use of multispectral satellite datasets to improve ecological understanding of the distribution of Invasive Alien Plants in a water-limited catchment, South Africa. Afr J Ecol 58, 709–718. https://doi.org/10.1111/aje.12751

Mtengwana, B., Dube, T., Mudereri, B.T., Shoko, C., 2021. Modeling the geographic spread and proliferation of invasive alien plants (IAPs) into new ecosystems using multi-source data and multiple predictive models in the Heuningnes catchment, South Africa. GIScience & Remote Sensing 58, 483–500. https://doi.org/10.1080/15481603.2021.1903281

Nagler, P., Scott, R., Westenburg, C., Cleverly, J., Glenn, E., Huete, A., 2005. Evapotranspiration on western U.S. rivers estimated using the Enhanced Vegetation Index from MODIS and data from eddy covariance and Bowen ratio flux towers. Remote Sensing of Environment 97, 337–351. https://doi.org/10.1016/j.rse.2005.05.011

Nel, J., Colvin, C., Le Maitre, D., Smith, J. and Haines, I., 2013. South Africa's strategic water source areas. *CSIR: Stellenbosch, South Africa*.

Nowell, M.S., 2011. *Determining the hydrological benefits of clearing invasive alien vegetation on the Agulhas Plain, South Africa* (Doctoral dissertation, Stellenbosch: University of Stellenbosch).

Ntshidi, Z., Dzikiti, S., Mazvimavi, D., 2018. Water use dynamics of young and mature apple trees planted in South African orchards: a case study of the Golden Delicious and Cripps' Pink cultivars. Proc. IAHS 378, 79–83. https://doi.org/10.5194/piahs- 378-79-2018

Pettit, N.E., Froend, R.H., 2018. How important is groundwater availability and stream perenniality to riparian and floodplain tree growth? Hydrological Processes 32, 1502–1514. https://doi.org/10.1002/hyp.11510

Pilgrim, D.H., Chapman, T.G., Doran, D.G., 1988. Problems of rainfall-runoff modelling in arid and semiarid regions. Hydrological Sciences Journal 33, 379–400. https://doi.org/10.1080/02626668809491261

Ping, Z., Xing-Quan, R. a. O., Ling, M.A., Xi-An, C. a. I., Xiao-Ping, Z., 2006. Sap flow-scaled stand transpiration and canopy stomatal

Conductance in an acacia mangium forest. Chinese Journal of Plant Ecology 30, 655. https://doi.org/10.17521/cjpe.2006.0086

Prinsloo, F.W., Scott, D.F., 1999. Streamflow responses to the clearing of alien invasive trees from riparian zones at three sites in the Western Cape Province. The Southern

African Forestry Journal 185, 1–7. https://doi.org/10.1080/10295925.1999.9631220

Ramjeawon, M.R., 2016. *Developing a method to estimate the water use of South African natural vegetation using remote sensing* (Doctoral dissertation).

Ramoelo, A., Majozi, N., Mathieu, R., Jovanovic, N., Nickless, A., Dzikiti, S., 2014. Validation of Global Evapotranspiration Product (MOD16) using Flux Tower Data in the African Savanna, South Africa. Remote Sensing 6, 7406–7423. https://doi.org/10.3390/rs6087406

Rascher, K.G., Große-Stoltenberg, A., Máguas, C., Meira-Neto, J.A.A., Werner, C., 2011a. Acacia longifolia invasion impacts vegetation structure and regeneration dynamics in open dunes and pine forests. Biol Invasions 13, 1099–1113. https://doi.org/10.1007/s10530-011-9949-2

Rascher, K.G., Große-Stoltenberg, A., Máguas, C., Werner, C., 2011b. Understory Invasion by Acacia longifolia Alters the Water Balance and Carbon Gain of a Mediterranean Pine Forest. Ecosystems 14, 904–919. https://doi.org/10.1007/s10021-011-9453-7

Rebelo, A.J., 2012. *An ecological and hydrological evaluation of the effects of restoration on ecosystem services in the Kromme River System, South Africa* (Doctoral dissertation, Stellenbosch: Stellenbosch University).

Revollo, A.I.S., 2010. *A study case on the upscaling of tree transpiration in water limited environments* (Master's thesis, University of Twente).

Reyes-Acosta, J.L., Lubczynski, M.W., 2013. Mapping dry-season tree transpiration of an oak woodland at the catchment scale, using object-attributes derived from satellite imagery and sap flow measurements. Agricultural and Forest Meteorology 174–175, 184–201. https://doi.org/10.1016/j.agrformet.2013.02.012

Richardson, D.M., Pysek, P., Rejmanek, M., Barbour, M.G., Panetta, F.D., West, C.J., 2000. Naturalization and invasion of alien plants: concepts and definitions. Divers Distrib 6, 93–107. https://doi.org/10.1046/j.1472-4642.2000.00083.x

Rogan, J., Miller, J., 2006. Integrating GIS and Remotely Sensed Data for Mapping Forest Disturbance and Change, in: Wulder, M., Franklin, S. (Eds.), Understanding Forest Disturbance and Spatial Pattern. CRC Press, pp. 133–171. https://doi.org/10.1201/9781420005189.ch6

Rossatto, D.R., de Carvalho Ramos Silva, L., Villalobos-Vega, R., Sternberg, L. da S.L., Franco, A.C., 2012. Depth of water uptake in woody plants relates to groundwater level and vegetation structure along a topographic gradient in a neotropical savanna. Environmental and Experimental Botany 77, 259–266. https://doi.org/10.1016/j.envexpbot.2011.11.025

Rouget, M., Richardson, D.M., Nel, J.L. and Van Wilgen, B.W., 2002. Commercially important trees as invasive aliens–towards spatially explicit risk assessment at a national scale. *Biological Invasions*, *4*, pp.397-412.

Said, A., Nachabe, M., Ross, M. and Vomacka, J., 2005. Methodology for estimating specific yield in shallow water environment using continuous soil moisture data. *Journal of irrigation and drainage engineering*, *131*(6), pp.533-538.

Schachtschneider, K. and Reinecke, K., 2014. Riparian trees as common denominators across the river flow spectrum: are ecophysiological methods useful tools in environmental flow assessments?. *Water SA*, *40*(2), pp.287-296. https://doi.org/10.4314/wsa.v40i2.11

Schlesinger, W.H., Jasechko, S., 2014. Transpiration in the global water cycle. Agricultural

and Forest Meteorology 189–190, 115–117. https://doi.org/10.1016/j.agrformet.2014.01.011

Scott, D.F., 1999. Managing riparian zone vegetation to sustain streamflow: results of paired catchment experiments in South Africa. *Canadian Journal of Forest Research*, *29*(7), pp.1149-1157.

Scott, D.F., Le Maitre, D.C., 1998. The interaction between vegetation and groundwater: research priorities for South Africa. Water Research Commission, Pretoria.

Scott, R.L., Huxman, T.E., Williams, D.G., Goodrich, D.C., 2006. Ecohydrological impacts of woody-plant encroachment: seasonal patterns of water and carbon dioxide exchange within a semiarid riparian environment. Global Change Biol 12, 311–324. https://doi.org/10.1111/j.1365-2486.2005.01093.x

Scott-Shaw, B.C., Everson, C.S., Geldenhuys, C.J., Starke, A., Atsame-Edda, A., Schutte, S.R. and Mupemba, M., 2016. Rehabilitation of alien invaded riparian zones and catchments using indigenous trees: an assessment of indigenous tree water-use volume 1. *WRC Report*, (2081/1/16).

Scott-Shaw, B.C., Everson, C.S., Clulow, A.D., 2017. Water-use dynamics of an alien- invaded riparian forest within the Mediterranean climate zone of the Western Cape, South Africa. Hydrol. Earth Syst. Sci. 21, 4551–4562. https://doi.org/10.5194/hess-21-4551-2017

Shackleton, R.T., Le Maitre, D.C., Van Wilgen, B.W., Richardson, D.M., 2015. The impact of invasive alien Prosopis species (mesquite) on native plants in different environments in South Africa. South African Journal of Botany 97, 25–31. https://doi.org/10.1016/j.sajb.2014.12.008

Shakhane, T., Fourie, F.D., Du Preez, P.J., 2017. Mapping riparian vegetation and charactersing its groundwater dependency at the modder river government water scheme. Groundwater for Sustainable Development 5, 216–228. https://doi.org/10.1016/j.gsd.2017.07.003

Shoko, C., 2014. *The effect of spatial resolution in remote sensing estimates of total evaporation in the uMgeni catchment* (Doctoral dissertation).

Smith, D.M., Allen, S.J., 1996. Measurement of sap flow in plant stems. J Exp Bot 47, 1833–1844. https://doi.org/10.1093/jxb/47.12.1833

Snyder, K., 2000. Water sources used by riparian trees varies among stream types on the San Pedro River, Arizona. Agricultural and Forest Meteorology 105, 227–240. https://doi.org/10.1016/S0168-1923(00)00193-3

Snyder, K.A., Williams, D.G., 2003. Defoliation Alters Water Uptake by Deep and Shallow Roots of Prosopis velutina (Velvet Mesquite). Functional Ecology 17, 363–374.

Song, X., Lyu, S., Wen, X., 2020. Limitation of soil moisture on the response of transpiration to vapor pressure deficit in a subtropical coniferous plantation subjected to seasonal drought. Journal of Hydrology 591, 125301. https://doi.org/10.1016/j.jhydrol.2020.125301

Souza-Alonso, P., Rodríguez, J., González, L., Lorenzo, P., 2017. Here to stay. Recent advances and perspectives about Acacia invasion in Mediterranean areas. Annals of Forest Science 74, 55. https://doi.org/10.1007/s13595-017-0651-0

Su, Z., 2002. The Surface Energy Balance System (SEBS) for estimation of turbulent heat fluxes. Hydrol. Earth Syst. Sci. 6, 85–100. https://doi.org/10.5194/hess-6-85- 2002

Tfwala, C.M., van Rensburg, L.D., Bello, Z.A., Zietsman, P.C., 2019. Transpiration dynamics and water sources for selected indigenous trees under varying soil water content. Agricultural and Forest Meteorology 275, 296–304. https://doi.org/10.1016/j.agrformet.2019.05.030

Council, I.S.A., 2006. Invasive species definition clarification and guidance white paper. *National Invasive Species Council, US Department of the Interior, Washington, DC. http://www. invasivespecies. gov/global/ISAC/ISAC_documents/ISAC% 20Definitions% 20White% 20Paper*, *20*.

Tromp-van Meerveld, H.J., McDonnell, J.J., 2006. On the interrelations between topography, soil depth, soil moisture, transpiration rates and species distribution at the hillslope scale. Advances in Water Resources 29, 293–310. https://doi.org/10.1016/j.advwatres.2005.02.016

Turk, K.G.B., Zeineldin, F.I., Alghannam, A.M., 2021. Mapping and Assessment of Evapotranspiration over Different Land-Use/Land-Cover Types in Arid Ecosystem, Climate Change in Asia and Africa - Examining the Biophysical and Social Consequences, and Society's Responses. IntechOpen. https://doi.org/10.5772/intechopen.96759

Van Wilgen, B.W., De Wit, M.P., Anderson, H.J., Le Maitre, D.C., Kotze, I.M., Ndala, S., Brown, B. and Rapholo, M.B., 2004. Costs and benefits of biological control of invasive alien plants: case studies from South Africa: working for water. *South African Journal of Science*, *100*(1), pp.113-122.

van Wilgen, B.W., Forsyth, G.G., Le Maitre, D.C., Wannenburgh, A., Kotzé, J.D.F., van den Berg, E., Henderson, L., 2012. An assessment of the effectiveness of a large, national-scale invasive alien plant control strategy in South Africa. Biological Conservation 148, 28–38. https://doi.org/10.1016/j.biocon.2011.12.035

van Wilgen, B.W., Measey, J., Richardson, D.M., Wilson, J.R., Zengeya, T.A. (Eds.), 2020. Biological Invasions in South Africa. Springer International Publishing, Cham. https://doi.org/10.1007/978-3-030-32394-3

White, D.A., Dunin, F.X., Turner, N.C., Ward, B.H., Galbraith, J.H., 2002. Water use by contour-planted belts of trees comprised of four Eucalyptus species. Agricultural Water Management, The Role of Agroforestry and Perennial Pasture in Mitigating Waterlogging and Secondary Salinity. 53, 133–152. https://doi.org/10.1016/S0378-3774(01)00161-5

White, W., 1932. A method of estimating ground-water supplies based on discharge by plants and evaporation from soil: Results of investigations in Escalante Valley, Utah. https://doi.org/10.3133/wsp659A

Wilgen, V., Brian, W., Faulkner, K.T., Chauke, O., Fill, J., Forsyth, T., Foxcroft, L., Greve, M., Griffiths, C., Herbert, D. and Holmes, P., 2018. The status of biological invasions and their management in South Africa. https://doi.org/10.13140/RG.2.2.31003.52002

Xu, S., Yu, Z., 2020a. Environmental Control on Transpiration: A Case Study of a Desert Ecosystem in Northwest China. Water 12, 1211. https://doi.org/10.3390/w12041211

Xu, X., Zhang, Q., Li, Y., Li, X., 2016. Evaluating the influence of water table depth on transpiration of two vegetation communities in a lake floodplain wetland. Hydrology Research 47, 293–312. https://doi.org/10.2166/nh.2016.011

Yang, D., Shao, W., Yeh, P.J.-F., Yang, H., Kanae, S., Oki, T., 2009. Impact of vegetation coverage on regional water balance in the non humid regions of China: impact of vegetation on water. Water Resour. Res. 45. https://doi.org/10.1029/2008WR006948

Yang, J., El-Kassaby, Y.A., Guan, W., 2020. The effect of slope aspect on vegetation attributes in a mountainous dry valley, Southwest China. Sci Rep 10, 1–11. https://doi.org/10.1038/s41598-020-73496-0

Yang, Z., 2018. Quantitative Assessment of Groundwater and Surface Water Interactions in the Hailiutu River Basin, Erdos Plateau, China, 1st ed. CRC Press. https://doi.org/10.1201/9780429487385

Zengeya, T.A., Wilson, J.R., 2021. The Status of Biological Invasions and their Management in South Africa in 2019. Zenodo. https://doi.org/10.5281/ZENODO.3947613

Zhang, W., Zhao, L., Yu, X., Zhang, L., Wang, N., 2020. Estimation of Groundwater Evapotranspiration Using Diurnal Groundwater Level Fluctuations under Three Vegetation Covers at the Hinterland of the Badain Jaran Desert. Advances in Meteorology 2020, 1–14. https://doi.org/10.1155/2020/8478140

Zhang, Y., Liu, J., Xu, X., Tian, Y., Li, Y., Gao, Q., 2010. The response of soil moisture content to rainfall events in semi-arid area of Inner Mongolia. Procedia Environmental Sciences 2,19701978. https://doi.org/10.1016/j.proenv.2010.10.211

Zhang, Y., Peña-Arancibia, J.L., McVicar, T.R., Chiew, F.H.S., Vaze, J., Liu, C., Lu, X., Zheng, H., Wang, Y., Liu, Y.Y., Miralles, D.G., Pan, M., 2016. Multi-decadal trends in global terrestrial evapotranspiration and its components. Sci Rep 6, 1–12. https://doi.org/10.1038/srep19124

Zhou, Y., Wenninger, J., Yang, Z., Yin, L., Huang, J., Hou, L., Wang, X., Zhang, D., Uhlenbrook, S., 2013. Groundwater–surface water interactions, vegetation dependencies and implications for water resources management in the semi-arid Hailiutu River catchment, China – a synthesis. Hydrol. Earth Syst. Sci. 17, 2435–2447. https://doi.org/10.5194/hess-17-2435-2013

Zolfaghar, S., Villalobos-Vega, R., Zeppel, M., Cleverly, J., Rumman, R., Hingee, M., Boulain, N., Li, Z., Eamus, D., 2017. Transpiration of Eucalyptus woodlands across a natural gradient of depth-to-groundwater. Tree Physiology 37, 961–975. https://doi.org/10.1093/treephys/tpx024